Order Number 9334001

Chemical reaction kinetics and bonding mechanisms of boron adsorption and desorption on alumina

Toner, Charles Vincent, IV, Ph.D.

University of Delaware, 1993

U·M·I
300 N. Zeeb Rd.
Ann Arbor, MI 48106

CHEMICAL REACTION KINETICS AND BONDING MECHANISMS OF BORON ADSORPTION AND DESORPTION ON ALUMINA

by

Charles V. Toner, IV

A dissertation submitted to the Faculty of the University of Delaware in partial fulfillment of the requirements for the degree of Doctor of Philosophy in Plant and Soil Sciences.

May 1993

CHEMICAL REACTION KINETICS AND BONDING MECHANISMS

OF BORON ADSORPTION AND DESORPTION ON ALUMINA

by

Charles V. Toner, IV

Approved: Donald L. Sparks

Donald L. Sparks, Ph.D.
Chairman of the Department of Plant and Soil Sciences

Approved: John C Nye

John C. Nye, Ph.D.
Dean of the College of Agricultural Sciences

Approved: Carol E. Hoffecker

Carol E. Hoffecker, Ph.D.
Associate Provost for Graduate Studies

I certify that I have read this dissertation and that in my opinion it meets the academic and professional standard required by the University as a dissertation for the degree of Doctor of Philosophy.

Signed: Donald L. Sparks

Donald L. Sparks, Ph.D.
Professor in charge of dissertation

I certify that I have read this dissertation and that in my opinion it meets the academic and professional standard required by the University as a dissertation for the degree of Doctor of Philosophy.

Signed: Jeffry J. Fuhrmann

Jeffry J. Fuhrmann, Ph.D.
Member of dissertation committee

I certify that I have read this dissertation and that in my opinion it meets the academic and professional standard required by the University as a dissertation for the degree of Doctor of Philosophy.

Signed: J. Thomas Sims

J. Thomas Sims, Ph.D.
Member of dissertation committee

I certify that I have read this dissertation and that in my opinion it meets the academic and professional standard required by the University as a dissertation for the degree of Doctor of Philosophy.

Signed: Robert A. Smith

Robert A. Smith, Ph.D.
Member of dissertation committee

ACKNOWLEDGMENTS

There are many people to whom I am indebted for their support and fellowship throughout my graduate sojourn. Due to the protracted length of my tenure, the list has grown to gargantuan proportions and space and raw materials prevent me from hailing each and every one. My failure to mention any of these people herein is not reflective of the extent of my indebtedness to them.

Several people deserve particular recognition. I would like to thank Dr. Donald L. Sparks for his generosity in providing me with this opportunity of a lifetime. His ongoing interest in both my professional and personal growth, and his gentle prodding are in every way responsible for bringing me to this juncture. I am most fortunate that our paths have crossed. I also wish to thank Dr. Jeffry J. Fuhrmann and Dr. J. Thomas Sims for serving on my graduate committee and for their thorough evaluation of my dissertation. Their thoughtful suggestions have made this a more cohesive treatise. Their artful instruction in the practical aspects of soil science has also provided me a much firmer footing on *terra firma.* I am especially indebted to Dr. Robert Smith for his participation on my graduate committee, which came at great personal inconvenience. His criticisms of my

spectroscopic efforts were invaluable and spared me professional embarrassment. His efforts were well above and beyond the call of duty.

Special thanks goes to Gerald Hendricks for his unerring cooperation and loyal friendship. If not for him, the lab would have fallen to ruin long ago. In this environment of unrelenting change, he was the one constant. Many graduate students, postdoctoral fellows, and professors, in soil chemistry, as well as other disciplines, have made my graduate studies more memorable. To mention only a few: a note of gratitude to Maria Saduski, you are one of the most thoughtful people I've ever known. Dr. Paul Grossl, thanks for the ashram, it was truly a refuge. Dr. Scott Fendorf and Dr. Pengchu Zhang, the soup was right on.

I am grateful to the University of Delaware for the provision of a competitive fellowship, which supported the bulk of my degree program, and the U. S. Borax Research Corporation for generously funding my research efforts and for their expressed interest in my investigations.

The deepest gratitude is extended to my family, particularly my parents, Charles V. Toner, III and Mary Meier Toner, for their unflagging devotion and encouragement. Your unabashed pride in my success was easily my greatest motivation. I love you all very much.

Finally, to Amy, mere words cannot express the depth of my appreciation. I owe it all to you in so many ways. I can only hope to repay you in the remainder of my earthly days. If not, there is always eternity.

TABLE OF CONTENTS

LIST OF FIGURES

LIST OF TABLES

Chapter 1

INTRODUCTION

1.1 Boron and Plant Nutrition

Boron (B) is one of several essential nutrients required for normal plant growth. Because of its efficacy in small quantities, it is classified as a micronutrient, where the range between deficiency and toxicity is rather narrow. Of the various micronutrients classified as essential, B deficiency in plants is the most pandemic, having been reported for one or more crops in 43 states in the United States, most provinces in Canada, as well as in many other countries throughout the world (Gupta, 1979).

Total soil B content for most soils ranges from 20 to 200 g kg^{-1}; however, usually less than 5% of total B is found in plant available forms (Gupta, 1979). Generally, plant growth suffers at soil solution B levels of less than 1 g m^{-3} and above levels of 5 g m^{-3} water-soluble B (Reisenauer et al., 1973). In the majority of agricultural soils from humid regions, water-soluble B levels fall

between 0.1 and 3.0 g m^{-3}. Water-soluble B represents that portion of total-B which is readily available to plants (Fleming, 1980).

The role of B in plant physiology has not been firmly established. Many possible roles have been suggested, most relating to the high affinity of B for polyhydroxyl compounds such as alcohols and sugars (Tisdale et al., 1985). Most evidence gathered to date indicates that B plays an important role in cell division and membrane function, and is a necessary constituent of the cell wall (Gupta et al., 1985).

Boron is unique among the essential plant nutrients in that no other is normally found in the soil solution as an uncharged species at pH levels suitable for plant growth. At pH 7, approximately 1% of boric acid (BA) is in the dissociated form, leading some researchers to assume that neutral BA is the form in which B is predominantly absorbed by plant roots (Oertli and Grgurevic, 1975; Tisdale et al., 1985). The possibility remains, however, that B is taken up as the conjugate base of boric acid, the borate anion (BT), and that BA subsequently dissociates to restore the acid/base equilibrium. The mechanism of B uptake by plants has not been fully elucidated but appears to be a passive process, occurring via mass flow to the root surface (Gupta et al., 1985; Tisdale et al., 1985).

Boron deficiency symptoms are most frequently encountered in the *Leguminosae*, most notably alfalfa, and in root and vegetable crops such as sugar beet, rutabaga, cauliflower, and other members of the *Brassicae* (Gupta, 1979;

Tisdale et al., 1985). Soil solution B levels that are adequate for these crops with high B requirements may be toxic for B sensitive crops such as small grains, beans, and peas (Tisdale et al., 1985).

Because B is immobile in plants, B deficiency affects the youngest growing parts of the plant first. Some of the observed effects of B deficiency include: slowdown of root extension, inhibition of cell division, abnormal cell wall thickening, accumulation of callose in conducting tissue, increased production of indole acetic acid, and browning of tissue as a result of accumulation of polyphenolic compounds (Gupta, 1979). Lee and Aranoff (1967) found that B forms complexes with 6-phosphogluconic acid, preventing excessive synthesis of phenolic acids which accumulate in B-deficient plants. Rajartnam et al. (1971) discovered that B-deficient oil palms were completely devoid of the normally present leucoanthocyanin phytohormones well before the onset of other pathological symptoms. This finding is consistent with the otherwise anomalous situation that B is essential for higher plants but not for animals, microorganisms or lower plants (Greulach, 1973; Tisdale et al., 1985).

Boron toxicity symptoms are quite similar for most plant species, consisting of marginal and tip chlorosis on foliage followed quickly by necrosis (Gupta, 1979). Symptoms typically appear first on older leaf tissues (Gupta et al., 1985). Few virgin soils contain enough soluble B to cause B toxicity injury. Boron toxicity arises most frequently on croplands from use of irrigation water with

elevated B levels resulting from repeated leaching and evapotranspiration cycles (Gupta et al., 1985).

Due to the aforementioned adverse effects on plant tissues, both B deficiency and B toxicity may result in reduction of crop yield and/or crop quality and economic losses to the producer (Gupta et al., 1985).

1.2 Boron Geochemistry

Boron is the fifth element in the periodic table. It is the only electron-deficient nonmetal and as such has a great affinity for oxygen and, in fact, always occurs covalently bonded to oxygen in the natural state (Smith, 1985). Generally the crystalline structure of B compounds in the regolith is analogous to that of the silicates with the exception that B occurs not only in four-fold tetrahedral coordination with oxygen but also in three-fold trigonal coordination as well (Heller, 1986). Crystalline orthoboric acid forms a monoclinic structure consisting of sheets of coplanar $B(OH)_3$ molecules linked by hydrogen bonds. The sheets are in turn weakly held together by van der Waals forces (Smith, 1985).

The most commonly encountered B containing mineral in soils and sediments is the boron-silicate, tourmaline, which is very resistant to both chemical and physical weathering. Tourmaline would therefore not be expected to contribute significantly to labile-B forms in the soil solution (Gupta, 1979; Stubican and Roy, 1962). Other common B minerals are the Na-borates, kernite and borax, which

often occur together in evaporite deposits. Borax is mined extensively and has many commercial and industrial uses (Klein and Hurlbut, 1985).

Boron occurs in solution predominantly as boric acid ($B(OH)_3$), which is a Lewis acid rather than a Brönsted acid (Edwards and Ross, 1960). Boric acid in dilute aqueous solution (i.e., < 0.05 mol L^{-1}) hydrolyzes to form the metaboric or borate anion ($B(OH)_4^-$) at pH > 7 with the pK_a = 9.24 for the hydrolysis reaction. At BA concentrations greater than 0.05 mol L^{-1}, various polyborate species will form in addition to the monomeric species (Bassett, 1980). Ingri and coworkers (1957) performed acid/base titrations on borate solutions adjusted to 3.0 mol L^{-1} ionic strength with $NaClO_4$ and proposed the existence of several polyanionic B species, the most prevalent being a monovalent trimer. Confirmation of three of these species was provided by Maeda et al. (1979) and Maya (1976) using Raman spectroscopy. Observed frequencies were ascribed to the $B_5O_6(OH)_4^-$, $B_3O_3(OH)_4^-$, and $B_4O_5(OH)_4^{2-}$ polyborate species. Spessard (1970) explained his BA-metaborate titration data by assuming the presence of the three aforementioned polyborate species as well as an additional $B_3O_3(OH)_5^{2-}$ solution species. Formation constants were calculated for all proposed aqueous polymeric species and again the monovalent trimer was found to predominate. The potentiometric data of Mesmer et al. (1972) indicated the presence of a dimer, $B_2(OH)_7^-$, in addition to the previously mentioned species. Several authors (Momii and Nachtrieb, 1967; Salentine, 1983; Smith and Wiersema, 1972) have shown through ^{11}B-NMR

spectroscopy that the trimeric species is the most significant of the aqueous polyborates.

1.3 Boron in soils

Boron is partitioned in soils amongst four forms: B in the soil solution, B incorporated in silicate mineral structures, B associated with clay mineral and sesquioxide surfaces, and organically combined B.

Boron has a valence of 3^+ and can assume either tetrahedral or trigonal coordination with oxygen, allowing it to substitute for Al^{3+} or Si^{4+} in various minerals (Fleming, 1980). Stubican and Roy (1962) successfully synthesized B-muscovite, B-saponite, and B-phlogopite under laboratory conditions in the absence of Al^{3+}. The B^{3+} readily substituted for the Si^{4+} in the tetrahedral layers. The extent of substitution was greater in the micas than in the saponites.

Adsorbed B plays a pivotal role in controlling plant-available B in that the amount of B in solution is largely determined by the equilibrium between adsorbed-B and solution-B. Organically combined B, either as inanimate organic-B complexes or biotically incorporated B, can also exert a sizable influence on dissolved B concentrations as it is assimilated or released (Naftel, 1937; Parks and White, 1952).

A number of soil factors have been shown to influence the amount of B in the soil solution including: type of clay minerals present, various metal oxides

and hydroxides, humic materials, soil pH and liming, soil texture, cations present, anions present, wetting and drying cycles, and soil moisture content.

Several soil minerals have been demonstrated to adsorb B in varying amounts. Rhoades et al. (1970) studied B adsorption on two orthosilicate minerals, six chain silicates, seven framework silicates, and six layer silicates. The authors found that all minerals tested, with the exception of two of the framework silicates, adsorbed B to a measurable extent. The layer silicates tested were chlorite, phlogopite, talc, muscovite, vermiculite, and biotite with chlorite adsorbing the most B and vermiculite the least. Boron adsorption has been documented for kaolinite (Goldberg and Glaubig, 1986b; Hingston, 1964; Mattigod et al., 1985; Parks and White, 1952; Sims and Bingham, 1967), bentonite (Keren and Talpaz, 1984; Parks and Shaw, 1941; Parks and White, 1952), montmorillonite (Goldberg and Glaubig, 1986b; Keren and Gast, 1981; Keren et al., 1981; Keren and Talpaz, 1984), vermiculite and hydrobiotite (Sims and Bingham, 1967) and calcite (Goldberg and Forster, 1991). Fleet (1965), Harder (1961), Hingston (1964), and Keren and Mezumen (1981) compared B adsorption on illite, montmorillonite, and kaolinite. Illite was found to be the most reactive in all four studies; however, only Hingston (1964) found that montmorillonite was the least reactive.

Various metal oxides have been shown to be very effective in adsorbing B from the soil solution. In a comparison of Al-oxides with Fe-oxides, Sims and Bingham (1968a) found that Al-oxides removed nearly an order of magnitude more

B from solution than Fe-oxides on a weight basis. The authors also studied B adsorption on freshly precipitated Al- and Fe-oxides vs. the same oxides after aging. The more crystalline aged oxides adsorbed substantially less B than did the freshly precipitated oxides. These same results were later substantiated by Goldberg and Glaubig (1985) and McPhail et al. (1972). In their survey of six Al-oxides and five Fe-oxides, Goldberg and Glaubig (1985) found that all but two of the Al-oxides studied, gibbsite and α-alumina, adsorbed substantial quantities of B. Magnesium hydroxide has also been shown to adsorb quantities of B comparable to other sesquioxides by Rhoades and coworkers (1970). The authors found that arid zone soils can have appreciable adsorption of B in the sand and silt size fractions and that the sites of adsorption appear to be on Mg-hydroxy coatings on weathered surfaces of ferromagnesian minerals. The frequent occurrence of these various metal oxides as coatings on mineral surfaces results in a physicochemical influence far in excess of what their contribution to the total soil mass would suggest due to their highly reactive nature and great surface exposure (Hatcher et al., 1967; Sims and Bingham, 1968b). Oxides and oxide coatings may therefore be the most important components in controlling B availability when present in soils.

1.4 Boron in Fly Ash

Boron is frequently found as a major component of fly ash, a waste material generated by coal burning and smelting operations. The disposal of fly ash has an increasing concern in the United States and throughout the world, mainly

due to a shift toward heavier dependence on coal as a source of energy for generation of electricity. Fly ash is that portion of the products of coal combustion or smelting processes that enters the flue gas stream (Adriano et al., 1980). Coal-fired electricity generating facilities located in the United States currently remove >99% of the particulates from the flue gas stream before emission into the atmosphere. Several billion tons of coal ash residue are generated each year in the United States with up to 20% being utilized in the making of cements and as a soil stabilizer. The remainder is currently being stockpiled as excess waste (Chang et al., 1977).

Coal combustion residues consist primarily of amorphous iron and aluminum silicates, with smaller quantities of Ca, Mg, K, Na and sulfur oxides (Chang et al., 1977). The type of coal consumed in the combustion process affects the composition of the coal ash. Ash residues from coal deposits of the western United States tend to have higher B levels than those mined in midwest and eastern states (Adriano et al., 1980).

As an alternative to stockpiling coal combustion waste materials, fly ash appears to have some utility as an amendment for soils or greenhouse growth media. Its principal benefit is as a micronutrient source since it contains appreciable quantities of several micronutrients, including B. However, the excessive B content of fly ash is most frequently the limiting factor in determining the amount of fly ash that can be safely applied to a growth medium (Adriano et

al., 1980). Leaching of B from the fly ash prior to its use as an amendment can lessen the likelihood of B phytotoxicity. Pagenkopf and Connolly (1982) have shown that adsorption of B by Fe-, Al- and Si-oxides is the most important process controlling the release of B during leaching of fly ash deposits.

1.5 Boron in Organic Complexes

Several researchers have found that humic substances in soils are very influential in B adsorption. Evans (1983) found that, of several soil properties studied, including soil mineralogy, B adsorption was best correlated with organic matter content in sandy soils of the Mid-Atlantic Coastal Plain. Yermiyaho et al. (1988) found B adsorption was more extensive on composted organic matter than on clays when expressed on an equivalent weight basis. Parks and Shaw (1941) saw significant B adsorption on electrodialyzed samples of humic material. Parks and White (1952) tested B adsorption on humic materials extracted with two different reagents, Na-pyrophosphate and Na_2CO_3/$NaHCO_3$, and saturated with two different cations, H^+ and Ca^{2+}. Hydrogen ion saturated humus adsorbed approximately twice the amount of B adsorbed by Ca-saturated humus, while humus extracted with Na-pyrophosphate adsorbed 15 to 30 times more B than did humus extracted with Na_2CO_3/$NaHCO_3$. The authors offered no explanation for this phenomenon, although humic acids extracted with pyrophosphate usually contain Fe and Al as contaminants (Stevenson, 1982).

Boron reaction studies have been conducted with isolated organic compounds, some of which are known to be common products of decomposition in soils. One of the earliest attempts to characterize reactions between B and organic compounds was the exhaustive work of Boeseken (1949) in which BA was used to identify the structures of various cyclic and non-cyclic polyhydroxy species. Reaction of the various compounds with BA was indicated by increases in conductivity due to the production of protons following complexation. It was found that the non-cyclic diols without adjacent hydroxyls cannot form cyclic complexes with BA. It was also determined that simple 1,2-glycols have their hydroxyl groups positioned unfavorably due to their mutual repulsion and ability to rotate freely around the bond connecting the two carbon atoms. In compounds with more than two adjacent hydroxyls, however, the mutual repulsion no longer allows them to be oriented 180° apart. In fact, the favorableness of hydroxyl orientation will increase with increasing numbers of adjacent hydroxyls, enhancing their reactivity with BA.

In the case of aromatic polyols, the hydroxyls will be held in the plane of the benzene ring and the reaction of BA with the hydroxyls can only be expected in the case of o-dihydroxybenzenes and not for m- and p-dihydroxybenzenes. Alicyclic compounds with five-membered rings, having their carbon atoms situated approximately in one plane, are disposed to reaction with BA only when the hydroxyls are located in a cis- arrangement, the trans- configuration being unfavorable. Six-membered ring alicyclic compounds do not have their ring carbon

atoms in one plane but are oscillating continuously around a certain equilibrium position so that neither configuration is more favorable. Cis- isomers of o-hydroxy acids, with their hydroxyl and carboxyl groups fixed on the same side of the plane of the benzene ring, have a positive effect on the conductivity of BA solutions indicating B complex formation. However, trans- isomers have no effect.

Oertel (1972) obtained Raman spectra for BT reacted with 1,2-propanediol, 1,3-butanediol, and 1,2,3-propanetriol which revealed that B remained four-coordinate in the reaction products. No features attributable to three-coordinate B appeared. Through quantitative Raman intensity studies in the monoborate-1,2-ethanediol system, it was established that both 1:1 and 2:1 (diol:B) complexes exist in solution. Pasdeloup and Brisson (1981) studied aqueous BA-catechol solutions by means of ^{11}B, ^{1}H, and ^{13}C NMR over wide ranges of pH and concentration and the presence of 1:1 and 2:1 (catechol:B) complexes were indicated. In aqueous media at pH 11 where the borate ion should predominate, Yoshino et al. (1979) identified ^{11}B NMR signals for both the 1:1 and 2:1 catechol:B complexes. However, solutions of L-dopa and B exhibited only the signals for the 1:1 complex, despite their structural similarity. Van Duin et al. (1985), in a survey of 25 polyols and polyhydroxycarboxylates by ^{11}B NMR, found all but two formed mono- and di-esters with borate. The remaining two, all-cis-cyclohexane-1,2,5-triol and epi-inositol, formed only tri-esters with the borate anion. Association constants for all species were determined and empirical rules

for predicting the stability of the borate esters in aqueous solution were proposed. The order of stability suggested by the results was: tridentate > bidentate > monodentate. Makkee et al. (1985) studied borate ester formation with D-mannitol, D-glucitol, D-fructose, and D-glucose using both ^{11}B and ^{13}C NMR. At high B:carboxylate ratios, mono-, di-, and sometimes tri-borate esters are formed. The stability of the esters depends on the favorableness of location of hydroxyls on the polyols and the flexibility of the carbon backbone of the diol.

Pizer and Babcock (1977) studied the complexation reaction mechanism between BA and catechol and substituted catechols using temperature-jump relaxation kinetic measurements. The study was conducted at a pH of approximately 4 and at BA concentrations of 0.1 mol L^{-1} or less to eliminate polyborate formation. Relaxations detected in B-catechol solutions were not detected in this concentration range for BA solutions without catechol. Relaxation time analysis indicated an addition-substitution type reaction mechanism, viz., one ligand donor occupies a previously vacant site on BA and one displaces an OH^- at another site. Both ligand protons are displaced during the reaction as well. Titration results indicated the formation of only 1:1 complexes.

1.6 Soil Properties and Boron Availability

Of the many soil properties which affect B adsorption and soil fixation, pH has been the most widely studied (Bingham and Page, 1971; Goldberg and Forster, 1991; Goldberg and Glaubig, 1985; 1986b; Keren and Gast, 1981; Keren et

al., 1981; McPhail et al., 1972; Mezumen and Keren, 1981; Parks and Shaw, 1941; Sims and Bingham, 1967). In all cases, B adsorption increased with pH to a maximum between pH 8 and 9 and then decreased with increasing pH. This observation has been ascribed to differences in the B species adsorbed at a given pH, and to changes in the surface functional groups of the adsorbent (Hingston, 1964). The increase in B adsorption as pH increases below pH 8-9 may be in response to changes on the surface of the adsorbent favoring the formation of more adsorption sites. This is indicated by an increase in the maximum adsorption constant obtained from the Langmuir equation as pH is increased to pH 8-9. At pH<7, the neutral BA molecule is prevalent and may be the dominant adsorbed species, whereas, at pH≥7, the BT anion increases in concentration and may be adsorbed preferentially. At pH above 8-9, the decrease in B adsorption with increasing pH may be due to the increase in competitiveness of OH^- relative to the BT anion.

Soil texture, particle size and resultant surface area also control the extent of reaction of B with soil components (Elrashidi and O'Connor, 1982; Goldberg and Glaubig, 1986a; Hatcher and Bower, 1958; Hatcher et al., 1967; Mezumen and Keren, 1981; Singh, 1964). Couch and Grim (1968) found that surface area determined the amount of B adsorbed by three illitic minerals. On a per weight basis, all three adsorbed dissimilar amounts of B; however, when compared on a surface area basis, the illites adsorbed remarkably similar amounts.

Evans (1983) found the total amount of B sorbed was highly correlated to the amount of clay present in sandy Coastal Plain soils of the Mid-Atlantic region. Keren and Talpaz (1984) studied the effect of particle size on the adsorption behavior of B on Na- and Ca-montmorillonite at two pH ranges (7.4-7.7 and 8.6-8.9). The clay suspensions were divided into two identical parts and one part was treated with an ultrasonic disintegrator to reduce the particle size. Transmission electron micrographs (TEM) were obtained to substantiate reduction in particle size. This reduction in particle size should result in increases in surface area on the broken edges of the clay particles only. In both cation systems, smaller clay particles adsorbed more B than the untreated clay suspensions.

There is evidence to suggest that the exchangeable cations present also influence the extent of B adsorption. Hadas and Hagin (1972) compared B adsorption on two soils with and without K^+ saturation. In both cases, the K-saturated soils adsorbed more B than the untreated soils. Parks and White (1952) saturated fine clay fractions of Wyoming bentonite and kaolinite with H^+, Ca^{2+}, Mg^{2+}, K^+, and NH_4^+ to assess their effects on B adsorption. All clay fractions were subjected to both a wet and dry treatment. The wet treatment consisted of shaking the clay suspensions periodically over 48 h. The dry treatment consisted of drying the suspension at 50 °C after shaking the suspension for the same 48 h period as the wet treatment. The dried suspension residue was then rewetted with distilled water and allowed to rehydrate for 24 h after which the B in solution was

determined. No B was adsorbed by the H^+-saturated clays subjected to the wet treatment, while, except for the NH_4^+-saturated bentonite, the base saturated wet clays fixed large amounts of B. In the dried systems, however, the H^+-saturated bentonite fixed amounts similar to the bentonite saturated with the other cations. Without exception, the dried clay suspensions adsorbed more B than did the undried suspensions.

Sims and Bingham (1967) compared B adsorption on Na- and K-saturated vermiculite, kaolinite, hydrobiotite, and montmorillonite. Reduction of interlayer spacing in the K-saturated vermiculite, as evidenced by X-ray analysis, resulted in a decrease in B fixed. Little effect of cation saturation was seen in the non-expanding kaolinite. When sesquioxides were extracted from the expandable montmorillonite and hydrobiotite prior to B addition, cation saturation had little effect on B adsorption, suggesting that access to interlayer sesquioxide coatings was the overriding factor in B fixation. Keren and Talpaz (1984) found greater B adsorbed on Ca-montmorillonite than on the Na- form in the pH range of 7.4 to 8.9. This was attributed to the greater repulsion of BT anions by the negatively charged Na-montmorillonite surfaces. This would result from the greater exposure of permanently charged negative planar surfaces of the Na-montmorillonite due to its occurrence as single platelets. Less planar surface and permanent negative charge is exposed in the Ca-montmorillonite since it occurs as tactoids which consist of several clay platelets stacked together.

Adsorption of B is believed to be specific in nature, occurring by ligand exchange with surface hydroxyl groups on broken edges of clays irrespective of the sign of the net surface charge (Hingston et al., 1972). Nonetheless, greater repulsion of the borate anion should result as more negative surface charge is exposed, thus decreasing the amount of B adsorbed .

The effect of liming of soils on B adsorption can be directly attributed to exchangeable cations. Several early studies of plant response to B fertility and liming status concluded that plant injury resulted from B deficiency caused by overliming (Cook and Millar, 1939; Jones and Scarseth, 1944). Naftel (1937) suggested a relationship between liming and increased microbial activity which would result in the biological fixation of available B. This was later discounted by Midgley and Dunklee (1939) who tested B availability before and after sterilization of the soil. No difference in B availability was observed, indicating biological incorporation was not a factor. Parks and Shaw (1941) cited two reasons for the reduction in B availability, both the formation of insoluble precipitates of Ca with B as well as the effect of pH on B fixation by aluminosilicates. Goldberg and Forster (1991) have shown that B adsorption on calcite particles could at least partially explain this phenomenon. Mattigod et al. (1985) suggested B retention on kaolinite was enhanced in the presence of Ca^{2+} is due to the adsorption of the $CaB(OH)_4^+$ ion-pair.

Soils subjected to various wetting and drying cycles may fix greater amounts of B irreversibly. Biggar and Fireman (1960) showed that an increase in the Langmuir maximum adsorption capacity value, as well as in bonding energy between the soil and B, resulted from wetting and drying following the adsorption of B. Parks and White (1952) found that an increase in the number of drying cycles increased the amount of B fixed by kaolinite but that B fixed by bentonite actually decreased slightly after the fourth drying cycle. Keren and Gast (1981) demonstrated that drying of the soil prior to B adsorption had no effect on the amount adsorbed, yet drying of the soil after B adsorption significantly reduced the desorbability of B. Keren and Bingham (1985) suggested that formation and adsorption of polyborate species as moisture content decreases and B concentration in the soil solution increases could explain this phenomenon. These polyborates may have a greater affinity for the adsorption sites than BA. Mezumen and Keren (1981) contend that solution:soil ratios, as expressed by adsorption parameters such as maximum B adsorption (per unit mass of adsorbent) and affinity coefficients, do not affect the B/soil interaction, at least in the range of ratios tested by the authors (1:2 to 12:1). The increased B fixation with drying is apparently unrelated to the volume of solution per unit mass of soil.

Parks and Shaw (1941) explored the possibility that a precipitation mechanism could explain B removal from the soil solution. Aqueous solutions containing Ca^{2+}, Al^{3+}, and B produced large amounts of precipitate indicating

fixation is at least partially due to the inclusion of B in a Ca-Al complex. In aqueous solutions of Ca^{2+}, Si^{4+}, and B, Ca^{2+} had the effect of reducing B removal from solution at low pH but enhanced B removal at high pH. In aqueous solutions containing Ca^{2+}, Al^{3+}, Si^{4+}, and B, all the original B in solution was fixed in a hot-water insoluble form.

The ability of other anions to compete for B adsorption sites has been studied by various researchers. Goldberg and Glaubig (1988) studied simultaneous adsorption of silicon (Si) and B on alon, an aluminum oxide and found a slight but significant reduction in B adsorption when compared to B sorption in the absence of Si. This indicated that some sites could adsorb both Si and B. The possibility exists that adsorbed Si forms new adsorption sites with reduced affinity for B relative to those on the clean alumina. Silicon adsorption was not significantly affected by the presence of B. McPhail et al. (1972) found that silicic acid, when adsorbed to freshly precipitated Fe- and Al-oxides, substantially reduced subsequent B adsorption. Bingham and Page (1971) tested B adsorption on hydrous oxides of Fe and Al in the presence of SO_4^{2-}, PO_4^{3-}, and monosilicic acid. Neither SO_4^{2-} nor PO_4^{3-} had any bearing on the amount of B adsorbed while the monosilicic acid caused only a mild reduction in B adsorbed by the oxides, indicating a specificity of sites for B. The results of Bloesch et al. (1987) indicated that PO_4^{3-} decreased B adsorption on goethite in the range of pH 5.2 to 10.6, indicating competition for

surface sites. Sulfate effects on B adsorption were less than what was observed with PO_4^{3-} and B adsorption was reduced only below pH 7.

1.7 Mathematical Models for Boron Adsorption Reactions

Various models have been employed in describing the adsorption behavior of B in soils, the most frequently used being the Langmuir adsorption isotherm (Bingham et al., 1971; Elrashidi and O'Connor, 1982; Goldberg and Forster, 1991; Goldberg and Glaubig, 1986a; Hingston, 1964; McPhail et al., 1972; Rhoades et al., 1970; Singh, 1964).

The Langmuir model was developed from studies of gas adsorption on solid surfaces. Many of the assumptions inherent in its development therefore do not apply to the adsorption of ions at the solid/liquid interface. One of these assumptions in particular, that the energy of interaction between the adsorptive and adsorbent is constant over the entire range of surface coverage, is certainly not applicable to specific adsorption of ions on variable-charged mineral surfaces. The electrostatic interaction between the adsorptive and the surface of the adsorbent changes as the charge on the colloidal surface is altered by the adsorption process.

Several of the aforementioned studies used the Langmuir model to infer mechanisms of B adsorption (Biggar and Fireman, 1960; Hadas and Hagin, 1972; Hatcher and Bower, 1958; Hingston, 1964; Okazaki and Chao, 1968). Deviations from linearity of isotherm plots at higher equilibrium B concentrations were interpreted as indicative of more than one type of reaction or site of reaction. The

possibility of concurrent B precipitation and adsorption was also suggested in light of the work of Parks and Shaw (1941) (Biggar and Fireman, 1960). However, adsorption isotherm data applied to the Langmuir model should not be used to infer reaction mechanisms (White and Zelazny, 1986), particularly for specific adsorption reactions of ionic species on charged surfaces.

The Freundlich equation has been widely used to describe B adsorption behavior (Elrashidi and O'Connor, 1982; Goldberg and Forster, 1991; Goldberg and Glaubig, 1986a). Both the Langmuir and Freundlich equations adequately described B adsorption on calcareous soils and reference calcites (0.1 to 23 mol m^{-3} initial B) from pH 5.5-12.0 (Goldberg and Forster, 1991). Elrashidi and O'Connor (1982) found deviations from linearity at high B concentrations in the Langmuir treatment of their B adsorption data for 10 soils from New Mexico. The Freundlich equation, however, successfully described the B adsorption data over the entire concentration range tested (0-9 mol m^{-3} initial B). Two mechanisms of B adsorption, reversible and hysteretic, were inferred from the adsorption/desorption data. However, the Freundlich equation suffers from many of the same deficiencies as the Langmuir model in its applicability to soil systems as well as in its ability to convey mechanistic information. Furthermore, since the parameters describing maximum B adsorption and strength of binding change with pH and equilibrium B concentration, both models are incapable of describing B adsorption under changing conditions of soil acidity and B activity.

Singh (1964) found that problems encountered when using the Langmuir model to describe B adsorption at high B concentrations could be avoided by using the BET equation, a model which was also originally developed to describe adsorption of gases onto solid surfaces. Multilayer coverage is assumed in the development of the model (Hair, 1967). When the entire range of equilibrium B concentrations was considered, the B adsorption data could be closely described by the resultant quadratic curve. Singh (1964) apparently did not test the ability of the BET equation to describe B adsorption under conditions of varying pH.

The use of a phenomenological equation developed by Keren and coworkers was successful in predicting B adsorption behavior over a wide range of soil acidity and solution B levels (Keren et al., 1981; Mezumen and Keren, 1981). It also allows for the possibility that two solution species, BA and BT, having different affinities for the solid surface, are competing for the same surface sites and that their relative concentrations vary with pH. The equation offers the same benefits as the Langmuir and Freundlich equations in that it includes parameters indicating maximum B adsorption and affinity of the various adsorptive species for the adsorbent. An affinity coefficient accounting for the competition of solution OH^- for surface sites is also included. The equation offers an added advantage in that it is able to relate total adsorbed B to total B present in the suspension. It can also be rearranged to describe B adsorption under conditions of varying solution-to-solid ratios.

In their study of B adsorption on kaolinite, montmorillonite, and illite, Keren and Mezumen (1981) concluded that the water content of the clay suspensions did not affect the B/surface interaction. This was indicated by the invariability of the adsorptive affinity coefficients with changes in solution-to-solid ratios. Keren and Talpaz (1984) found insignificant variation in affinity coefficients with changes in particle size, indicating the equation could accurately predict B adsorption with changes in texture. Boron adsorption maxima for the montmorillonite and illite were very similar despite the much greater surface area measured for the montmorillonite. The two minerals have similar edge surface areas exposed, however, indicating that edges of the minerals may be significant in B adsorption. Increases in both ionic strength and pH did not decrease the B adsorption maxima, although both would bring about increases in negative charge on the amphoteric edge surfaces, increasing repulsion of the BT anion. Ligand exchange would thus appear to be an important B adsorption mechanism.

The constant capacitance model, developed by Stumm and coworkers, (1980) has been used with some success to model B/surface interactions (Goldberg and Glaubig, 1988). This model of the solid/liquid interface in aqueous suspensions explicitly defines surface adsorbed species and addresses the effect of pH on adsorption. The model is based on the premise that all surface complexes, including those with protons and hydroxyls, are of the ligand exchange variety and are situated in the same plane of adsorption. The possibility of surface complexes

with ions of the background electrolyte is not considered. A linear relationship between surface charge and electrical potential at the plane of adsorption is assumed. A computer program (e.g., the FITEQL program (Westall, 1982)) is used to fit intrinsic surface complexation constants to the experimental data.

The constant capacitance model was successful in describing B adsorption behavior on several Fe- and Al-oxides throughout the pH range of 4 to 11 by adjusting only one parameter, the B surface complexation constant (Goldberg and Glaubig, 1985). These same authors used the constant capacitance model to simulate B adsorption on 15 arid-zone soils (Goldberg and Glaubig, 1986a). The model described B adsorption on the majority of the soils within the pH range 5.5 to 11.5, using a set of surface complexation constants averaged over all 15 soils. In each application of the model to B adsorption, the authors assumed that BA is the only B solution species adsorbed and only neutral OH sites participate in the ligand exchange, with water the leaving ligand. Since this reaction mechanism involves no charged species, surface charge has no effect on the adsorption process. Because the model does not consider adsorption of the background electrolyte, the B adsorption constant is only valid for a given ionic strength.

The triple layer model (Hayes and Leckie, 1987) has also been used to model B adsorption behavior. Singh and Mattigod (1992) used this model to describe B adsorption on kaolinite in the pH range of 6.0 to 10.5 at constant ionic strength (0.01 mol L^{-1}), with either $Ca(ClO_4)_2$ or $KClO_4$ as the background

electrolyte. In the Ca^{2+} system, B was assumed to adsorb as BA or BT, as well as Ca^{2+}-B ion-pairs. An intrinsic equilibrium constant, valid over a range of background electrolyte concentrations, is the primary advantage of the triple layer model over the constant capacitance model. This version of the triple layer model (Hayes and Leckie, 1988) assumes that the adsorptive may form both inner- and outer-sphere coordination complexes with the surface, a more realistic assumption considering that the specifically adsorbed ion is also a component of the electric double layer (EDL). An inner-sphere complex results from adsorption at the surface by ligand exchange. An outer-sphere complex is an ion-pair type complex between the surface and the adsorbate, with the adsorbate retaining its water of hydration. The authors assumed that adsorbed B could form any of six surface species in the presence of Ca^{2+}: adsorbed BA, monodentate adsorbed BT, bidentate adsorbed BT, adsorbed Ca^{2+}-BA ion-pair, adsorbed Ca^{2+}-BT ion-pair, and bidentate adsorbed Ca^{2+}-BT ion-pair. The FITEQL program was used to simultaneously optimize these six equilibrium constants.

Bloesch et al. (1987) were successful in modeling B adsorption on goethite using the model of Bowden et al. (1980). This model is similar to the constant capacitance model and the triple layer model in that it is an adaptation of the Stern EDL model. Like the triple layer model, three planes of adsorption are considered; however, the plane of specific adsorption of B is at some small distance from the surface, where OH^- and H^+ are adsorbed. The authors assumed that B

could adsorb as one of four solution B species including: BT, $B_3O_3(OH)_4^-$, $B_4O_5(OH)_4^{2-}$, and $B_5O_6(OH)_4^-$, but was adsorbed predominantly as BT. The adsorption of BA was not considered.

1.8 Kinetics of Boron Adsorption/Desorption

At this time, the kinetics of B reactions in soils have not been extensively studied. Most of the kinetic information currently available pertains to B desorption and release. What is particularly lacking is kinetic information pertaining to B reactions with Fe- and Al-oxide materials, which are often the soil components most reactive with B.

The few kinetic studies reporting the rates associated with B adsorption phenomena that have appeared in the literature have utilized methods which measure relatively slow processes. It is likely that the reaction step, whereby the B solution species bonds to a surface site of a soil colloid, is far too rapid to be monitored by the techniques thus far employed. Surface complexation reactions involving ligand exchange are typically very rapid, with reaction times of a few seconds or less.

The rates of B desorption from four California desert soils with high native B levels were studied using a batch technique with a large excess of mannitol in the desorptive solution to create pseudo-first order conditions (Griffin and Burau, 1974). It was assumed that diffusion was not rate-limiting since the reaction vessels were shaken continuously throughout the experiments. For each

soil, pseudo first-order treatment of the data yielded three distinct linear regions which were interpreted as evidence of three separate B-desorption reactions. The rates of B dissolution from borax and BA were also measured and found to be much faster than the rates measured for B release from the four soils. The authors proposed that the two fastest B release rates were due to desorption from surfaces of soil hydroxy compounds. Two of the observed rates were ascribed to desorption from similar surface sites with two different crystal field exposures. The third slowest rate was attributed to diffusion of B from tetrahedral positions in the crystal lattice of clay minerals. However, no sample agitation rates were reported, nor surface area determinations made before and after the desorption measurements, and it is not known what effect, if any, particle abrasion may have had on B release.

Peryea et al. (1985a) measured the rates of B release from four cultivated soils from California which contained B at phytotoxic levels. Their objective was to compile information which could be used to assess the potential for re-elevation of B levels in the soil solution following reclamation of B toxic soils by leaching. A batch technique, using a B specific exchange resin as a sink for desorbed B, was employed in the kinetic study. In all cases, the B desorption data were accurately described using an integrated form of the Elovich equation. The Elovichian treatment of the data proved useful in predicting the rate of B release to the soil solution for a given soil and degree of reclamation. However, the physical significance of this equation has not been well established and may be

essentially no more than a mathematical manipulation of kinetic data (Hingston, 1981).

Use of the Elovich equation to describe one unique mechanism may not be appropriate since it can be used to describe several unrelated processes (Sparks, 1986). The applicability of the Elovich equation to kinetic data may in fact be indicative of a diffusion process (Aharoni and Sparks, 1991). Therefore, no mechanistic inferences regarding B desorption can be made from the study of Peryea et al. (1985a).

To determine whether B regeneration in the soil solution is due to dissolution and desorption or to B release from soil pores occluded from the leachate, Peryea et al. (1985b) compared B and Cl^- release under both batch and column flow conditions. Chloride was assumed to be physically retained and therefore any Cl^- release after reclamation would be due to release from occluded pores. Essentially no Cl^- was recovered from the soils tested after one 48 h batch extraction period whereas B was recovered continuously throughout 10 batch extraction periods. Furthermore, following a 30 d regeneration period subsequent to the 10 batch extractions, an increase in extracted B was found, yet still no Cl^- was detected in the supernatant. In the column study, no Cl^- was detected in the leachate following four pore volume displacements (PVD); however, B remained detectable after 40 PVD. The columns were allowed a 30 d regeneration period following the 40 PVD. Similar amounts of B and Cl^- were found in the first PVD

of leachate following regeneration. The Cl^- was reduced to nondetectable levels with one additional PVD in contrast to the continued detection of B after an additional 6 PVD. In light of both the batch and column results, it appears that a dissolution and/or desorption process as well as diffusion from occluded pores contribute to soil solution B regeneration in previously reclaimed soils. The methodology chosen by the authors fails to distinguish between a dissolution and a desorption process, however, and the most fundamental questions regarding B desorption and regeneration remain unanswered.

The kinetics of B retention in a heavy textured soil and on Fithian illite, both adjusted to pH 7.8 by addition of $CaCO_3$, were investigated by equilibration with BA solutions over periods of up to 6 months (Evans, 1988). At fixed time intervals, pH and B remaining in the supernatant were determined. An initial fast reaction followed by a subsequent slow reaction was observed. Both reactions were adequately described by pseudo-first-order equations. The pH increased over the length of the equilibration period, suggesting a ligand exchange of B solution species for surface hydroxyls was taking place. The change in pH alone could not account for the total amount of B lost from solution, however. Evans (1988) therefore suggested that the slower reaction rate may be ascribed to diffusion of B into the tetrahedral sheet of the clay mica structure. Closer examination of the data would seem to indicate that ligand exchange continues into the slow phase of the B removal process. The data indicate an increase in pH in the supernatant beyond the

initial rapid phase of the experiments. The possibility of the formation of an insoluble B mineral phase is also indicated since the soil solutions were supersaturated with respect to the Ca-borate mineral, nobleite. Goldberg and Forster (1991) have shown that B is adsorbed to $CaCO_3$ particles as well. The fact that no definitive reaction mechanisms were established from these experiments is perhaps a consequence of the batch method chosen for this kinetic study.

Evans (1983) used a variety of kinetic equations to describe B adsorption and desorption from several sandy soils of the Mid-Atlantic Coastal Plain. The Elovich equation, the parabolic diffusion law, as well as zero-order, first-order, and second-order equations were evaluated. Boron reaction rates in the soils with the greatest sand content were too rapid to be measured using a miscible displacement technique. In the remainder of the soils, B adsorption and desorption kinetics were described by the Elovich equation. The absence of discontinuities in the Elovich plots for all of the soils suggested that only one type of reaction occurred for both adsorption and desorption (Hingston, 1981). The data for these soils also conformed to the parabolic diffusion law indicating that the rates of B adsorption and desorption were diffusion controlled (Boyd et al., 1947). Very little variation in diffusion rate parameters was found among the various soils for the forward and reverse processes. This finding indicated that adsorption and desorption rates may be controlled by the same mechanisms in all the soils tested. Boron adsorption conformed to first-order kinetics for all of the soils. Boron

desorption for the majority of the soils also conformed to first-order kinetics. Desorption for three of the soils did not conform to either zero-, first-, or second-order kinetics. Attempts to establish a fractional rate law were unsuccessful.

Sharma et al. (1989) studied the rates of B desorption from four salt-affected soils from India using a batch technique with mannitol as a sink for desorbed B. Boron desorption kinetics conformed well to the power-function, the pseudo first-order, and Elovich equations but not to the parabolic diffusion equation.

The rates and mechanisms of B adsorption reactions with oxide soil components are still largely unknown. The fact that several different kinetic models will fit a given set of adsorption data (Evans, 1983; Sharma et al., 1989) indicates that the kinetic measurements thus far obtained do not pertain to the chemical kinetics of B adsorption and desorption. Knowledge of B chemical kinetics and the exact nature of B adsorption mechanisms is essential to accurately predict the ultimate fate and availability of soil B.

1.9 Spectroscopic Investigations of Boron

Much spectroscopic information has been accumulated from ^{10}B- and ^{11}B-nuclear magnetic resonance (NMR) spectroscopy pertaining to B speciation and polymerization in solution (Momii and Nachtrieb, 1967; Smith and Wiersema, 1972; Epperlein et al., 1975; Janda and Heller, 1979; Salentine, 1983; Balz et al., 1986). Boron solution species have also been studied using Raman spectroscopy

(Maya, 1976; Maeda et al., 1979; Oertel, 1972). The polymeric aqueous B species proposed by Ingri (1962) have been confirmed as a result of these NMR and Raman studies of B solutions.

The bonding and stereochemistry of B complexation reactions with OH functional groups of organic compounds have also been well characterized using NMR spectroscopy (Yoshino et al., 1979; Pasdeloup and Brisson, 1981; Makee et al., 1985; Van Duin et al., 1985).

Edwards et al. (1955) provided direct evidence through Raman spectroscopy of the Lewis acid/base relationship of trigonal BA and its hydrolysis product, tetrahedral BT. Edwards and Ross (1960) surveyed several X-ray and NMR studies of borate minerals and formulated a set of postulates governing the structures of hydrated polyborates. They contend that the fundamental unit of polyanionic B species is a trimeric ring containing both trigonal and tetrahedral B atoms.

Infrared spectroscopic studies of adsorbed B species, in most cases, have relied on precipitation of the solid adsorbent in the presence of B rather than adsorption of B on previously precipitated and stabilized minerals (Beyrouty et al., 1984; Stubican and Roy, 1962). Infrared spectra obtained from these studies are therefore subject to interpretation regarding the association of the B with the surface. Although these authors assumed that B was in the adsorbed state, under these experimental conditions B may be adsorbed and/or co-precipitated with the

mineral adsorbent. Volkhin and coworkers (1983) obtained IR spectra of B adsorbed on stabilized $Ni(OH)_2$ surfaces which indicated that $B(OH)_3$ and $B_4O_7^{2-}$, from BA and $Na_2B_4O_7$ solutions, respectively, were adsorbed via ligand exchange and hydrogen bonds.

Direct spectroscopic examination of adsorbed B species on the surfaces of oxide soil components, obtained from mineral phases precipitated prior to the adsorption step, would advance considerably our understanding of B fixation reactions in soils.

1.10 Objectives

One of the most important objectives in choosing a suitable method for measurement of reaction rates in aqueous colloidal systems is the elimination of diffusion as the overall rate-limiting step in the reaction (Ogwada and Sparks, 1986). This is an absolute requirement if the rates of actual chemical exchange or reaction are to be measured, allowing one to determine the mechanism of the reaction (Sparks, 1986). In the past, the experimental techniques traditionally employed in kinetic studies of B soil reactions, such as batch techniques (Evans, 1988; Griffin and Burau, 1974; Peryea et al., 1985a; Sharma et al., 1989) and miscible displacement techniques (Evans, 1983; Peryea et al., 1985b) sought to minimize transport influences; yet, it is unlikely that transport effects were completely eliminated. Agitation in batch experiments, and flowing and stirring in miscible displacement experiments, are used for this purpose. These agitation

techniques also may have some undesirable side effects such as particle abrasion and may require unrealistic soil-to-solution ratios (Sparks, 1989). In addition, these methods are severely limited in their ability to monitor very fast reactions, those which may reach completion in a minute or less. Because of these experimental deficiencies, the rates and mechanisms of B adsorption reactions with sesquioxides have not been determined.

Boron sesquioxide surface complexes have not been analyzed spectroscopically under natural temperature and moisture conditions. Boron containing minerals synthesized by co-precipitation of B have been used to infer the nature of the adsorbed-B surface complex (Stubican and Roy, 1962; Beyrouty et al., 1984).

The objectives of this study are to measure the rates of B adsorption and desorption reactions on an aluminum oxide using the pressure-jump chemical relaxation technique. Chemical relaxation techniques are capable of measuring reaction kinetics on millisecond time scales, while eliminating liquid transport effects in the overall reaction process (Sparks, 1989). The chemical kinetics will thus be measured with this technique, allowing the chemical reaction mechanisms of B adsorption and desorption to be determined. Additionally, horizontal attenuated total reflectance Fourier transform infrared (HATR-FTIR) spectra of adsorbed B in aqueous aluminum oxide suspensions will be obtained as an independent determination of B surface complexation mechanisms. Attenuated total

reflectance FTIR spectra can provide an in-situ analysis of adsorbed B in colloidal oxide suspensions (Zeltner et al., 1986). The results from these studies should greatly enhance our predictive capabilities regarding B adsorption and release in soils containing sesquioxide materials.

Chapter 2

PRESSURE-JUMP RELAXATION ANALYSIS OF BORON ADSORPTION/DESORPTION REACTIONS

2.1 Introduction

2.1.1 Chemical Relaxation Kinetics

Chemical relaxation kinetics refers to the measurement of the equilibration rates of a chemical system following inducement of chemical disequilibrium by an external perturbation. Any chemical system at equilibrium, when perturbed chemically or physically, will respond to that perturbation by relaxing to a new equilibrium state. The process whereby the chemical system establishes a new equilibrium position in response to the perturbation can be monitored as a function of time to yield the fundamental forward and reverse rate parameters governing the dynamic equilibrium.

The dynamic equilibrium of any chemical system is determined by its physical and chemical variables of state (Eisenberg and Crothers, 1979). The chemical parameters which control the equilibrium positioning of a reaction include

the reactant and product concentrations, the activity of other reactant species providing alternate reaction pathways, if present, and in the case of reactions in solution or suspension, the nature of the solvent and ionic strength. The physical parameters which determine the equilibrium positioning include the pressure, temperature, and in the case of charged, ionic, or dipolar reactant species, the electric field.

Several advantages are gained in selecting a relaxation technique over other kinetic techniques. Many reaction rates, particularly those of reactions involving soil constituents, are too rapid to measure by batch techniques or flow techniques, the kinetic methods most commonly used to measure reaction rates in aqueous systems (Sparks and Zhang, 1991). Although several chemical relaxation techniques are quite suitable for measuring slow reaction rates, their greatest advantage lies in their ability to measure the rates of extremely rapid reactions. Virtually all of the currently accepted chemical relaxation techniques are capable of measuring reaction rates which attain equilibrium in less than a second (Sparks, 1989).

Chemical reactions involving soil solution species, such as ion exchange or adsorption, generally comprise both diffusion and actual chemical reaction processes. In the past, most kinetic studies of soil chemical reactions have used batch and/or flow reactor techniques. In the majority of cases, these kinetic apparatus have measured the rates of diffusion which precede or follow the actual

chemical reactions (Sparks, 1989). Depending on the nature of the adsorbent and the type of reaction, one of several diffusion events may control the overall rate of reaction. These may include: diffusion of the adsorptive or desorbed species through the static hydrodynamic film surrounding the adsorbent particle and diffusion through the hydrated interlayers of layered adsorbent particles (Sparks, 1986). The slowest of these sequential diffusion and reaction processes will be the rate-determining step for the overall reaction. Typically one of the diffusion steps will be rate-determining.

Often the investigator's primary impetus for obtaining kinetic information is to determine the mechanisms of a reaction. Under such circumstances, it is essential that the kinetic method chosen yield rate parameters which pertain to the chemical reaction alone and not accompanying transport phenomena (Sparks, 1989). Since relaxation experiments are conducted in a premixed system, diffusion processes, as well as the time required for mixing, can be circumvented and the reaction rates that are measured pertain to the chemical reaction itself (Eisenberg and Crothers, 1979).

Batch and flow techniques require separate experiments to measure the rates of both forward and reverse reaction processes, such as the adsorption and desorption of a particular adsorptive. Relaxation experiments yield the kinetic parameters associated with both the forward and reverse processes from a single set of experimental results.

Relaxation methods require that only small perturbations be applied, i.e., in moving from the perturbed to the relaxed equilibrium state, the change in concentration of the reactants must be insignificant relative to the initial and final concentrations. With a small change in reactant concentrations, all higher order terms in the rate expression become negligible and the rate equations are reduced to linear relationships (Bernasconi, 1976). This aspect greatly facilitates the kinetic analysis of complex chemical reaction schemes. For pressure changes on the order of 10 MPa or less, molar volume changes in aqueous solutions are sufficiently small to ensure that only small perturbations will result (Takahashi and Alberty, 1969).

Relaxation techniques are capable of revealing the nature of intermediate steps in multi-step reaction processes, as well as alternate reaction pathways (Eisenberg and Crothers, 1979). This is only true, however, when the difference in the relaxation times associated with the individual steps are of such magnitude that their relaxation spectra can be differentiated from one another. Two relaxation times can be distinguished from one another if the slower of the two times is at least twice the faster (Knoche and Strehlow, 1979).

2.1.2 The Pressure-jump Technique

Of the several relaxation techniques available, the pressure-jump (P-jump) technique is perhaps the one best suited for adsorption reactions involving

ionic adsorptives in colloidal suspensions. This technique relies on a sudden change in pressure to perturb a chemical equilibrium.

The pressure (P) dependence of an equilibrium constant (K) derives from the thermodynamic relationship

$$\left(\frac{\partial \ln K}{\partial p}\right)_T = -\frac{\Delta V}{RT} \tag{2.1}$$

where ΔV is the standard molar volume change of the reaction (L), R is the universal gas constant (8.3144 J K^{-1} mol^{-1}), and T is the absolute temperature (K). The magnitude of the pressure dependence of K is thus largely dependent on ΔV. For reactions in solution, ΔV is most pronounced when a concentration change of ionic species results; whereas, the ΔV for a reaction involving only nonionic solution species may be so small as to yield an immeasurable relaxation effect. The large molar volume change associated with changes in ionic makeup of solutions results from electrostriction effects on the solvent structure (Takahashi and Alberty, 1969).

Several detection methods are acceptable for measuring reactant concentration changes following a P-jump, including conductometry, spectrophotometry, fluorimetry, and polarimetry. The principal detector requirement is that the time interval for reactant concentration measurement be substantially shorter than the time required for equilibration, such that the exponential decay of the equilibrium imbalance can be sampled repeatedly.

Colorimetric measurements can be used but are generally less useful since the time for formation of the color producing species is often too slow to allow sufficiently rapid sampling. Since the P-jump method is best suited for reactions of ionic species in solution, conductivity detection provides a sensitive monitoring tool and is most often utilized.

2.1.3 Pressure-jump Studies in Colloidal Systems

Pressure-jump reaction rate measurements in colloidal suspensions are subject to other experimental constraints in addition to those of solutions. The integral task of a P-jump experiment entails evaluating the variation in the relaxation time as equilibrium reactant concentrations are varied. The relaxation time (τ) is defined as the time required for the difference between the initial and final equilibrium reactant concentrations to decrease to a value e^{-1} of its initial value, where e is the base of the natural logarithm.

In compiling the data necessary to complete a P-jump study, several relaxations must be recorded for each sample, since the precision in calculated relaxation times is greatly enhanced by signal-averaging. Signal-averaging increases signal-to-noise ratios of relaxation amplitude measurements by a factor of $N^{0.5}$, where N is the number of superimposed relaxations (Krizan and Strehlow, 1974). Therefore, the maintenance of a stable suspension throughout the data collection period is of critical importance to the success of the experiments. As colloidal particles settle in an unstable suspension, the active concentration of one

or more of the reactants in an adsorption process (i.e., the adsorption sites) will vary. Since the relaxation time is dependent on the reactant concentrations, this will result in an uncontrolled variation in the relaxation time measured.

In a typical P-jump study, even for reactions which equilibrate in less than a second, several minutes are required between repeat measurements. Turn around time is largely determined by the time required for transfer of digitized data to a computer, visual inspection of the relaxation spectrum on an oscilloscope or computer screen, and adjustment of the Wheatstone bridge for the next measurement. Signal-averaging of several relaxations thus requires that suspensions remain stable for an hour or more, depending on the actual time of equilibration following the pressure drop. Studies of slower reactions which require longer periods of time to relax to a new equilibrium after perturbation will of course require longer time intervals between repeat measurements.

For P-jump studies of colloidal suspensions in aqueous electrolytes, care must be taken to maintain a constant ionic strength, as the activities of the reactants in solution, as well as the electrical potential at the colloid's surface, will vary with ionic strength. However, the use of a swamping electrolyte, which is a commonly used device for controlling ionic strength, is not practical when relying on conductivity detection. Because conductance measurements are nonspecific regarding the conducting species in multi-electrolyte solutions, small changes in reactant concentrations relative to large indifferent electrolyte concentrations will

not be accurately measured (Hoffmann et al., 1964). Ionic strength must therefore be sufficiently low to maintain detector sensitivity.

Since suspension stability decreases with increasing ionic strength, a constant ionic strength below which flocculation is induced must be maintained throughout the relaxation study. For the case of ionic reactants, ionic strength can be no lower than that dictated by the highest reactant concentration for which a relaxation time is to be obtained. Additionally, for any detection method chosen for monitoring the relaxation, there is a minimum quantity of reactant for which an accurate concentration measurement is feasible.

For certain solution species, high reactant concentrations may lead to side reactions such as polymerization and precipitation which may be misinterpreted as adsorption reactions. The maximum adsorptive concentration should not exceed the level where these side effects become appreciable.

In order to linearize the rate expressions for a given reaction mechanism, the reactant concentration changes following a perturbation must be small relative to the absolute reactant concentrations (Bernasconi, 1976). Thus, in order for the perturbation to be detectable yet yield a small concentration change relative to the absolute concentration, a certain minimum of reactant must be present in solution. The extent of perturbation can be adjusted to some extent, however, by altering the magnitude of the forcing function (e.g., the pressure drop).

It becomes apparent that some considerations require that ionic reactant concentrations and ionic strength be low, whereas others dictate higher concentrations. Finding the range of experimental conditions where all these requirements are satisfied can be arduous. Many relaxation studies of colloidal suspensions, which at first appear feasible, may prove impracticable due to an inability to maintain a stable suspension for a period of time sufficient for accurate relaxation time measurement. Thus, prior to recording relaxation curves for calculation of relaxation times, it is essential that various combinations of colloid particle concentrations, reactant solution concentrations, and background electrolyte concentrations be tested so that an optimal range of experimental conditions can be chosen.

2.1.4 Pressure-jump Apparatus with Conductivity Detection

A schematic of a typical P-jump apparatus, such as that devised by Knoche and Weise (1974), is depicted in Fig. 2.1. The apparatus consists of a mechanical pressure inducing device, the P-jump autoclave, and various electronic devices to detect and record the reactant concentration changes during the equilibration process following a rapid pressure change.

The P-jump autoclave is a brass chamber with two removable cells mounted diametrically on its sides, each capable of holding approximately 1 mL of solution or suspension. Both cells, one containing the sample and the other containing a reference, have internally mounted electrodes which provide a

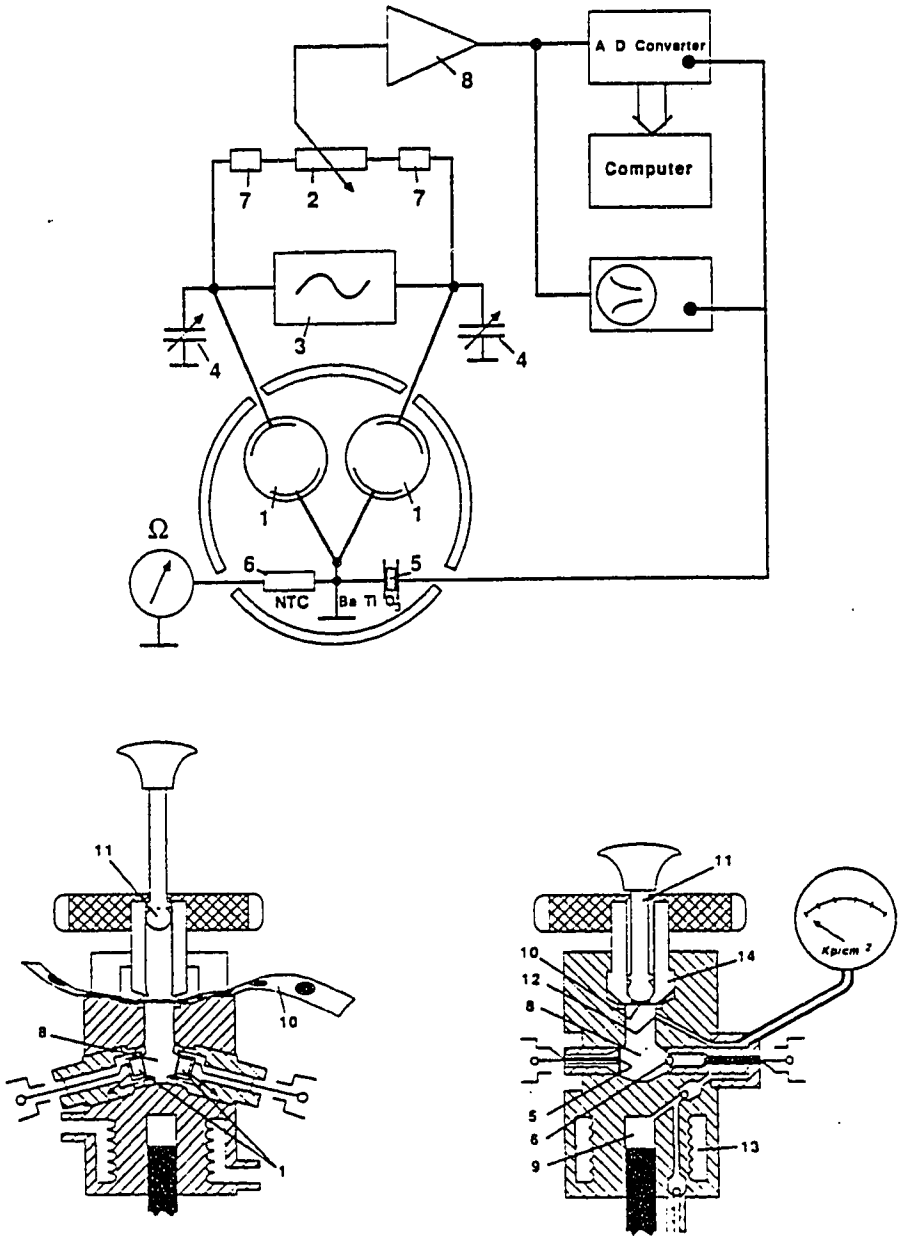

Figure 2.1 Schematic diagram and sectional views of the pressure-jump apparatus: 1, conductivity cells; 2, potentiometer; 3, 40-KHz generator; 4, tunable capacitors; 5, piezo-electric capacitor; 6, thermistor; 7, 10-turn helipot; 8, experimental chamber; 9, pressure pump; 10, rupture diaphragm; 11, vacuum pump; 12, pressure inlet; 13, heat exchanger; 14, bayonet socket. Reprinted from Chem. Instrum., p. 91-98 by courtesy of Marcel Dekker Inc.

measurement of the electrical conductivity of the cell contents. The reference cell functions to compensate for non-chemical side effects on the measurement of reactant concentrations as a result of the P-jump. For conductivity detection, the reference cell contains an electrolyte solution of similar conductivity and ionic mobility to that of the sample. The suspension supernatant is often the best reference solution since it should be nearly identical in chemical makeup to the conducting medium of the sample.

Temperature fluctuations in the autoclave, due to heat exchange with the surroundings, are prevented by circulating water maintained at a constant temperature through a water jacket built into the autoclave walls. An internally mounted thermistor provides a continuous reading of the temperature inside the autoclave.

Following the sudden pressure drop, the contents of both the sample and the reference cell experience the same change in solution volume. Therefore, the physical effects on sample conductivity during the relaxation are nullified. The cumulative effect of the relaxation on the electrical conductivity of the sample ($\Delta\sigma$, Ω^{-1} cm^{-1}) can be represented mathematically by

$$\Delta\sigma = F/1000[\rho \sum |z_j| \mu_j \Delta m_j + \rho \sum |z_j| m_j \Delta \mu_j + \sum |z_j| m_j \mu_j \Delta \rho] \qquad (2.2)$$

where F is the Faraday constant, ρ is the density of the solution, z_j is the valence of ion j, μ_j is the mobility of ion j (cm^2 V^{-1} s^{-1}), and m_j is the molal concentration of

ion j (Eigen and DeMaeyer, 1963). The physical effects brought about by the volume change which might otherwise contribute to the relaxation effect are changes in density ($\Delta\rho$) and ionic mobility ($\Delta\mu_j$). Because the pressure drop results in an adiabatic expansion of the solutions, a small simultaneous temperature drop also occurs (< 0.1 °C) (Takahashi and Alberty, 1969). This temperature jump is also nullified by the reference cell, leaving a relaxation due only to the chemical changes (Δm_j) resulting from the pressure-induced perturbation. The temperature equilibration time in the sample and reference cells following the adiabatic pressure drop is approximately 10 s (Krizan and Strehlow, 1974).

Both the sample and reference cells are sealed with a flexible plastic membrane which allows the pressure to be transmitted to the contents of both cells. Pressure is increased by pumping water into the autoclave which has been sealed with a thin strip of brass foil. When the pressure in the chamber exceeds that which the brass foil can withstand, the foil bursts, rapidly releasing the pressure. The foil is milled to an exact thickness which provides a reproducible bursting pressure in the autoclave for each repetition of the relaxation time measurement. The time required for the pressure in the autoclave to return to ambient conditions is approximately 60 μs (Knoche, 1974). Since the pressure drop must be instantaneous on the time scale of the relaxation to be measured, this represents the lower time scale limit for reactions that can be studied with this apparatus.

The electronic components of the P-jump apparatus comprise a Wheatstone bridge, an analog-to-digital (AD) converter, a computer, and oscilloscope. The two conductivity cells in the autoclave are connected to the Wheatstone bridge. The total resistances of the sample and reference cells, including their electrical connections and conducting contents, represent two of the four arms of the Wheatstone bridge. The total resistance of the reference cell arm of the bridge is adjustable by means of a potentiometer, which allows the reference cell resistance and the sample cell resistance to be balanced artificially. As pressure is increased in the autoclave, the equilibrium of the chemical system in the sample cell is altered, resulting in a change in the ionic makeup of the supernatant. An imbalance in the resistance (i.e., the conductivity) between the sample and reference arms of the Wheatstone bridge results. The sample is given sufficient time to attain the equilibrium dictated by the high pressure condition. At this point, the brass foil is burst, the chemical system relaxes to the low pressure equilibrium, and the balance in resistance is restored between the two arms of the bridge.

As the chemical system in the sample cell relaxes to the ambient pressure equilibrium, the AD-converter captures the decaying analog signal of the resistance imbalance in the bridge and converts it to a digital signal. The capture and digitization of the resistance measurement from the bridge is triggered at the point of pressure release by a piezo-electric capacitor built into the walls of the autoclave. Following capture of the relaxation signal, the digitized information is

transferred to a computer for data storage and analysis. An oscilloscope is used to display the digitized relaxation spectrum of resistance imbalance amplitude versus time for each relaxation measurement. Several digitized relaxation spectra for each sample can be fed to the computer for signal-averaging and data manipulation. The computer is also equipped with software designed to calculate relaxation times from the exponential decay of the bridge signal. Statistical parameters associated with the relaxation time measurement are also calculated by the program.

2.1.5 Preliminary Static Measurements for P-jump Studies in Colloidal Systems

A convenient aspect arises from the development of chemical relaxation theory, in that the rates of the equilibration process following the perturbation are dependent on the final (i.e., the low pressure) equilibrium concentrations. The absolute concentrations of the various products, reactants and intermediates need not be known throughout the equilibration phase following the pressure drop. One need only measure the equilibrium concentrations of the various reactants at ambient pressure (Bernasconi, 1976). This equilibrium information is then used to determine the intrinsic reaction rate constants for the adsorption process from calculated relaxation times.

In studies of reactions of ionic adsorptives and charged colloidal adsorbate surfaces, the electrical potential at the plane of adsorption must be considered. The electrical potential at the surface has an effect on both the

equilibrium constant for the adsorption process as well as on the kinetics of adsorption. Unfortunately, values for the electrical potentials at or near the particle surface cannot be measured directly but can only be obtained by modeling of potentiometric titration data.

Various models of the electrical double layer (EDL) have been developed which differ in the relationship between surface charge and potential. Therefore, the values for the electrical potential at the plane of adsorption will vary with the model chosen. The majority of P-jump studies in colloidal systems have focused on reactions involving metal oxides with pH-dependent variable surface charge. The triple layer model with inner-sphere (TLM-IS) adsorption (Hayes and Leckie, 1987) has been used extensively for modeling of adsorption behavior on colloid surfaces and has been very successful in yielding the desired agreement between static and kinetic measurements from chemical relaxation studies. Yet this model is not universally accepted as the best representation of the aqueous interface of a charged surface, and new models continue to be developed (Hiemstra et al., 1989). The TLM-IS and other models will be discussed in greater depth later.

In adsorption studies, where surface functional groups are considered to be reactant species, the specific surface area and the surface site density of the adsorbent must be determined. For variable-charge surfaces, surface acidity constants determined by acid/base titration data, using either a graphical procedure or equilibrium speciation modeling, provide a means of determining the relative

concentrations of positive, neutral, and negative charge sites on amphoteric colloid surfaces at a given pH. This information is essential since only one form of the amphoteric surface site can be assumed to be reactive for each reaction mechanism tested.

Once the essential static measurements have been completed, preliminary relaxation studies of the system can proceed. The primary objective of this phase is to determine if a measurable relaxation effect can be obtained. Once a measurable relaxation has been detected, the various time regions that the AD-converter is capable of monitoring must be probed to determine if more than one relaxation occurs. Multiple relaxations indicate more than one reaction step or reaction mechanism is occurring in the system. Thus, the appropriate time region(s) for measurement of each sample's relaxation time(s) will be known in advance once actual relaxation data collection begins.

Once it has been confirmed that one or more relaxations can be measured, it must be established that the relaxations are only obtained when all of the proposed reactants are present. All other sample constituents, alone and in all possible combinations, must be tested for the ability to produce the relaxation effect. Once it has been established that the relaxation occurs only in the presence of the proposed reactants, the actual relaxation time measurements can be taken.

Several approaches may be used to vary the concentrations of the proposed reactants, eliciting a change in the relaxation time(s). The first approach

is to change the total amount of one of the reactants added to the suspension. For example, either the particle concentration or solution concentration of the adsorptive can be varied. Another approach is to vary the pH of the suspension. In the case of a variable-charge colloid, this will alter the distribution of the three interdependent protonation states that the amphoteric surface functional groups can assume. Varying the pH is also a convenient device for chemical relaxation studies of adsorption reactions of weak acid anions. The relative concentrations of the undissociated and dissociated forms of the adsorptive can be shifted by varying the pH, providing a means of determining which adsorptive species are active in the adsorption process.

2.1.6 Measurement of Relaxation Times

Preparation of the P-jump apparatus for recording of relaxation curves begins with a measurement of the absolute resistance (Ω) of the sample in its autoclave cell. Once determined, a reference solution of similar resistance ($\pm$ 10% absolute resistance) (Takahashi and Alberty, 1969) is placed in the reference cell and both cells are mounted in the autoclave. The potentiometer on the Wheatstone bridge can then be used to artificially balance the resistances of the two cells. Once balance is obtained, the AD-converter is programmed to monitor the equilibration process throughout the previously determined time region.

To obtain the high pressure equilibrium, the P-jump autoclave is sealed with the brass foil and water is forcibly pumped into the chamber. To avoid

pressure oscillations following the pressure release, the pressure transducing water must be degassed and any air bubbles which may be trapped in the experimental chamber (Fig. 2.1) must be removed prior to sealing the chamber. The pressure is brought to within 0.5 MPa of the bursting pressure and the sample is given sufficient time to reach the high pressure equilibrium ($\geq$ 6 times the slowest relaxation time) (Gruenewald and Knoche, 1979). To avoid the interference of acoustical noise, the pressure above the foil is reduced below ambient pressure by pulling up on the vacuum pump prior to the pressure release. A rapid thrust of the water pump is then applied to burst the foil and restore the pressure in the autoclave to ambient.

At the instant that the pressure is released, the piezo-electric transducer triggers the recording of the relaxation spectrum over the specified time interval. The captured relaxation is transferred to the computer for signal averaging and analysis. Once transferred to the computer, the relaxation can be displayed on the oscilloscope screen for a visual determination of the signal quality. Signals which are of obviously poor quality due to mechanical or electronic disturbances can be discarded at this point, so that high quality relaxation spectra will not be degraded by the averaging process. The average of two or more relaxation spectra can also be displayed for a visual inspection of the signal enhancement with each additional spectrum recorded and averaged. The relaxations can also be qualitatively

inspected for multiple relaxation effects (single, double or more relaxations) at this time.

Once several relaxation spectra have been measured and recorded, the computer can be used for calculation and statistical evaluation of relaxation times. This process is initiated by first choosing a portion of the relaxation spectrum where the relaxation effect is most pronounced. The relaxation spectrum represents the relationship between the amplitude of the resistance imbalance (the dependent variable) and time (the independent variable). Based on the time interval chosen, the computer obtains 16 relaxation amplitudes equally spaced in time which will be used to calculate τ. The relaxation time can be calculated from the amplitude decay over time using the relationship

$$y = A \quad \exp(-t/\tau) + C \tag{2.3}$$

where y is the amplitude at time t (s), A is the initial amplitude, and C, the final amplitude. Five τ values (τ_1 to τ_5) are calculated from the 16 amplitudes by first evaluating the first through eighth amplitude values, then the second through ninth amplitude values, and so on. If there is no systematic variation in the five τ values, it can be assumed that the relaxation effect is a single exponential (or two relaxations with the same relaxation time). A systematic increase in the τ values from τ_1 through τ_5 indicates that two or more relaxation effects with different equilibration rates are superimposed. Random variation from τ_1 to τ_5 due to

experimental error is expected. The standard deviation of τ_1 through τ_5 can be used as a statistical evaluation of the precision of the τ measurement.

If two or more relaxation effects are superimposed, the relaxation curve can be segmented and the latter portion of the relaxation spectrum analyzed for the longer τ. Subsequently, the early portion of the curve can be analyzed for the fast relaxation. Of the 16 amplitude values sampled, the first three values can be ignored in calculating five τ values for the slow relaxation. Thus, τ_1 is calculated from the fourth through eleventh amplitude values, τ_2 is calculated from the fifth through twelfth amplitudes, etc. Once the slower relaxation time has been determined, the first portion of the curve is analyzed for the fast relaxation time. If the two effects are not readily separated in this manner, the digitizer can be programmed to record both shorter and longer time periods. It is therefore possible for the fast relaxation to be detected in a shorter time region where the slow relaxation has as yet little influence on the amplitude decay. The slow relaxation can be isolated in a longer time region where the influence of the fast relaxation has run its course. Alteration of other experimental conditions, such as temperature, may be required to separate the relaxations, however.

Based on the proposed reaction mechanism, an equation describing the dependence of the relaxation time(s) on the concentrations of the proposed reactants can be derived. The form of the equation is dependent on the stoichiometry, the number of reactants, the number of products, the number of intermediate steps, as

well as the number of side reactions in which the reactants and/or products can participate (Bernasconi, 1976). The rate expression and the relaxation data analysis can be simplified in some cases by maintaining some reactants or products quasi-constant through the use of large reactant excesses or buffers.

As stated before, all τ vs. reactant concentration expressions can be reduced to linear relationships regardless of their simplicity or complexity. Any such equation relating the τ dependence on reactant concentrations can be arranged to yield the intrinsic forward rate constant (k_f^{int}) and reverse rate constant (k_r^{int}) for each step in the reaction mechanism using a graphical procedure. The preliminary test of the validity of the proposed reaction mechanism is then to determine if the τ vs. reactant concentration expression yields a linear relationship. If the plot is linear, and none of the other possible reaction mechanisms yields a similar adherence, this indicates that the reaction mechanism is valid. Depending on the reaction mechanism, a relationship between the various rate constants and the equilibrium constants involved in the overall adsorption process can be found.

From chemical kinetic theory, the equilibrium constant for a particular reaction or reaction step is equal to the ratio of the associated forward and reverse rate constants. As a more rigorous test of the validity of the reaction mechanism, the value of the ratio of the forward and reverse rate constants should be in substantial agreement with the intrinsic equilibrium constant for the reaction or related reaction steps as obtained from the static measurements.

2.2 Previous Relaxation Studies Relevant to Soil Chemistry

The P-jump relaxation method has been used successfully by several researchers to study the rates and mechanisms of a variety of reactions involving ionic species in aqueous media. Many of these involve ionic interactions with colloidal surfaces.

Pressure-jump relaxation studies of hydrolysis reactions of zeolite surfaces have been conducted (Ikeda et al., 1981; 1982b), as well as ion exchange reactions between protons and NH_4^+ on zeolite surfaces (Ikeda and Yasunaga, 1984). Ion exchange of various quaternary alkylammonium ions with Na^+ within the cage structure of a zeolite was also studied (Ikeda et al., 1983).

The reaction mechanisms of proton adsorption and desorption from hematite and magnetite surfaces were determined by the P-jump method (Astumian et al., 1981), as were Pb^+ adsorption and desorption mechanisms on goethite (Hayes and Leckie, 1986). The rates and mechanisms of IO_3^- adsorption and desorption (Hachiya et al., 1980), and proton adsorption and desorption reactions (Ashida et al., 1978) with TiO_2 surfaces have also been determined. Ikeda and coworkers (1982a) used the P-jump relaxation method to study acetic acid adsorption and desorption reactions with silica-alumina particles.

Zhang and Sparks have studied the adsorption of MoO_4^{2-} (1989), SO_4^{2-} (1990a), SeO_3^{2-}, and SeO_4^{2-} (1990b) in aqueous goethite suspensions using the P-jump method. Experimental results indicate MoO_4^{2-} adsorbs on goethite by ligand

exchange following the formation of an ion-pair complex between a protonated surface site and the MoO_4^{2-} anion. Sulfate and SeO_4^{2-} undergo adsorption simultaneously with the formation of the OH_2^+ surface group by protonation of a neutral surface site. In each case an outer-sphere ion-pair complex is formed. Selenite adsorbs as either $HSeO_3^-$ or SeO_3^{2-} via ligand exchange, forming an inner-sphere coordination complex.

Adsorption and desorption reactions on γ-Al_2O_3 have been investigated for Pb^+ (Hachiya et al., 1979), the uranyl ion (UO_2^{2+}) (Mikami et al., 1983b), the CrO_4^{2-} and $HCrO_4^-$ anions (Mikami et al., 1983c), as well as the PO_4^{3-} anion (Mikami et al., 1983a). Results of P-jump experiments focusing on adsorption-desorption reactions of the divalent metal cations, Cu^{2+}, Mn^{2+}, Zn^{2+}, Co^{2+}, and Pb^{2+} on γ-Al_2O_3 indicate inner-sphere adsorption at two distinct sites on the Al-oxide surface (Hachiya et al., 1984). Two distinct reaction rates were measured for each type of site.

Chemical relaxation studies of B reactions have been limited to investigations of polymerization reactions in aqueous BA solutions as well as B complexation reactions with organics (Pizer and Babcock, 1977). Osugi et al. (1968) used P-jump spectrometry to determine the forward and reverse rate constants for the formation of the trimeric B solution species $B_3O_3(OH)_4^-$, postulated by Ingri (1962). Relaxations attributable to formation of the B trimer were obtained from pH 5 to 9, and total B concentrations of 0.025 and 0.2 mol L^{-1}.

Anderson et al. (1964), using the temperature-jump technique, determined the rate constants associated with this same polymerization reaction as well as for the formation of a pentamer, $B_5O_6(OH)_4^-$. The trimer was in evidence from pH 5 through 9 with total B concentrations of 0.06 to 0.6 mol L^{-1} while the pentamer was the second most abundant B polymer found between pH 5 and 7 with total B concentrations of 0.3 to 0.6 mol L^{-1}. The rate constants for the trimer formation reaction were in substantial agreement with those obtained by Osugi and coworkers (1968). While acknowledging that more than one step may occur during trimer formation, Anderson et al. (1964) reported rate constants for the overall processes only, as insufficient information was obtained to determine the rates of individual steps which may have been involved.

The rapid kinetics of B adsorption reactions on soil constituents have not as yet been studied using relaxation kinetic techniques. The mechanisms associated with these reactions remain conjecture at this time.

2.3 Materials and Methods

2.3.1 Aluminum Oxide Characterization and Static Measurements

Aluminum Oxide C, a manufactured alumina (γ-Al_2O_3) (Degussa Corp., Teterboro, NJ) was used as the adsorbent for all phases of the static and kinetic studies of B adsorption. Although not a common soil mineral, alumina has been widely used as a soil oxide analog and its chemical and physical properties are well

documented due to its extensive applications as a chemical catalyst. It has been perhaps the most frequently used adsorbent in past chemical relaxation studies of colloidal suspensions (Sparks, 1989). Its electrochemical surface properties are similar to naturally occurring soil oxides yet its uniform composition lends itself to interpretation of complex adsorption processes occurring on its surface. The pertinent physical and chemical properties of the alumina were determined prior to collection of chemical relaxation data and are elaborated on later.

All reagents were analytical grade and used without further purification. Polyethylene containers were used for storage and analysis of all suspensions and solutions throughout the entire study to avoid B and/or silicate contamination from boro-silicate glassware.

An alumina stock suspension in deionized H_2O was prepared and used in both the static and kinetic studies. The stock suspension was dialyzed repeatedly to remove entrained electrolytes until the conductivity of the dialyzate was nearly equal ($\pm$ 1 $\mu S\ cm^{-1}$) to that of deionized H_2O (0.9 $\pm$ 0.1 $\mu S\ cm^{-1}$) after a 24 h period. The final concentration of the stock alumina suspension after dialysis was determined gravimetrically by drying a known volume of the stock suspension at 105 °C.

The specific surface area of the alumina as supplied by the manufacturer without further treatment and after the dialysis treatment was determined by the ethylene glycol monoethyl ether (EGME) method (Heilman et

al., 1965). Specific surface area measurements using the BET-N_2 gas adsorption method were also supplied by the manufacturer (100 ± 15 m^2 g^{-1}). The EGME specific surface area measurements were not significantly different from the BET-N_2 values. Dialysis had no significant effect on the specific surface area of the alumina.

Surface acidity constants were determined by potentiometric titration of the alumina suspensions (13.1 g L^{-1}) with NaOH and HCl in 0.001, 0.01, and 0.5 mol L^{-1} $NaNO_3$. The pH of the suspension was monitored throughout the titration using a Radiometer PHM 82 pH-meter equipped with a Radiometer GK2401B combination electrode (Radiometer Copenhagen, Denmark). A non-linear least squares optimization procedure (FITEQL Version 2.0, Westall, 1982) was used to model the titration data and determine the first and second acid dissociation constants (K_+^{int}, and K_-^{int}, respectively) for the alumina surface (Table 2.1). Surface site density (0.9 nm^{-2}) was also determined using the FITEQL program. The two capacitance values required for the triple layer model (TLM), the inner capacitance between α- and β-layers (C_1) and outer capacitance between the β-layer and the diffuse layer (C_2), were obtained from the literature (Westall, 1982) (Table 2.1). The single inner capacitances used when testing the constant capacitance model (CCM) and the modified Stern model (MSM) were also obtained from the literature (Goldberg and Glaubig, 1985; and Westall, 1982, respectively). These same

capacitances values were also used when modeling the B adsorption data using these three EDL models.

The FITEQL program provides four EDL model options for modeling of surface acidity and adsorption phenomena (Westall and Hohl, 1980): the CCM (Schindler and Gamsjäger, 1972), the diffuse layer model (DLM) (Stumm et al., 1970), the (MSM) (Bowden et al., 1977), and the (TLM) (Hayes and Leckie, 1987). The surface acidity constants were determined using each of the four models as all four models were subsequently tested for their ability to simulate the B adsorption data. The values of K_+^{int} and K_-^{int}, as determined by a given EDL model, were held constant in optimizing the equilibrium constants for B adsorption using the same model.

Equilibrium constants for the outer-sphere adsorption of Na^+ and NO_3^- (K_{Na}^{int}, and K_{NO3}^{int}, respectively), which are also required for the TLM, were obtained from the literature as well (Westall, 1982) (Table 2.1).

The mass law expressions describing the surface acidity and electrolyte adsorption reactions are

$$K_+^{int} = \frac{[AlOH][H^+]}{[AlOH_2^+]} \exp(-F\psi_\alpha/RT) \qquad (2.4)$$

$$K_-^{int} = \frac{[AlO^-][H^+]}{[AlOH]} \exp(-F\psi_\alpha/RT) \qquad (2.5)$$

$$K_{NO_3}^{int} = \frac{[AlOH_2^+ - NO_3^-]}{[AlOH_2^+][NO_3^-]} \exp(-\psi_\beta F/RT) \quad (2.6)$$

$$K_{Na}^{int} = \frac{[AlO^- - Na^+]}{[AlO^-][Na^+]} \exp(\psi_\beta F/RT) \quad (2.7)$$

Table 2.1 **Electric double layer model parameters for alumina surface acidity reactions used in the four FITEQL model options.**

MODEL	$-logK_+^{int}$	$-logK_-^{int}$	CAPACITANCES F m^{-2}	$logK_{Na}^{int}$ $logK_{NO3}^{int}$
CCM	6.7	9.0	C=1.06[#]	NA[*]
DLM	7.3	8.6	NA	NA
MSM	7.3	8.5	C=2.40[‡]	NA
TLM[†]	7.0	8.8	C_1=1.2 C_2=0.2	$logK_{Na}^{int}$=-8.3 $logK_{NO3}^{int}$=8.3

[#] From Goldberg and Glaubig (1985).

[*] Not Applicable.

[‡] From Westall (1982).

[†] C_1, C_2, $logK_{Na}^{int}$, and $logK_{NO3}^{int}$ from Westall (1982).

where F is the Faraday constant. The exponential terms represent surface activity coefficients for a charged surface and the brackets denote concentrations (mol L^{-1}).

The terms, ψ_α and ψ_β, represent the electrical potentials at the α- and β-layers, respectively.

Boron adsorption was measured over the pH range of 7.0 to 10.8 in 35 g L^{-1} alumina suspensions. The pH of the suspensions was adjusted with additions of either HNO_3 or NaOH.

Boron was added to the alumina suspensions as $B(OH)_3$. Total B in the suspensions was held constant at 0.012 mol L^{-1}. Boron speciation as BA and BT was controlled by changing the pH of the suspensions. Total B-adsorbed was assumed to be the difference between initial total B added and that remaining in the suspension supernatant after a 2h equilibration period. The sample suspensions were equilibrated on a reciprocal shaker at low speed. The supernatant was obtained by high speed centrifugation at 34,500 g for 30 min (Sorvall RC-5B, DuPont Instruments, Newtown, CT), followed by filtration through a 0.2 μm membrane filter (Gelman Sciences, Ann Arbor, MI). Total B remaining in the supernatant was determined by the azomethine-H photocolorimetry method (Parker and Gardner, 1981) at 420 nm with a Hewlett Packard 8452A diode array spectrophotometer (Hewlett Packard Company, Palo Alto, CA). Boron speciation in the equilibrium supernatant was predicted using the formation constant for BT calculated as a function of temperature and ionic strength (Mesmer et al., 1972) assuming no aqueous polyborates were formed (Ingri, 1962).

Boron adsorption data were modeled using each of the four FITEQL EDL models assuming either BA could be adsorbed, BT could be adsorbed, or both BA and BT could be adsorbed. Depending on the assumptions inherent in each of the models, the data were also modeled assuming B could be adsorbed as an outer-sphere or inner-sphere complex. The FITEQL program was then used to determine intrinsic equilibrium constants for the various adsorbed B species. In addition to optimized adsorption constants, the program output also included the equilibrium concentrations of all defined chemical species for each datum point of the adsorption isotherm, both on the alumina surface and in the supernatant. The equilibrium information provided was dependent on both the reaction mechanism proposed and the model used. For instance, the CCM does not take into account adsorption of background electrolyte ions or allow for the assumption of outer-sphere adsorption. Information regarding the concentrations of solution and adsorbed background electrolyte as well as outer-sphere adsorbed B species is therefore not provided as output from this model.

2.3.2 Pressure-jump Measurements of Boron Adsorption/Desorption Rates

The rate constants associated with adsorption and desorption reactions of B solution species on γ-Al_2O_3 surfaces were determined by analysis of the dependence of P-jump relaxation times on proposed reactant species concentrations, based on a particular assumed reaction mechanism. This procedure was also used

to test the validity of the various possible reaction mechanisms which could account for the removal of B species from solution in oxide suspensions.

Relaxation spectra in response to a pressure perturbation were sought in aqueous alumina suspensions with 0.012 mol B L^{-1} at various ionic strengths up to 0.1 mol L^{-1}. A 0.05 mm thick brass foil was used to seal the autoclave, producing a pressure drop of 13.2 MPa following bursting. Relaxations were induced, detected, and recorded using a DIA-RPC P-jump autoclave in combination with a DIA-RPM Wheatstone bridge, and DIA-RRC analog-to digital converter (Dia-log Co., Düsseldorf, Germany), respectively. An AIM-65 computer (Rockwell International, Anaheim, CA) was used to calculate τ from the relaxation curves and provide statistical parameters regarding τ measurement precision. Relaxation curves were displayed on a Kenwood CS-1021 oscilloscope (Kenwood, Japan) for visual inspection.

Maximum concentrations of 0.012 mol total B L^{-1} were used to avoid formation of aqueous B polymer species (Ingri, 1962) which might also undergo adsorption reactions (Keren and Bingham, 1985). An iterative procedure was used to calculate the portion of total B as BT in each sample, as dictated by the pH, to account for the contribution of BT to the ionic strength of the supernatant. The amount of $NaNO_3$ needed to bring the ionic strength to the desired level was then added. Preliminary studies of the aqueous B/alumina suspensions with ionic strength adjusted to 0.01 mol L^{-1} indicated a chemical relaxation effect in response

to a pressure drop from pH 7 to 10. All other components of the P-jump sample suspensions were tested in all possible combinations to ensure that the relaxations were detected only when alumina and B were both present in the suspensions.

These same suspensions were tested for their stability by placing them in the P-jump cell and balancing the Wheatstone bridge with an appropriate electrolyte solution in the reference cell. The stability of the balanced signal from the bridge was then observed and found to be essentially stable for a period of an hour or more, indicating equilibrium and insignificant particle settling occurred.

Portions of the P-jump samples used for τ determinations were set aside for subsequent equilibrium reactant concentration measurements. Relaxation times for a series of BA/BT/alumina suspensions of constant total B (0.012 mol L^{-1}) were obtained from pH 7.3 to 9.7. By changing the pH, the concentrations of the various possible reactants, BA, BT, and the negatively-charged (AlO^-), neutral (AlOH), and positively-charged ($AlOH_2^+$) alumina surface sites were varied. Several relaxation signals were averaged for each sample ($\geq$5 relaxation curves) to enhance the signal-to-noise ratio for each relaxation time measurement. The recording of relaxations following placement of each sample in the P-jump cell was limited to a period of not more than 1 h to avoid changes in τ due to particle settling.

Equilibrium determinations for τ analysis consisted of measuring the pH of the sample suspension and total B remaining in solution following adsorption. Total B was determined by the azomethine-H colorimetric method

given previously. The amount of BA and BT remaining in the suspension supernatant was then calculated based on the conditional equilibrium constant for the BA/BT equilibrium (Mesmer et al., 1972), the amount of total B, and the pH. Total B remaining in the supernatant, free BT and pH at equilibrium were then used as input for the FITEQL equilibrium speciation program.

Output obtained from the FITEQL program included all concentrations of model-defined adsorbed and aqueous species. These included: the proposed adsorbed B species for a given reaction mechanism tested, outer-sphere background electrolyte surface complexes (if applicable to the model), and the concentrations of the remaining free pH-dependent surface sites. The electrical potential at the various planes of adsorption, pertinent to each model tested, were also provided based on the previously determined surface acidity constants and the calculated surface charge.

Using the equilibrium output obtained for each model and mechanism tested, the τ dependence on the concentrations of the various reactants for a particular assumed reaction mechanism was then tested. The influence of the surface potential on the extent and rate of B adsorption at the assumed plane of adsorption was also accounted for in testing each reaction mechanism.

Rate constants for the adsorption of B species were obtained by a graphical analysis stemming from the derived dependence of τ on the proposed

reactant species concentrations. The relationship between the rate constants and τ varies with the particular reaction mechanism assumed.

Once conformity of relaxation data to a proposed reaction mechanism was found, agreement between an intrinsic equilibrium constant obtained from static measurements and a kinetic equilibrium constant obtained from the ratio of k_f^{int} and k_r^{int} was tested. Such agreement between equilibrium and kinetic derived constants was considered validation of the reaction mechanism.

2.4 Results and Discussion

2.4.1 Static Measurements

Throughout the pH range studied, varying amounts of B were removed from the supernatant of B/alumina suspensions following a 2 h equilibration period. The total amount of B removed from B/alumina suspensions (0.012 mol L^{-1} initial B) as a function of pH follows a pattern of increasing B adsorbed as pH increases, with a maximum at pH 8.5, followed by a decrease in B adsorbed as pH was increased further (Fig. 2.2).

A similar behavior was found for B adsorption on clays and oxide surfaces by other authors (Hingston, 1964; Sims and Bingham, 1968a; McPhail et al., 1972). Goldberg and Glaubig (1985) studied B adsorption on several Al-oxides and found that B adsorption was greatly affected by pH, exhibiting sharp maxima near pH 6 to 7. Boron adsorption on alumina (γ-Al_2O_3) was the exception,

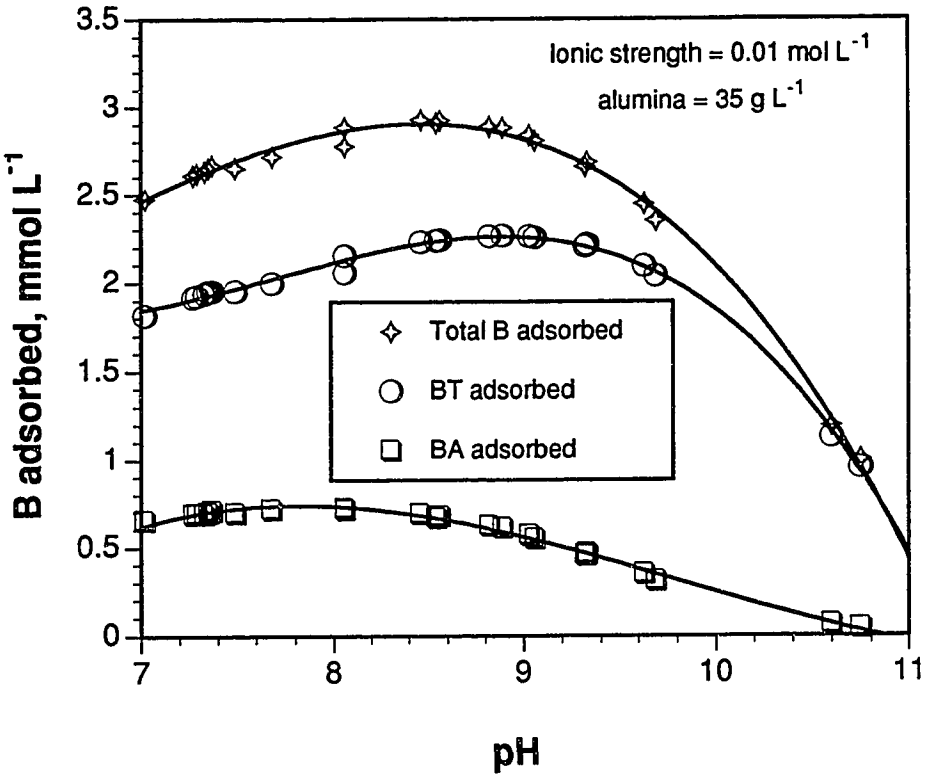

Figure 2.2 **Adsorption of boric acid (BA), borate (BT), and total B on alumina as a function of pH. Boric acid and BT adsorption were modeled using the TLM-IS.**

however, exhibiting a flattened adsorption envelope with a more gradual response to changes in pH. Maximum B adsorption occurred over a broad range of pH 5 to 8. Similar results were obtained in this study of B adsorption on alumina (Fig. 2.2).

Modeling of the B adsorption data obtained in this study yielded varying results depending on the model chosen and the B species assumed to be adsorbed. All four models included in the FITEQL program adequately simulated the B adsorption behavior over the pH range tested. As modeling of the B adsorption data using the four EDL models was central to the objectives of the P-jump investigation, these results will be discussed later within the context of interpreting the P-jump results.

Alumina suspensions (35 g L^{-1}) with 0.012 mol L^{-1} total B and ionic strength maintained at 0.01 mol L^{-1} remained stable for a minimum of 1 h. All P-jump samples were subsequently adjusted to 0.01 mol L^{-1} ionic strength with $NaNO_3$ as the background electrolyte.

2.4.2 Pressure-jump Measurements

Pressure-jump relaxations were detected in alumina/BA suspensions from pH 7.3 to 9.7, within a time region of 1.6 s. These same relaxations were not detected in solutions or suspensions containing the various other components of the B/alumina suspensions unless both the alumina and B were present. This indicated that the relaxation spectrum was due to an interaction between B and alumina. No

additional relaxations were detected in the B/alumina suspensions in time regions up to 1.75 min.

Relaxation times for each sample in the P-jump study were calculated from a minimum of five recorded and signal-averaged relaxation spectra. No systematic variation was found in τ_1 through τ_5 for each P-jump sample, indicating that only a single relaxation occurred. The average τ for P-jump samples with equal particle and total B concentrations varied with the pH of the sample (Fig. 2.3), indicating that the detected relaxation was due to one or more of the pH-dependent surface or solution species present in the suspension. Since τ is related to the forward and reverse rate constants governing the reaction, a smaller τ indicates the equilibration rate is occurring more rapidly. Although the rate constants remain unchanged, the rate of the forward reaction will increase as the concentration of the reactants increases.

The relationship between τ and the amount of free BT in solution is shown in Fig. 2.4. The relaxation time decreases with an increase in BT in the suspension indicating that the relaxation could be attributable to BT adsorption reactions.

2.4.3 Triple Layer Model Application to Boron Adsorption Isotherm Data

Since the intrinsic rate and equilibrium constants for the adsorption reaction are dependent on the activity of the adsorptive in the EDL surrounding the adsorbate particles and not on their bulk solution concentrations, per se, the effect

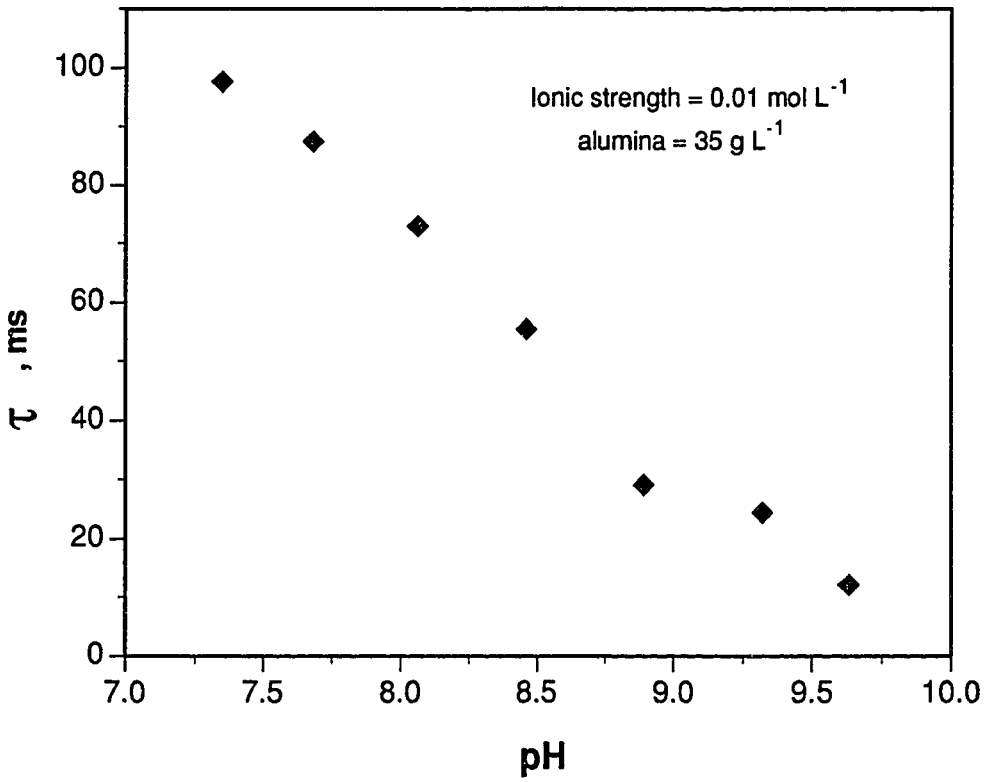

Figure 2.3 **The pH dependence of relaxation times (τ) measured in alumina suspensions with 0.012 mol total B L^{-1}.**

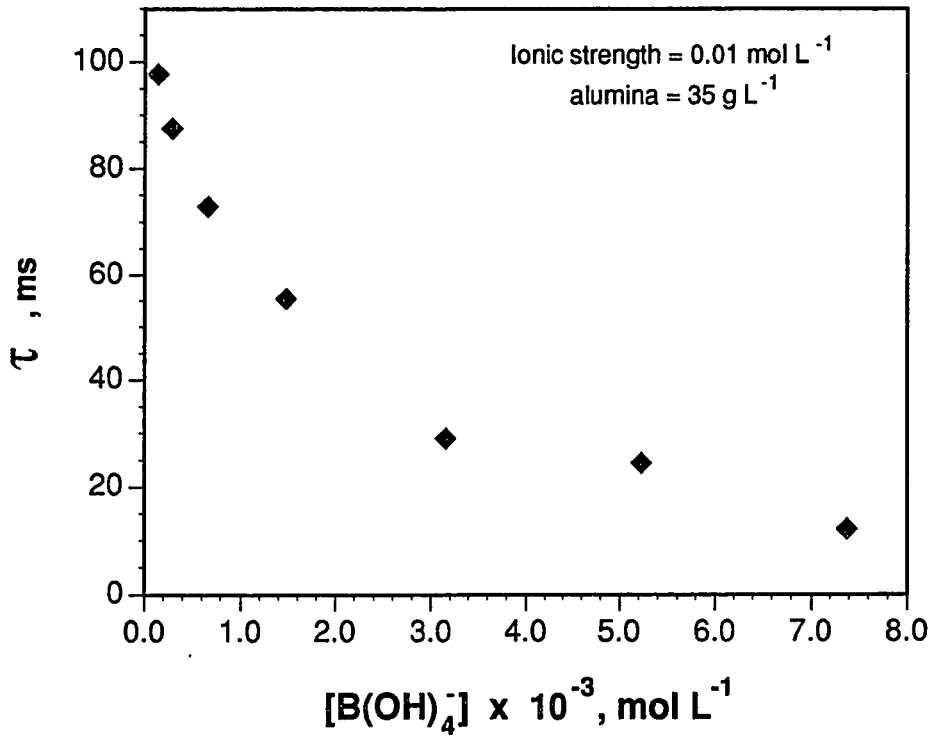

Figure 2.4 The effect of $B(OH)_4^-$ concentration on relaxation times (τ) measured in alumina suspensions with 0.012 mol total B L^{-1}.

of the electrical potential at the plane of adsorption on the adsorptive activity must be considered.

The mechanisms proposed for B adsorption on the alumina surface were tested under the following assumptions. Several authors have suggested that B can be adsorbed from solution as both the neutral BA and BT species (Hingston, 1964; Keren et al., 1981) and possibly as one or more of the several polyborate species (Harder, 1961). In designing the experiments, total B concentrations were kept below levels which would promote the formation of aqueous polyborates, therefore, the latter possibility could be ignored. It was then assumed that B could be adsorbed as either BA or BT, or both BA and BT. The first criterion for (EDL) model validity was the ability to simulate the B adsorption data. If the model was successful in this capacity, it was then tested for its ability to fit the kinetic data.

Because P-jump with conductivity detection can only be used to monitor reactions which involve a change in concentration of ionic species, the adsorption of neutral BA molecules can only be detected if it results in the desorption of an ionic product, such as a hydronium ion or hydroxyl ion. Modeling of the BA adsorption reaction with the appropriate stoichiometry which would yield either of these two ionic product species was attempted using the TLM-IS.

The stoichiometry and coordination restrictions of the adsorption of neutral BA on a negatively-charged AlO^- group would require that OH^- be the leaving group, with the result being a net loss of negative charge from the alumina

and formation of a neutral adsorbed B surface species. This reaction mechanism could not be successfully modeled using the TLM-IS.

The stoichiometry of the adsorption of BA on a positively-charged $AlOH_2^+$ site would require that H_3O^+ be the leaving group, resulting in a neutral adsorbed B site on the alumina surface. Modeling of this reaction scheme was also unsuccessful using the TLM-IS to simulate the B adsorption data.

The adsorption of BA on a neutral AlOH site would require that the leaving group be H_2O. Since all reactants and products in this reaction scheme are uncharged, no change in conductivity would result from this adsorption reaction. Therefore, the relaxation effect could not be attributed to this process. Nonetheless, an attempt was made to model this B adsorption reaction mechanism using the TLM-IS but was unsuccessful when it was assumed that BA was the only species adsorbed.

Although the relaxation in B/alumina suspensions cannot be attributed to BA adsorption, and BA adsorption could not account for all adsorbed B in the P-jump suspensions, this reaction may occur concurrently with BT adsorption. Modeling of the B adsorption isotherm was successful under the assumption of BA adsorption on a neutral AlOH site when it was assumed that BT was also competitively adsorbed on a neutral site using the TLM-IS (Fig. 2.2).

Boron adsorption on the three amphoteric forms of the alumina surface functional group offered three possible reaction schemes for the inner-sphere

adsorption of BT on alumina. Borate adsorption on a negatively charged AlO^- site, ignoring the fact that the electrical repulsion between like charges would be unfavorable, would require that OH^- be the leaving group and would result in a negatively-charged adsorbed-B site. This reaction mechanism could not be successfully modeled with the TLM-IS.

Borate adsorption on a positively-charged $AlOH_2^+$ site would require that H_3O^+ be the leaving group, resulting in a negatively-charged adsorbed B site. Despite the favorable electrical attraction expected between the $AlOH_2^+$ surface site and the BT anion, this reaction scheme could not be successfully modeled using the TLM-IS.

The TLM-IS was only successful in modeling BT adsorption when it was assumed that both the neutral BA species as well as the anionic BT species were adsorbed on a neutral AlOH group, resulting in a neutral and negatively-charged adsorbed-B site, respectively. In each reaction scheme, H_2O is the leaving group. Throughout the pH range studied, the amount of BT adsorbed was ≥ 3 times the amount of BA adsorbed as simulated by the FITEQL program (Fig. 2.2). This reaction scheme for B adsorption is consistent with the observation that B adsorbs regardless of the overall charge on the surface of the oxide and that it adsorbs over a wide range of pH. The adsorption of BA would occur at $pH < 10$ as long as neutral AlOH surface groups remain available. However, under increasingly acidic conditions ($pH < 5$), protonation of the neutral AlOH site and

formation of the $AlOH_2^+$ surface group decreases the number of sites favorable for B adsorption. As pH increases above pH 7, the BT solution species becomes more prevalent and total B adsorption increases. At pH > 10, deprotonation of the neutral surface site and formation of the AlO^- site reduces the number of sites available for B adsorption.

2.4.4 Analysis of Relaxation Data Using the TLM-IS

Since only the BA and BT adsorption reactions involving the neutral surface site could be modeled successfully with the TLM-IS, and only the adsorption of BT would result in a change in conductivity, the correlation between P-jump relaxation times and the BT adsorption reaction mechanism was tested using the FITEQL equilibrium output.

The reaction mechanism for the adsorption of BT on a neutral AlOH surface group, involving two reactants and two products, of which one of the products, H_2O, is quasi-constant can be written as

$$AlOH + BT \rightleftharpoons AlOBT^- + H_2O \tag{2.8}$$

The symbol $AlOBT^-$ is used to represent the BT inner-sphere adsorption complex on the alumina surface, and the minus sign denotes that adsorption of the BT anion imparts a negative charge to the surface. The mass law expression for Eqn. (1.1) is

$$K_{BIS} = \frac{[AlOBT^-][H_2O]}{[AlOH][BT]} \tag{2.9}$$

The terms in brackets denote concentrations of neutral surface sites, BT, $AlOBT^-$ and H_2O.

From chemical relaxation theory (Bernasconi, 1976), for a reaction mechanism of this form, the dependence of the reciprocal of the relaxation time (τ^{-1}) on the reactant concentrations is given by

$$\tau^{-1} = k_f\{[AlOH] + [BT]\} + k_r[H_2O] \tag{2.10}$$

where k_f is the conditional forward rate constant and k_r is the conditional reverse rate constant. The relationship between the conditional rate constants (k_f and k_r) and the intrinsic forward rate constant (k_f^{int}) and the intrinsic reverse rate constant (k_r^{int}) can be derived as follows.

From chemical kinetics,

$$K_{BIS} = \frac{k_f}{k_r} \tag{2.11}$$

The intrinsic equilibrium constant for BT inner-sphere adsorption (K_{BIS}^{int}) is related to K_{BIS} by

$$K_{BIS}^{int} = K_{BIS}\exp(\frac{-\psi_\alpha F}{RT}) \tag{2.12}$$

where ψ_α is the surface potential at the plane of inner-sphere adsorption.

Combining Eqns. (2.11) and (2.12) leads to

$$K_{BIS}^{int} = \frac{k_f^{int}}{k_r^{int}} = \frac{k_f}{k_r}\exp\left(\frac{-\psi_\alpha F}{RT}\right) \tag{2.13}$$

For the condition of a small perturbation following a sudden pressure drop, ψ_α remains essentially constant and the activation potentials for the forward and reverse processes are equal and opposite in sign (Hayes and Leckie, 1986). Therefore,

$$K_{BIS}^{int} = \frac{k_f \exp(-\psi_\alpha F/2RT)}{k_r \exp(\psi_\alpha F/2RT)} \tag{2.14}$$

Combining Eqns. (2.13) and (2.14) yields

$$k_f = k_f^{int}\exp(\psi_\alpha F/2RT) \tag{2.15}$$

and

$$k_r = k_r^{int}\exp(-\psi_\alpha F/2RT) \tag{2.16}$$

Combining Eqns. (2.10), (2.15), and (2.16) yields

$$\begin{aligned}\tau^{-1} = {} & k_f^{int}\exp(\psi_\alpha F/2RT)\{[AlOH] + [BT]\} \\ & + k_r^{int}\exp(-\psi_\alpha F/2RT)[H_2O]\end{aligned} \tag{2.17}$$

Rearrangement of Eqn (2.17) leads to

$$\begin{aligned}\tau^{-1}\exp(\psi_\alpha F/2RT) = {} & k_f^{int}\exp(\psi_\alpha F/RT)\{[AlOH]+[BT]\} \\ & + k_r^{int}[H_2O]\end{aligned} \tag{2.18}$$

or

$$T = k_f^{int} P + k_r^{int}[H_2O] \tag{2.19}$$

where

$$P = \exp(\psi_\alpha F/RT)\{[AlOH] + [BT]\} \tag{2.20}$$

and

$$T = \tau^{-1}\exp(\psi_\alpha F/2RT) \tag{2.21}$$

Therefore, a plot of T versus P will yield a linear relationship with a slope, k_f^{int}, and the intercept equal to the product of k_r^{int} and the quasi-constant concentration of H_2O if the proposed reaction mechanism is valid. By dividing the intercept by the concentration of H_2O in the suspension (55.5 mol L^{-1}), the intrinsic rate constant for the desorption process is obtained.

A plot of T versus P for the relaxation times measured for B adsorption on alumina obtains a linear relationship (R^2=0.92) with a slope equal to $10^{5.52}$ and an intercept equal to 0.10021 (Fig. 2.5). Upon division of the intercept by the concentration of H_2O, the rate constant for the desorption of borate from the oxide surface is obtained ($10^{-2.74}$). The ratio, k_f^{int}/k_r^{int}, yields an equilibrium constant obtained through kinetic analysis ($K_{KIN}^{int} = 10^{8.26}$). Comparison of equilibrium constants for the adsorption of borate on the alumina surface from kinetic (K_{KIN}^{int}) and static analysis using the TLM-IS shows substantial agreement between the two (Table 2.2). This indicates the proposed BT adsorption reaction mechanism is valid.

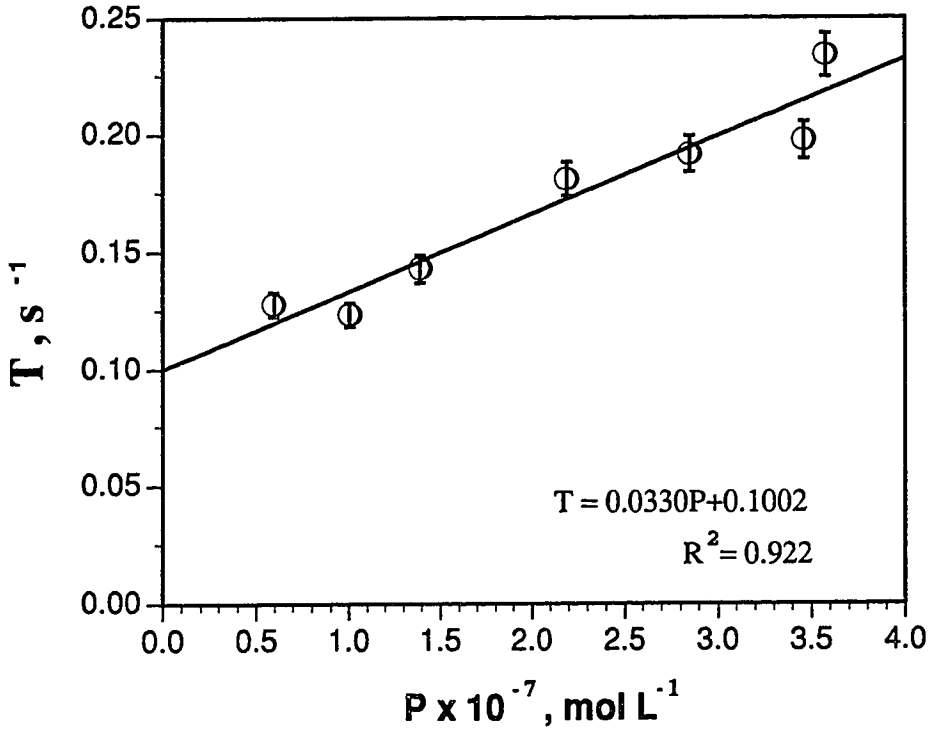

Figure 2.5 **Plot of T vs. P in Eqn. 2.21 for the borate inner-sphere adsorption mechanism.**

Table 2.2 **Model-dependent intrinsic equilibrium constants for B adsorption obtained using the FITEQL program.**

Model	BT Adsorption Constant	BA Adsorption Constant
TLM-IS†	7.69	2.16
CCM	6.28	NC*
DLM†	6.39	1.47
MSM‡	12.09	2.24
TLM-OS	12.48	NC

* No convergence of the FITEQL optimization procedure was obtained with inclusion of BA adsorption.

† BT adsorption constant was unaffected by inclusion of BA adsorption.

‡ Convergence obtained only with inclusion of BA adsorption.

2.4.5 Pressure-jump Data Analysis Using Other EDL Models

The three other surface complexation model options provided by the FITEQL program, the CCM (Schindler and Gamsjäger, 1972), the DLM (Stumm et al., 1970), and the MSM (Bowden et al., 1977), as well as the TLM assuming outer-sphere adsorption (TLM-OS) (Hayes and Leckie, 1987) were tested for their

ability to describe the kinetic data. These models are alike in their inclusion of both mass law and material balance constraints on equilibrium concentrations but differ in their interpretation of the EDL. These differences include the particular definition of the type of surface complex formed in the adsorption process, the number and location of planes of adsorption, and the equation describing the relationship between surface charge (σ) and surface potential (ψ) at the plane of adsorption (Westall and Hohl, 1980). The models also differ in the number of parameters which are adjustable in fitting the data. All the models mentioned herein are adaptations of the original Stern model of the oxide surface/electrolyte solution interface (Westall and Hohl, 1980).

Each of the models divides the surface/solution interface into discreet layers (Fig. 2.6), each with their associated σ and ψ. The surface of the oxide itself is characterized by O^{2-} and OH^- groups which have a lesser degree of metal ion coordination than O^{2-} and OH^- groups in the bulk of the solid. This results in an insufficient charge neutralization of surface O^{2-} and OH^- groups which is countered by the adsorption of protons from solution. The plane at which the surface O^{2-} and OH^- groups are located is referred to as the α-layer. All the FITEQL models assume surface O^{2-} and OH^-, and adsorbed protons are located in the α-layer. Depending on the model in question, other ions adsorbed to the surface in what is known as specific adsorption or inner-sphere complex formation are assigned to either the α-layer, and/or assigned to a separate plane of adsorption,

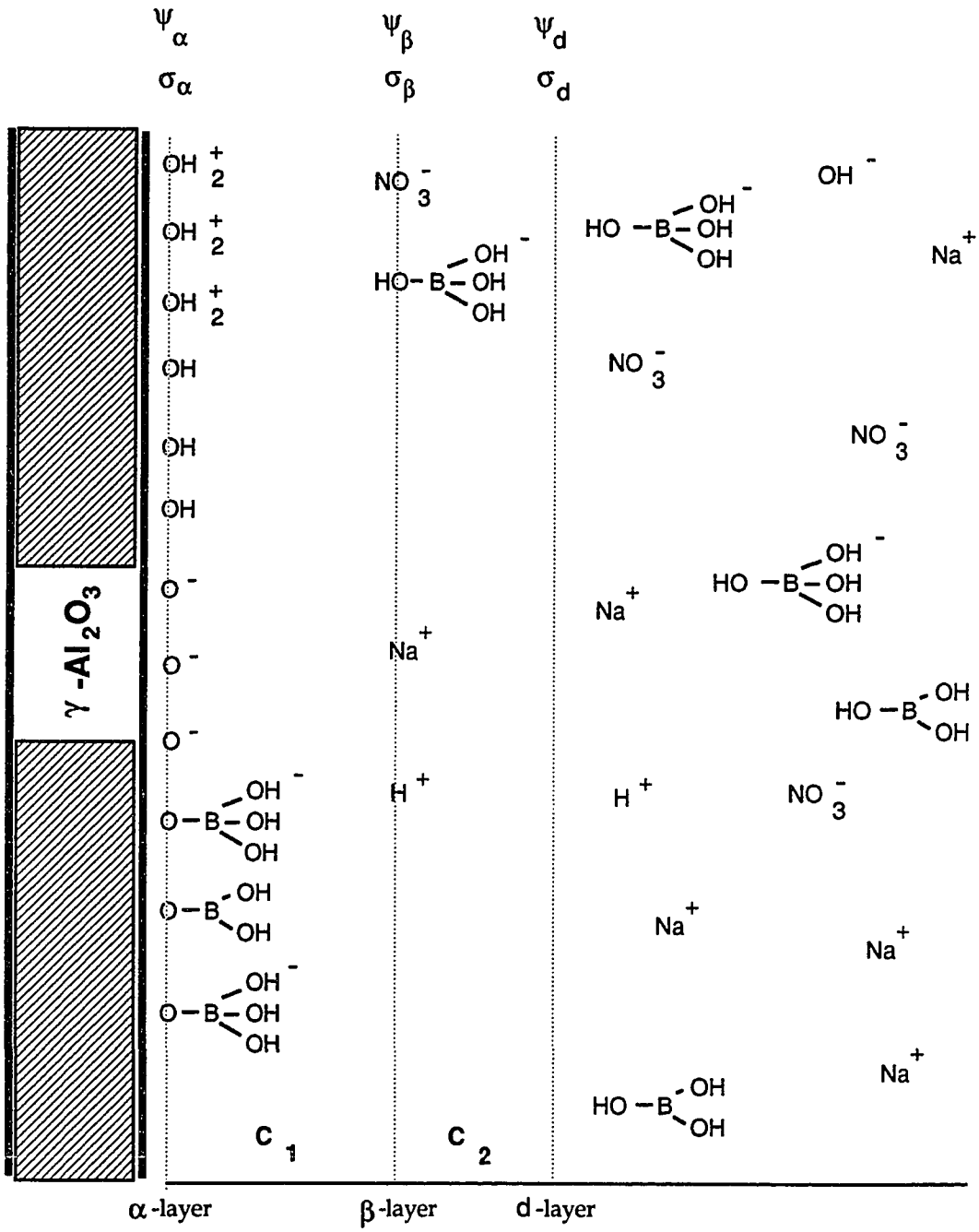

Figure 2.6 **A schematic diagram of the alumina surface/solution interface according to Stern (Westall and Hohl, 1980).**

the β-layer, at some small distance from the surface. Ions adsorbed in the α-layer contribute to the charge in the α-layer, σ_α, and their chemical activity is influenced by the potential, ψ_α. Ions in the α-layer are considered to have no water of hydration retained between the surface and the adsorbate molecule. With the exception of the MSM, ions adsorbed forming what are referred to as outer-sphere complexes are located in the β-layer. These ions are adsorbed by electrostatic attraction and are considered to retain their hydration sphere in the adsorbed state which dictates the separation between the α- and β-layers. Ions adsorbed as outer-sphere complexes create a plane of charge, σ_β, and are influenced by the associated electrical potential, ψ_β. The diffuse layer of adsorbed counterions has the **d**-layer as its inner boundary. Ions located in the diffuse layer create σ_d and are under the influence of ψ_d. Electroneutrality constraints dictate that

$$\sigma_\alpha + \sigma_\beta + \sigma_d = 0 \tag{2.22}$$

The CCM, developed by Stumm and Schindler, and others (Schindler and Gamsjäger, 1972; Stumm et al., 1976) is a Stern model adaptation which takes into account only inner-sphere surface complexes while ignoring the formation of outer-sphere complexes. It is explicitly assumed that adsorption results from a ligand exchange reaction between the adsorptive and a surface functional group. The relationship between the charge and potential at the plane of adsorption is linear, where

$$\sigma_\alpha = C_1 \psi_\alpha \qquad (2.23)$$

and C_1 is the Helmholz capacitance between the α- and β-layers (F m^{-2}). No distinction is made between the plane of adsorbed protons or hydroxyls and other adsorbed ions, as all surface complexes are bound in the α-layer. The value of the Helmholz capacitance is adjusted to provide the desired fit of the data to the model. In actuality, the value of C_1 is not constant, but varies with the particular cation/anion combination and concentration of the background electrolyte. However, the fit of experimental data to the CCM is rather insensitive to changes in C_1 and a single value will fit a wide range of conditions and adsorptives (Goldberg and Glaubig, 1986b). Goldberg and Glaubig have modeled B adsorption reactions on a wide variety of soil mineral and oxide surfaces with a capacitance value set at 1.06 F m^{-2} (Goldberg and Glaubig, 1985; Goldberg and Glaubig, 1986a; Goldberg and Glaubig, 1986b). This same capacitance value was used for modeling of PO_4^{2-} adsorption on Fe- and Al-oxides, as well (Goldberg and Sposito, 1984).

In the DLM (Stumm et al., 1970), it is assumed that the relationship between σ and ψ is as from the Stern-Grahame modifications of the Gouy-Chapman theory and thus the capacitance is fixed by theory and not adjustable, as it is in the CCM. Inner-sphere adsorption is as described for the CCM; however, retention of counterions in the **d**-layer and thus ionic strength is considered.

The MSM, as included in the FITEQL program, is an adaptation for colloid surfaces of Stern's original EDL model of electrode surfaces proposed by

Bowden and coworkers (1977). This model differs from the previous two in that only protons and hydroxyls are assumed to be adsorbed at the α-layer. All other specifically adsorbed ions are adsorbed at the β-layer, contributing to charge σ_β and influenced by ψ_β. The MSM is unique in that it is not assumed that water of hydration is retained between the adsorbent and adsorbate at the β-layer. All nonspecifically adsorbed ions are assigned to the diffuse counterion swarm. Thus, there is no designated plane of adsorption for outer-sphere complexes. As in the original Stern model, the inner boundary of the diffuse ion swarm is at the **d**-layer.

The TLM, which was developed by Yates and coworkers (Yates et al., 1974), is similar to the aforementioned MSM in its number and location of planes of adsorption of the various surface/adsorbate complexes. It differs from the MSM in the relationship between σ and ψ and in the conceptualization of the Helmholz capacitances between the α- and β-layers (C_1) and β- and **d**-layers (C_2). In the MSM, the potential at the β-layer is assumed to be equal to the **d**-layer potential, i. e., the outer Helmholz capacitance is infinite. Whereas, in the TLM, there are two constant capacitance layers, each with a finite capacitance. In the original form of the TLM (Davis and Leckie, 1980), it was assumed that only protons and hydroxyls could enter the α-layer; other specifically adsorbed ions were assigned to the β-layer. It has since been modified by Hayes and Leckie (1987) to allow for specific adsorption of ions other than H^+ and OH^- into the α-layer. This modified TLM accounts for ionic strength effects on adsorption in two ways. First in the

manner of the DLM, where the Gouy-Chapman charge/potential relationship has an explicit ionic strength dependence. Secondly, it allows for ion-pair complexes between surface sites and solution species, and thus is able to model surface complexation reactions over a wider range of ionic strength (Hayes et al., 1991). These ion-pair surface complexes are assigned to the β-layer. The TLM thus provides two possibilities for modeling B surface complexation reactions, the TLM-IS, which was tested previously in this study, and the TLM assuming outer-sphere adsorption of B (TLM-OS).

In modeling the B adsorption data obtained in this study using the CCM, DLM, MSM, and TLM-IS assuming inner-sphere adsorption, the models succeeded only under the assumption that B, either as BA or BT, was adsorbed on neutral surface sites of the alumina, and only when H_2O was assumed to be the leaving ligand in the exchange process. For all of the models used, as in TLM-IS, the model equilibrium speciation output indicated that B adsorption in the pH range of this study (pH 7 to 10.75) was predominantly or entirely as BT.

The intrinsic equilibrium constant for B adsorption on alumina provided as output from the FITEQL program using the CCM is presented in Table 2.2. As required by the assumptions inherent in the development of this model, only adsorption in the α-layer is considered.

The CCM was unsuccessful in modeling the B adsorption data when it was assumed that both nonionic BA and the BT anion could be adsorbed

simultaneously. It successfully simulated the adsorption data when it was assumed that BT was the sole adsorptive, however.

The model-generated electrical potentials at the plane of adsorption and equilibrium concentrations of the reactant species in the alumina/B suspensions were used in testing the proposed reaction mechanism for B adsorption. The relationship between τ and the reactant concentrations is the same as for the TLM-IS (Eqn. 2.18). The plot of T versus P in Eqn. (2.19) using the CCM output provided only marginal agreement between the kinetic and static equilibrium constants with the kinetic constant (K_{KIN}^{int} = 7.34) being more than an order of magnitude greater than the static constant (Table 2.2). Goldberg and Glaubig have used the CCM extensively to model B adsorption reactions on various adsorbents (Goldberg and Glaubig, 1985; 1986a; 1986b). In each case, the authors assumed neutral BA adsorption on a neutral surface site with no net change in charge on the alumina surface. The magnitude of the FITEQL equilibrium constant for B adsorption obtained in their studies of various adsorbents was similar to that obtained in this study. Since they assume adsorption of an uncharged solution species in their reaction scheme, there is no electrostatic effect on the B adsorption process, however.

The equilibrium constant for BT adsorption given by the DLM was of similar magnitude to the CCM static equilibrium constant (Table 2.2). The DLM successfully modeled the B adsorption data assuming either both BA and BT could

be adsorbed or only BT could be adsorbed. The value of the BT adsorption constant was largely unaffected by the assumption of simultaneous BA adsorption (Table 2.2).

The relationship between τ and the reactant concentrations for the DLM is similar to the TLM-IS and the CCM (Eqn. 2.18) but different values for ψ_α and the AlOH concentration are generated. Neither DLM assumption (BT adsorption, or BT and BA adsorption) yielded a rational T vs. P plot, however, as in either case the intercept was negative, indicating a negative rate constant for the BT desorption process. This was largely due to the value of ψ_α in the exponential terms in Eqn. (2.18) generated as DLM output. Since ψ_α has an exponential effect on the values of T and P in Eqn (2.19), its influence is much greater than the reactant concentrations themselves. Due to the negative intercept of Eqn. (2.19), no kinetic equilibrium constant was obtainable from the DLM output.

The MSM was successful in modeling B adsorption only when assuming both BA and BT were adsorbed (Table 2.2). The intrinsic equilibrium constant for BT adsorption obtained from the MSM treatment of the isotherm data (Table 2.2) differs substantially from those obtained from the TLM-IS, DLM, and CCM. The MSM static equilibrium constant for BT adsorption was nearly six orders of magnitude greater than the CCM and DLM constants, and nearly five orders of magnitude greater than the TLM-IS constant. This was a result of the exponential effect of the β-layer potentials predicted by the MSM, which were

large (-0.5 to -0.6 V) relative to the α-layer potentials predicted by the other models (-0.1 to -0.3 V).

The kinetic test of the model output indicated the MSM was not an accurate representation of B adsorption at the charged alumina interface, however. The τ vs. reactant concentration expression was as in the TLM-IS, CCM, and the DLM (Eqn. 2.18). However, assuming specific adsorption occurs at the β-layer, the MSM generated values of ψ_β are used instead of ψ_α in the exponential terms in Eqn. (2.18). The T vs. P plot (Eqn. 2.19) of the MSM output yielded a negative slope, indicating a negative k_f^{int} for BT adsorption. A negative rate constant for the adsorption process is an illogical result; therefore, no kinetic equilibrium constant was obtained from the MSM.

The TLM-OS was used in modeling outer-sphere complexation of B by the alumina surface as well. The TLM-OS simulated the B adsorption data successfully only when it was assumed that BT was adsorbed electrostatically by a protonated $AlOH_2^+$ site (Table 2.2). Since outer-sphere adsorption is considered to be an electrostatic attraction between a charged surface site and an ionic adsorbate, convergence of the FITEQL program was not expected when assuming the neutral BA species was also adsorbed.

The outer-sphere B adsorption mechanism can actually be represented in either of two forms,

$$AlOH_2^+ + BT \rightleftharpoons AlOH_2^+\text{-}BT^- \quad (2.24)$$

where the BT anion is adsorbed at a previously protonated site, or

$$AlOH + H^+ + BT \rightleftharpoons AlOH_2^+\text{-}BT^- \quad (2.25)$$

where the protonation of the surface site and formation of the outer-sphere BT surface complex occur simultaneously. The symbol $AlOH_2^+$-BT^- represents the BT ion-pair complex with the positively charged alumina surface group.

One shortcoming that becomes apparent in using the FITEQL program is its inability to distinguish between single- and multiple-step reactions in model species matrix construction. The FITEQL program is designed such that all chemical species, reactant and product, in the equilibrium chemical system to be modeled are represented as the sum of their components. Species are defined as all of the individual chemical entities to be considered in the chemical equilibrium system of interest, whereas, components are defined as those chemical entities whose products make up all the species in the system. No component can be written as a product of a reaction of any of the other components (Westall, 1982). A species can be made up of a single component, however. The end result is that a single reactant species in Eqn. (2.24), the protonated surface site, is codified in the FITEQL species input matrix in the same form as two reactant species in Eqn. (2.25), the neutral surface site and proton. Although the FITEQL model input matrix and model output are identical for each of the rate law expressions (Eqns.

2.24 and 2.25), the form of the τ vs. reactant concentration expression is different for each reaction mechanism.

For a reaction in which two reactants yield a single product, as in Eqn. (2.24), from chemical relaxation kinetic theory (Bernasconi, 1976), the relationship between τ and the reactant concentrations at the final equilibrium is

$$\tau^{-1} = k_{fO2}\{[AlOH_2^+] + [BT]\} + k_{rO2} \tag{2.26}$$

Since it is assumed that BT is adsorbed at the β-layer, the intrinsic equilibrium constant for the outer-sphere adsorption process (K_{BO2}^{int}) is given by

$$K_{BO2}^{int} = \frac{[AlOH_2^+ - BT^-]}{[AlOH_2^+][BT]}\exp(\frac{-\psi_\beta F}{RT}) = K_{BO2}\exp(\frac{-\psi_\beta F}{RT}) \tag{2.27}$$

and

$$K_{BO2} = \frac{k_{fO2}}{k_{rO2}} \tag{2.28}$$

Therefore,

$$K_{BO2}^{int} = \frac{k_{fO2}^{int}}{k_{rO2}^{int}} = \frac{k_{fO2}}{k_{rO2}}\exp(\frac{-\psi_\beta F}{RT}) \tag{2.29}$$

As in Eqn. (2.14), for a small perturbation, the exponential term in Eqn. (2.29) can be divided between the forward and reverse rate constants such that

$$k_{fO2}^{int} = k_{fO2}\exp(-\psi_\beta F/2RT) \tag{2.30}$$

and

$$k_{rO2}^{int} = k_{rO2}\exp(\psi_\beta F/2RT) \tag{2.31}$$

Rearranging Eqns. (2.30) and (2.31) yields

$$k_{fO2} = k_{fO2}^{int}\exp(\psi_\beta F/2RT) \tag{2.32}$$

and

$$k_{rO2} = k_{rO2}^{int}\exp(-\psi_\beta F/2RT) \tag{2.33}$$

Combining Eqns. (2.26), (2.32), and (2.33) leads to

$$\begin{aligned}\tau^{-1} = {} & k_{fO2}^{int}\exp(\psi_\beta F/2RT)\{[AlOH_2^+] + [BT]\} \\ & + k_{rO2}^{int}\exp(-\psi_\beta F/2RT)\end{aligned} \tag{2.34}$$

Rearrangement of Eqn. (2.34) obtains

$$\begin{aligned}\tau^{-1}\exp(\psi_\beta F/2RT) = {} & k_{fO2}^{int}[\![\exp(\psi_\beta F/RT) \\ & \{[AlOH_2^+] + [BT]\}]\!] + k_{rO2}^{int}\end{aligned} \tag{2.35}$$

Therefore, if the two-reactant outer-sphere reaction mechanism (Eqn. 2.24) for B adsorption is valid, a plot of the left hand side of Eqn. (2.35) vs. the terms enclosed within double brackets will be linear with the slope equal to k_{fO2}^{int} and the intercept equal to k_{rO2}^{int}.

When plotting the FITEQL output for the TLM-OS according to Eqn. (2.35), a negative intercept was obtained. This indicates a negative reverse rate constant which is untenable. Therefore no kinetic equilibrium constant was obtained from this exercise.

The form of the τ vs. reactant concentration expression for the outer-sphere adsorption reaction mechanism as proposed in Eqn. (2.25), involving three reactants and a single product, is unlike that of the two-reactant outer-sphere mechanism (Eqn. 2.24). For a reaction mechanism of this form, the relationship between τ and the equilibrium concentrations of the three reactants is given by (Bernasconi, 1976)

$$\tau^{-1} = k_{fO3}\{[AlOH][BT] + [AlOH][H^+] + [H^+][BT]\} + k_{rO3} \tag{2.36}$$

Since the adsorption data were obtained in the region pH 7 to 10.75, the H^+ concentration was negligible relative to the neutral surface site and BT anion concentrations in the suspensions. The second and third terms enclosed within the brackets in Eqn. (2.36) can therefore be ignored and Eqn. (2.36) reduces to

$$\tau^{-1} = k_{fO3}\{[AlOH][BT]\} + k_{rO3} \tag{2.37}$$

The relationship between the intrinsic and conditional equilibrium constants for BT outer-sphere adsorption (K_{BO3}^{int} and K_{BO3}, respectively), where two of the reactants are solution species, H^+, which must adsorb at the α-layer to form an OH_2^+ group, and BT which adsorbs at the β-layer, thus becomes

$$K_{BO3} = \frac{[AlOH_2^+\text{-}BT^-]}{[AlOH][BT][H^+]} = \frac{k_{fO3}}{k_{rO3}} \tag{2.38}$$

and

$$K_{BO3}^{int} = K_{BO3}\exp\left(\frac{(\psi_\alpha - \psi_\beta)F}{RT}\right) \tag{2.39}$$

Therefore,

$$K_{BO3}^{int} = \frac{k_{fO3}^{int}}{k_{rO3}^{int}} = \frac{k_{fO3}}{k_{rO3}}\exp\left(\frac{(\psi_\alpha - \psi_\beta)F}{RT}\right) \tag{2.40}$$

For a P-jump perturbation of small magnitude

$$k_{fO3}^{int} = k_{fO3}\exp((\psi_\alpha - \psi_\beta)F/2RT) \tag{2.41}$$

and

$$k_{rO3}^{intr} = k_{rO3}\exp((\psi_\beta - \psi_\alpha)F/2RT) \tag{2.42}$$

Combining Eqns. (2.37), (2.41), and (2.42) yields

$$\begin{aligned}\tau^{-1} = {} & k_{fO3}^{int}\exp((\psi_\beta - \psi_\alpha)F/2RT)\{[AlOH][BT]\} \\ & + k_{rO3}^{int}\exp((\psi_\alpha - \psi_\beta)F/2RT)\end{aligned} \tag{2.43}$$

which upon rearrangement becomes

$$\begin{aligned}\tau^{-1}\exp((\psi_\beta - \psi_\alpha)F/2RT) = {} & k_{fO3}^{int}\exp((\psi_\beta - \psi_\alpha)F/RT) \\ & \{[AlOH][BT]\} + k_{rO3}^{int}\end{aligned} \tag{2.44}$$

A plot of the left hand side of Eqn. (2.44) vs. the product of the right hand exponential term and the reactant concentrations in Eqn. (2.44) will yield a linear relationship if the relaxation measurements pertain to the three-reactant outer-sphere adsorption mechanism for BT adsorption.

The K_{KIN}^{int} obtained from the ratio of the slope ($k_{fO3}^{int} = 10^{7.35}$) and intercept ($k_{rO3}^{int} = 10^{0.464}$) of the plot of Eqn. (2.44) yields $K_{KIN}^{int} = 10^{6.89}$. The equilibrium constant obtained from the FITEQL program using the TLM-OS differs from the K_{KIN}^{int} obtained from Eqn. (2.44) by six orders of magnitude (Table 2.2), indicating the chemical relaxation detected in the B/alumina suspensions is not attributable to outer-sphere adsorption of BT at the β-layer of the alumina surface.

There is little difference between the CCM, DLM, MSM, TLM-IS, AND TLM-OS in their ability to simulate B adsorption on alumina, despite having dissimilar descriptions of the charged colloid/solution interface. Westall and Hohl (1980) concluded that these same EDL models were equally suitable for modeling surface acidity using potentiometric titration data. Since all are equally capable of simulating equilibrium data, none of the models yields an unambiguous description of the adsorption energies and electrostatic potentials at the oxide surface, based on equilibrium measurements alone.

Since the electrostatic properties of the surface affect not only the equilibrium positioning of reactions involving charged adsorptives, but also the kinetics of these reactions, a more stringent test of model validity then becomes which model can best fit both static and kinetic data.

Only the TLM-IS was successful in fitting both static and kinetic data for the adsorption of B on alumina. This indicates that the TLM-IS provides the

most accurate description of the interaction between adsorbed BT and the adsorbent at the colloid/solution interface of the four EDL models tested in this study.

Chapter 3

INFRARED SPECTROSCOPIC ANALYSIS OF AQUEOUS ALUMINA AND ADSORBED BORON

3.1 Introduction

3.1.1 Vibrational Spectroscopy of Surfaces

Infrared (IR) spectroscopy, due to its great sensitivity to the composition of surfaces and its ability to detect a wide array of compounds, is well suited to the study of colloidal surfaces and their reactions (Kiselev and Lygin, 1975).

The infrared spectra of molecules arise from the vibratory motions of their constituent atoms. The symmetry of the atoms comprising the molecular unit and the strength of the bonds between the atoms determine the number of vibrational modes and frequency of the vibrations. The frequency of vibration is also dependent on the mass of the vibrating atoms. It is evident that, upon adsorption, the unidirectional influence of the adsorbate will influence the symmetry and therefore the vibrational spectrum of the surface atom(s) to which it is bound.

Infrared spectroscopy can detect changes in the vibrational energy of both adsorbate and adsorbent molecules following adsorption. Adsorption that results in perturbation of the electronic and stereochemical states of the adsorbate molecule, but otherwise leaves the molecule and its entire electron complement intact, is considered physical adsorption (Hair, 1967). Physical adsorption involves only relatively weak van der Waals or electrostatic forces between the adsorbate and adsorbent and the symmetry is perturbed only slightly from that of the free (bulk solution) state. The frequency of vibration and hence, the IR spectral bands of the surface are altered only slightly, with surface group band shifts of approximately 1% being typical (Hair, 1967).

Chemisorption results in a change in symmetry of the surface atoms, and the bond between the adsorbate and adsorbent is much stronger than that of physical adsorption. Chemisorption results in the formation of new chemical species by alteration of the electronic structure of both the adsorptive and the surface (Hair, 1967). As a result, a new IR spectrum, unique to these newly formed species, is obtained. Physical and chemical binding of adsorptive molecules to surfaces can occur concurrently.

Changes in vibrational frequencies of the adsorptive or adsorbent as a result of adsorption can be interpreted as changes in bond strength. Shifting of bands to lower frequencies indicates bond weakening, whereas, a shift to higher frequencies indicates an increase in bond strength.

Shifts in vibrational frequency due to isotopic exchange can be used to identify absorption bands associated with surface functional groups. Isotopic exchange of deuterium (D) for hydrogen (H) occurs readily in surface hydroxyl groups at room temperature by exposure of the mineral surface to liquid or gaseous D_2O or D_2 gas (Farmer, 1974). Since the frequency of vibration is a function of the mass of the constituent atoms in a bond, changing the mass of either constituent will change the vibrational frequency. This effect is most pronounced when D is exchanged for H in end groups of molecules, since the mass of the D atom is twice that of the H atom (Kiselev and Lygin, 1975).

3.1.2 Physical Chemistry of Infrared Spectroscopy

When a molecule absorbs electromagnetic radiation, there is an increase in its total energy. According to quantum mechanical theory, only discrete units of energy, called quanta, can be absorbed. If the energy difference (ΔE) between two quantized energy levels of a molecule placed in an electromagnetic field is a constant multiple of the frequency of the electromagnetic radiation (ν), an exchange of energy between the radiation and the molecule can occur. This constant is known as Planck's constant (h=6.26 x 10^{-34} J s) where:

$$\Delta E = h\nu \tag{3.1}$$

When transitions between energy levels occur, a plot of the intensity of the electromagnetic radiation versus frequency of the radiation results in a

spectrum. If ΔE is positive, i.e., energy is absorbed, an absorption spectrum results. If ΔE is negative, i.e., energy is emitted, an emission spectrum results.

The relationship between the frequency (ν) and wavelength (λ) of electromagnetic radiation is given by

$$\lambda\nu = c \tag{3.2}$$

where c is the velocity of light (3.3×10^{10} cm s^{-1}). The most widely accepted expression for the frequency of infrared radiation is the reciprocal of λ, the wave number ($\bar{\nu}$), and reciprocal centimeters (cm^{-1}) the most commonly used units.

The total energy of a molecule is the sum of its electronic energy, rotational energy, translational energy, and vibrational energy (E_{vib}). To a reasonable approximation, transitions in vibrational energy can be separated from those of rotational, translational, and electronic energy since the separation between E_{vib} levels are much smaller than electronic energy transitions and rotational energy transitions generally correspond to frequencies below 500 cm^{-1} (the far infrared region) (Hair, 1967). Translational energy is only a minor contributor to total energy. Transitions between vibrational energy levels correspond to energies associated with electromagnetic radiation in the infrared radiation region (4000 to 400 cm^{-1}).

As a heteronuclear molecule vibrates, its interatomic distances change at the frequency of vibration, resulting in an oscillating change in its dipole moment, thus creating an alternating electric field. It is this electric field which interacts

with the electrical component of infrared radiation, resulting in absorption of energy and transitions between vibrational energy levels (Anderson et al., 1980). Vibrations of homonuclear diatomic molecules do not result in a change in dipole moment. Since vibrations of this type do not yield an alternating electrical field, no absorption of energy from IR radiation can occur.

The theoretical treatment of the interaction of IR radiation with the vibrational energy of a diatomic molecule involves the consideration of the classical harmonic oscillator comprising two objects (with masses, m_1 and m_2) joined by a spring of length r_0. When the spring is extended to a distance of $r_0 + r$, or compressed to a distance of $r_0 - r$, a restoring force, f, which is proportional to the magnitude of r, will reestablish the distance between the two objects to r_0. The restoring force of a harmonic oscillator is analogous to the strength of a chemical bond. The frequency of oscillation of the harmonic oscillator is a function of f (i.e., the bond strength) as well as the magnitude of m_1 and m_2. For a diatomic oscillator, the frequency of vibration is related to the square root of the reduced mass (μ) (Eisenberg and Crothers, 1979) where

$$\mu = \frac{m_1 m_2}{m_1 + m_2} \tag{3.3}$$

In contrast to classical mechanics, quantum mechanics requires that only discrete amounts of energy can be imparted to the vibrator.

With diatomic molecules, only one mode of vibration exists between the two atoms. If a molecule consists of three or more atoms, new modes of vibration arise.

For a polyatomic molecule of n atoms, $3n$ coordinates are required to completely describe the various motions of the atoms. Three coordinates are required to describe the translational motion of the molecule's center of gravity. In the case of linear molecules, only two coordinates are needed to describe the rotation of the molecule, since there is no rotation considered about the axis. Thus, $3n$ - 5 coordinates remain to describe the motions associated with the atomic vibrations of linear molecules (Anderson et al., 1980). For a diatomic (linear) molecule, it follows that only one mode of vibration is possible. For nonlinear polyatomic molecules, three coordinates are required to describe the rotational motions and three coordinates to describe the translational motions of the molecule, leaving $3n$ - 6 coordinates to describe vibrational modes. Of these n - 1 are stretching vibrations, and $2n$ - 5 are bending vibrations.

In molecules comprising three or more atoms, two general types of vibrational motion are possible. Vibrations which result in a change in bond length are known as stretching or valence vibrations and those which result in a change in bond angle are known as deformation or bending vibrations. Vibrations that lead to a symmetric relocation of atoms about a central point in a bond are known as symmetric vibrations and those which lead to asymmetric changes in the location of

atoms are antisymmetric vibrations. In the case of planar molecules, changes in the position of atoms within the plane of the molecule are called planar vibrations and those outside the plane are called extraplanar vibrations (Kiselev and Lygin, 1975).

When two vibrations differ only in that they are perpendicular to one another, they are said to be degenerate and only one vibration will be detected. Vibrations which result in a change in the dipole moment of the molecule, giving rise to an absorbance of IR radiation, are said to be IR-active. Vibrations that result in a change in the polarizability of the molecule, such as those associated with homonuclear diatomic molecules, are Raman-active (and IR-inactive) and can be detected by Raman spectroscopy.

In many instances, the locations of bands in an IR spectrum are indicative of the molecular groups present. The vibrational frequencies of many organic and inorganic functional groups are largely independent of the rest of the molecule of which they are constituents. These vibrations behave almost as though the vibrating group is isolated from the rest of the molecule (Anderson et al., 1980).

Characteristic functional group frequencies have been extensively tabulated and offer an identifying tool for the IR spectroscopist. This tendency applies mainly to groups that are, or contain, end atoms of molecules and where this end group is of low mass relative to the rest of the molecule (Hair, 1967).

The occurrence of characteristic group frequencies in spectra must be regarded as phenomenological and caution must be exercised in their use in

interpreting the spectra (Anderson et al., 1980). Absorbance at a given frequency is not unequivocal evidence of the presence of a particular molecular group. Moreover, several different functional groups in a sample may have similar band positions. Usually, confirmatory bands due to other vibrational modes can be found in different regions of the spectrum to determine which functional groups are giving rise to these bands.

3.1.3 Infrared Spectroscopy of Minerals

Infrared spectroscopy has been used most extensively in the characterization of organic compounds and their reactions (Skoog, 1985), yet is equally suitable for the study of inorganic substances (Farmer, 1974). The spectra of inorganic materials, which will be the focus of this research, tend to have fewer and broader bands than the spectra of organic substances. Many IR bands resulting from vibrations of inorganic compounds occur at relatively low wave numbers due to the high atomic weights of their constituent atoms (Anderson et al., 1980).

In complex crystals, absorption of IR radiation will occur due to any of three types of vibrations in the unit cell of the crystal: internal vibrations, external or lattice vibrations, and torsional vibrations. Some atoms in the crystal may form anionic units, such as CO_3^{2-} and SiO_3^{2-}, which are more tightly bound within themselves than to other units or atoms in the crystal lattice. Motions within these units are referred to as internal vibrations. Because of the strong bonds within these units, internal vibration bands tend to exhibit the highest frequencies of the

three types. Internal vibrations are also associated with molecules sheathed by water of hydration. Motions of strongly bonded anionic units within crystals relative to the cations to which they are attached are known as external or lattice vibrations. The bands associated with these vibrations are usually located at lower frequencies due to the weaker bond forces involved. The third type of vibration arises from the torsional motion of H_2O molecules within the mineral and the resultant bands occur at very low wave numbers because of the relatively low energy of these motions (Anderson et al., 1980). The interpretation of most metal-oxide spectra, which are of particular interest in this study, involves the characterization of stretching frequencies of metal-oxygen bonds (Anderson et al., 1980).

3.1.4 Developments in IR Analysis of Powders and Surfaces in Aqueous Suspensions

When electromagnetic radiation strikes an object, it can be reflected and scattered, transmitted, or absorbed (Hair, 1967). In transmission spectroscopy, reflection and scattering effects must be minimized in order to obtain high quality spectra of surfaces. The transmittance and absorption of radiation can be controlled by altering the amount of substance in the path of the incident radiation, according to the well known Beer's Law. This property of IR spectroscopy can often be exploited to determine the concentration of a certain molecular unit present.

The energy change upon absorption of radiation at a particular frequency can be used for quantitative analysis by measuring the absorbance (A), which is defined as

$$A = -\log(\frac{I}{I_0}) \tag{3.4}$$

where I is the intensity of the transmitted radiation, and I_0 is the intensity of the incident radiation. The ratio, I/I_0, called the transmittance, is the fraction of incident radiation transmitted by the sample. Quantitation is usually achieved by measuring A at the absorption maximum of the analytical band frequency (Anderson et al., 1980). Absorbance is related to the concentration of the species of interest in a mixture by

$$A = \varepsilon b C \tag{3.5}$$

where ε is the molar extinction coefficient of the chemical species of interest at a given frequency (L mol^{-1} cm^{-1}), b is the pathlength through the sample (cm), and C is the concentration (mol L^{-1}). Surface spectroscopists have been aided by the fact that the molar extinction coefficient of a given molecular vibration is greatly increased when the molecular unit giving rise to the infrared absorption is in the adsorbed state. This increase in ε for surface species relative to bulk species is as much as two orders of magnitude (Hair, 1967).

When attempting to obtain IR spectra of solids, scattering of the incident radiation becomes an important consideration. Scattering results in a

decrease in the amount of radiation striking the detector with a subsequent decrease in signal. Scattering is inversely proportional to the particle size of the adsorbent. A particle size of less than 1 μm is generally regarded as sufficient to minimize light scattering (Hair, 1967). If the surface of the solid is to be probed, this will provide the added benefit of a large surface area-to-mass ratio, thereby increasing the intensity of surface group absorbances relative to bulk absorbances.

The degree of scattering is inversely proportional to the frequency of the incident radiation, therefore, transmission increases as one moves to the lower energy regions of the spectrum. Another means of minimizing scattering effects of particulate solids and increasing spectral resolution is to immerse the particles in a liquid of similar refractive index. However, choosing a solvent of suitable refractive index may not be a viable solution to scattering problems if solvent effects on the interaction between the adsorbent and adsorptive are to be considered.

An additional problem arises when the surface to be studied is that of a particle in aqueous suspension. Since water is a very strong absorber of IR radiation, particularly in the regions between 3800 and 3000 cm^{-1}, obtaining information regarding other functional groups with bands in these same regions is difficult. Unfortunately, the functional group often of most interest in the study of oxides and minerals is the surface OH group which has a characteristic frequency found in the 3650 and 3400 cm^{-1} region.

The total internal reflection method, developed by Harrick (Harrick and Riederman, 1965), is well suited for studies of adsorbed molecules and their associated surfaces. In the attenuated total reflection (ATR) method, the IR beam passes through an IR-transparent solid prism of relatively high refractive index, with the solid material or suspension to be studied in contact with its surface. The angle of incidence of the radiation at the sample/prism interface must be greater than the critical angle for total reflection. Although the angle of incidence is greater than the critical angle, some radiation penetrates the sample phase. By choosing an appropriate prism geometry and angle of incidence, the beam can be made to reflect several times at the prism/sample interface, with beam attenuation occurring with each reflection. The depth of penetration of the IR beam is dependent on the angle of incidence and refractive indices of the sample and prism. Thus the effective pathlength can be controlled by varying the angle of incidence and/or refractive indices. Because the depth of penetration into the sample is so small (on the order of one wavelength of the incident radiation, 2.5 to 25 μm), the absorbance intensity is independent of sample thickness (Skoog, 1985). The internal reflection spectra differ slightly from transmission spectra in their intensity and frequency profile but are nonetheless of equivalent utility despite the lack of direct correlation with typical transmission spectra. The method is particularly useful for recording of spectra of molecules adsorbed from solution (Zeltner et al., 1986).

The success of an ATR experiment depends on adequate contact between the sample and the ATR crystal, yielding sufficient sample penetration of the IR beam. The most common ATR applications employ a vertical prism which may result in inadequate sample contact with the prism. The horizontal ATR (HATR) method, which employs a horizontally arranged internal reflectance prism, improves contact between particles in a suspension and the prism, thus ensuring penetration of the IR beam into the suspended solid (Spectra-Tech Contact Sampler™ Users Manual).

3.2 Infrared Applications in Mineralogy and Surface Chemistry

Infrared spectroscopy has been used extensively to characterize a variety of minerals and oxides and to elucidate their structure, composition and reactivity (Hair, 1967; Farmer, 1974). The IR spectra of unknown mineral substances can, in many cases, be used as an identifying tool, as characteristic absorption bands have been established for a variety of minerals. Due to its nonselectivity, IR spectroscopy is also a valuable tool in assessing mineral sample purity.

Infrared spectroscopy of inorganic minerals supplements X-ray diffraction analysis by providing information regarding complex anions in mineral structures. Furthermore, it is more universally applicable than X-ray analysis in that it is sensitive to both crystalline and noncrystalline substances. This becomes an important advantage when studying amorphous oxide materials. It can also

provide valuable information regarding isomorphous substitutions in mineral structures (Farmer, 1974).

The bulk of IR spectra of minerals recorded to date have been obtained from dried samples under vacuum which had been heated to eliminate surface-adsorbed water (Russell, 1974). This is an acceptable procedure for the identification of mineral substances and for characterization of their internal structure. However, extrapolation of this information, obtained under unnatural moisture, temperature, and pressure conditions, to an aqueous environment, may be inappropriate. The similarity between natural and dried samples is even less certain when studying the surfaces of minerals or surface-adsorbed species. Removal of surface hydration water will almost certainly affect the energy of interaction between the adsorbate and surface.

Relatively few spectra have been obtained of minerals in an aqueous environment due to the strong interference of H_2O absorbance bands. Recently, IR studies of minerals under natural moisture conditions have been facilitated by the development of the ATR method (Harrick and Riederman, 1965) and by computer-aided spectral subtraction. The ATR-FTIR technique has been used successfully to obtain spectra of goethite, an Fe-oxide, in aqueous suspensions (Tejedor-Tejedor and Anderson, 1986; Yost et al., 1990; Zeltner et al., 1986). Through appropriate subtraction procedures, the spectrum of the supernatant is effectively removed, resulting in a spectrum of the oxide surface/solution interface.

The surface properties of alumina have been extensively studied using IR spectroscopy, due to its wide application as a catalyst in organic synthesis reactions (Hair, 1967). Some of the earliest and most complete studies were conducted by Peri (Peri and Hannan, 1960; Peri, 1965). Most of the spectral information currently available regarding this mineral has been obtained under high temperature and/or vacuum conditions, however (Kiselev and Lygin, 1975).

Infrared studies of goethite (α-FeOOH) suspensions have been conducted by Anderson and coworkers using the ATR-FTIR technique (Tejedor-Tejedor and Anderson, 1986; Yost et al., 1990; Zeltner et al., 1986). Yost et al. (1990) determined the nature of the salicylate/goethite surface complex formed in aqueous suspension. The mechanism of PO_4^{3-} adsorption in aqueous goethite suspensions has been studied as well (Tejedor-Tejedor and Anderson, 1986).

Edwards et al. (1955) determined the structure of the aqueous borate (BT) anion in 10 mol L^{-1} B solutions using IR and Raman spectroscopies, and X-ray diffraction. The IR spectra of aqueous BT solutions were comparable to those of synthetic teepleite, which was shown by IR, Raman and X-ray analyses, to comprise four-coordinate BT anion units. This provided concrete evidence that aqueous boric acid (BA) is a Lewis acid rather than a Brönsted acid.

Volkhin et al. (1983) studied B interactions with hydroxides of the divalent metal ions Mg, Mn, Fe, Co, Ni, and Cd. Boron was coprecipitated with and/or sorbed to $Ni(OH)_2$ from solutions containing either BA or $Na_2B_4O_7$. Infrared

spectra were recorded of the air-dried products suspended in fluorinated oil or liquid paraffin. The spectra of the products obtained from each B adsorptive solution were similar and indicated that B forms three-coordinate complexes with Ni-hydroxide. The hydroxide ion is released during the B complexation process. It is not known what effects the organic solvents may have had on the oxide spectra.

Beyrouty et al. (1984), using IR spectroscopy, characterized the interaction of B with amorphous aluminum hydroxide following coprecipitation of an $Al(OH)_3$ gel from $AlCl_3$ and BA solutions. Spectra of the air-dried gel were obtained from KBr pellets pressed at 910 MPa pressure for 30 min under vacuum. The authors concluded that B associated with the gel was in the adsorbed state, despite the fact that the Al-hydroxide mineral phase had not been precipitated and stabilized prior to the B adsorption process. Thus, the possibility remains that at least some B was incorporated into the gel structure. It is not known what effect the air-drying or KBr die pressing processes had on the B interaction with the Al-gel surface.

Aluminum hydroxide gel surface complexes of NO_3^-, CO_3^{2-}, and SO_4^{2-} have been analyzed by IR spectroscopy (Serna et al., 1977). The Al-gels were precipitated by neutralizing 0.25 mol L^{-1} Al salt solutions of the respective anions. Spectra were obtained from liquid gels prior to drying, as well as air-dried films supported on AgCl windows. No differences resulting from air-drying the sample were noted in the spectra. These authors also assumed that the coprecipitated

anions were in the adsorbed state. The results suggested an electrostatic adsorption of NO_3^-, whereas, specific adsorption of CO_3^{2-}, and SO_4^{2-} were indicated.

Stubican and Roy (1962) synthesized micas and smectite clay minerals in solutions containing $Na_2B_4O_7$. Infrared spectra obtained from KBr pellets indicated that B was readily incorporated into the mineral structures and that B^{3+} ions substituted for Si^{4+} in the tetrahedral layers.

Infrared studies of adsorbed B have been restricted to air-dried or evacuated samples, pressed in alkali halide discs (Beyrouty et al., 1984; Stubican and Roy, 1962) or suspended in paraffin or fluorinated oils (Volkhin et al., 1983). Precipitation of the adsorptive may occur as the sample is dried, giving misleading information regarding the association between the adsorbate and surface. No IR spectra of B adsorbed on Al-oxide surfaces under normal pressure, temperature, and humidity conditions have been reported. An HATR-FTIR study of adsorbed B in aqueous oxide suspensions should provide valuable insight into the bonding mechanisms involved.

3.3 Materials and Methods

The commercially synthesized alumina, Aluminum Oxide C, (γ-Al_2O_3) (DeGussa Corp., Teterboro, NJ) was the adsorbent used in this study of B adsorption. A stock alumina suspension was dialyzed to remove any entrained salts following the procedure outlined previously (Chapter 2). Results of the

characterization of the alumina were presented in Chapter 2 (Table 2.1). Boron adsorption isotherms were determined prior to the FTIR study (Chapter 2).

The FTIR spectra were obtained using a Perkin Elmer 1720-X FTIR spectrometer (Perkin Elmer Corp., Norwalk, CT) equipped with a triglycine sulfate detector and a Contact Sampler (Spectra-Tech Inc., Stamford, CT) horizontal attenuated total reflectance (HATR) cell equipped with a ZnSe element. The spectra were recorded between 4000 and 500 cm^{-1} at a resolution of 4 cm^{-1}. All spectra were obtained by co-adding 1000 individual scans. The spectra of aqueous alumina suspensions (in H_2O and D_2O) were referenced against the spectrum of their supernatant to yield spectra of the oxide, its surface, and the solvent interface (Tejedor-Tejedor and Anderson, 1985).

The suspension supernatant was obtained by centrifugation (Sorvall RC-5B, DuPont Instruments, Newtown, CT) for 30 min at 34,500 *g* followed by filtration through a 0.2 μm Supor-200 membrane filter (Gelman Sciences, Ann Arbor, MI).

The sample compartment of the spectrometer was purged with N_2 gas during acquisition of spectra for all D_2O containing samples to limit D_2O dilution by atmospheric H_2O.

Infrared spectra were obtained of aqueous alumina suspensions of varying particle concentrations (28, 56, and 112 g L^{-1}) suspended in deionized H_2O to identify IR absorptions associated with the oxide in the suspension. A spectrum

of an alumina paste obtained by centrifuging the alumina stock suspension (30 min at 34,500 *g*) was also recorded. This paste was pressed to the HATR crystal with a rubber spatula to provide adequate sample contact with the crystal. Within this series of spectra of varying particle density, an increase in absorbance intensity with increasing alumina concentration for a particular absorption peak was deemed evidence of that band being due to the alumina present.

Since surface functional groups of alumina undergo protonation and deprotonation reactions, the relative concentrations of protonated, neutral, and deprotonated surface hydroxyls is dependent on the pH of the suspension. In an effort to differentiate between absorption bands associated with the bulk of the alumina and those attributable to surface functional groups, the pH of the alumina suspensions was varied, in effect, varying the interdependent surface site concentrations. This was accomplished by adding varying amounts of HCl and NaOH while maintaining the particle concentration of the suspension constant. Absorption bands previously identified as oxide related and whose intensity maxima occurred near the ZPC of the oxide (pH~8.0) and decreased in intensity with an increase or decrease in pH from the ZPC were tentatively attributed to surface hydroxyl groups.

To corroborate the assignments of the low-pH alumina bands, spectra were obtained of suspensions of equal pH (4.15) and varying particle concentration (13, 28, and 56 g L^{-1}).

As further verification of surface group band assignments, spectra were obtained of alumina suspended in D_2O in varying particle concentrations. All suspensions and solutions containing D_2O were prepared and stored under a N_2 atmosphere to limit isotopic dilution. A D_2O-alumina stock suspension (55 g L^{-1}) was prepared by repeated centrifugation and washing of alumina in D_2O. After each centrifugation, the supernatant was decanted and replaced by fresh D_2O and the alumina was then resuspended and shaken overnight. This procedure was repeated three times. Just prior to obtaining spectra of D_2O-alumina suspensions, the stock suspension was centrifuged and the supernatant replaced with fresh D_2O from sealed ampules. The solid was then resuspended and shaken for 30 min.

The D_2O-alumina stock suspension was diluted with D_2O to vary the particle concentration (11, 26, and 55 g L^{-1}). A deuterated oxide paste was also obtained by centrifugation following the procedure outlined for the H_2O-alumina paste. It was assumed that only surface OH and OH_2^+ groups of the alumina could exchange with the D_2O to form surface OD and OD_2^+, respectively. Due to the likelihood of residual H in the D_2O-alumina suspensions, the possibility of OHD^+ surface group formation was also recognized. If the alumina absorption bands found in the H_2O suspensions were due to the presence of surface OH, these bands should be relocated in the spectra of the D_2O suspensions. The location of new OD bands in D_2O-alumina spectra can be predicted from the difference in mass of D relative to H in the surface groups. New bands found near these predicted

frequencies, which increased in intensity with increasing particle concentration, were considered evidence of a surface OD band.

The effect of D^+ activity in the supernatant (pD) on the spectrum of alumina suspended in D_2O was studied. The D_2O-alumina stock suspension was acidified by addition of DCl sufficient to bring the suspension to pD 2.0. The pD of the suspension was estimated with a H^+-specific combination electrode.

To determine if surface precipitation/dissolution of soluble polymeric aluminum species could explain the pH effects on the IR spectra of alumina, a Al-hydroxide gel was precipitated from a 0.2 mol L^{-1} $Al(NO_3)_3$ solution by addition of NaOH sufficient to bring the solution to pH 6.5. Spectra were obtained of the resultant gel suspension (41.4 g L^{-1}) as well as a paste obtained by centrifuging this suspension. The supernatant spectrum was again subtracted to remove strong solvent absorbances. Spectra of a 0.2 mol L^{-1} $Al(NO_3)_3$ solution as well as 0.6 mol L^{-1} $NaNO_3$ were obtained to distinguish Al-gel bands from bands of NO_3^- solution species. The spectrum of deionized H_2O was subtracted from these solution spectra.

Spectra were obtained of 0.35 mol L^{-1} B dissolved in H_2O and D_2O (pH/pD 4.6) to locate bands associated with aqueous B species. The spectrum of the respective pure solvent was subtracted from the solution spectra to reveal solvent-obscured solute bands. Particular attention was given to the relocation of

H_2O/B bands in D_2O/B solution spectra, as this may signify bands due to D-exchangeable OH ligands of B solute species.

A 0.7 mol L^{-1} BA solution was diluted with 5 mol L^{-1} NaOH and H_2O to yield a 0.35 mol L^{-1} B solution at pH 10.6. The spectrum of this solution was obtained and the solvent spectrum was removed by subtraction. This spectrum was compared to the B solution spectra at low pH to distinguish bands of trigonal B solution species, which predominate at low pH, from bands of tetrahedral B solution species which predominate at pH > 10.

Infrared spectra were obtained of aqueous suspensions of alumina with B adsorbed to identify the nature of the adsorbed-B/alumina surface complex. These spectra were obtained from a series of suspensions varying in total B concentration (0.01, 0.02, 0.05, 0.18 mol L^{-1} B) with constant alumina particle concentration (56 g L^{-1}). The suspensions were equilibrated overnight prior to recording the suspension and supernatant spectra. A portion of the 56 g L^{-1} alumina suspension with 0.18 mol L^{-1} B was equilibrated for 7 d and subsequently centrifuged for 30 min at 34,500 *g* to obtain supernatant and paste. A spectrum of this B/alumina paste was obtained and the supernatant spectrum was subtracted. The resultant subtraction spectra of the B/alumina suspensions and paste were presumed to yield spectral features of the alumina and its surface only, including any adsorbed B. Since previous results (Chapter 2) indicated that the B solution species, BA, and the BT anion, interact with neutral surface OH groups in the

adsorption process, effects of adsorbed B on purported surface functional group bands were noted. If B adsorbs on the alumina surface by ligand exchange, the surface OH bands should decrease in intensity with increasing amounts of B adsorbed. New absorption bands that could be attributed to adsorbed B were also noted.

To test the validity of adsorbed-B band assignments, spectra of B/alumina suspensions prepared in D_2O were also obtained. The BA and BT solution species are alike in that they are coordination compounds comprising a central atom (B) surrounded by OH ligands. This molecular arrangement can be exploited to yield deuterated B-adsorptive species in D_2O solutions. A BA stock solution in D_2O was prepared under N_2 and allowed to equilibrate for a period of several weeks to allow isotopic exchange of D for H in the dissolved B species. It was assumed that D could readily displace H in the dissolved B species and that an exchange equilibrium was attained. Based on the ratio of D to H in the solutions (> 98% D), the B species were predominantly as $B(OD)_3$ and $B(OD)_4^-$. This D_2O-B stock solution and the D_2O-alumina stock suspension were combined to make a series of suspensions of equal particle concentration (55 g L^{-1}) and varying B concentration (0.02, 0.05, and 0.18 mol L^{-1} B). The D_2O-B suspensions were equilibrated overnight prior to recording their spectra. These D_2O-B spectra were compared to the B concentration series spectra obtained from H_2O suspensions.

Spectra were recorded of a paste obtained from a D_2O-alumina suspension with 0.18 mol L^{-1} total B. The suspension was allowed to equilibrate for 7 d at which time it was centrifuged to obtain supernatant and paste. The locations of new adsorbed-B bands in the deuterated suspensions were predicted from the location of adsorbed B bands in the H_2O-alumina suspensions and the change in reduced mass resulting from deuteration. Diminution or elimination of alumina surface OD absorption peaks was also noted and considered evidence of B adsorption.

3.4 Results and Discussion

3.4.1 Aqueous Alumina Spectra

Unless otherwise indicated, all spectra presented are the result of subtracting the supernatant spectrum from the spectrum of its corresponding suspension.

Absorption bands whose intensities are directly correlated to the concentration of dialyzed alumina suspended in deionized H_2O can be tentatively ascribed to the alumina. The spectra of a 56 g L^{-1} alumina suspension and a paste obtained by centrifuging the stock alumina suspension exhibit several bands which grow in intensity with an increase in the suspended alumina (Figs. 3.1 and 3.2). The spectrum of a 28 g L^{-1} alumina suspension exhibited a similar band intensity dependence on suspension density (not shown).

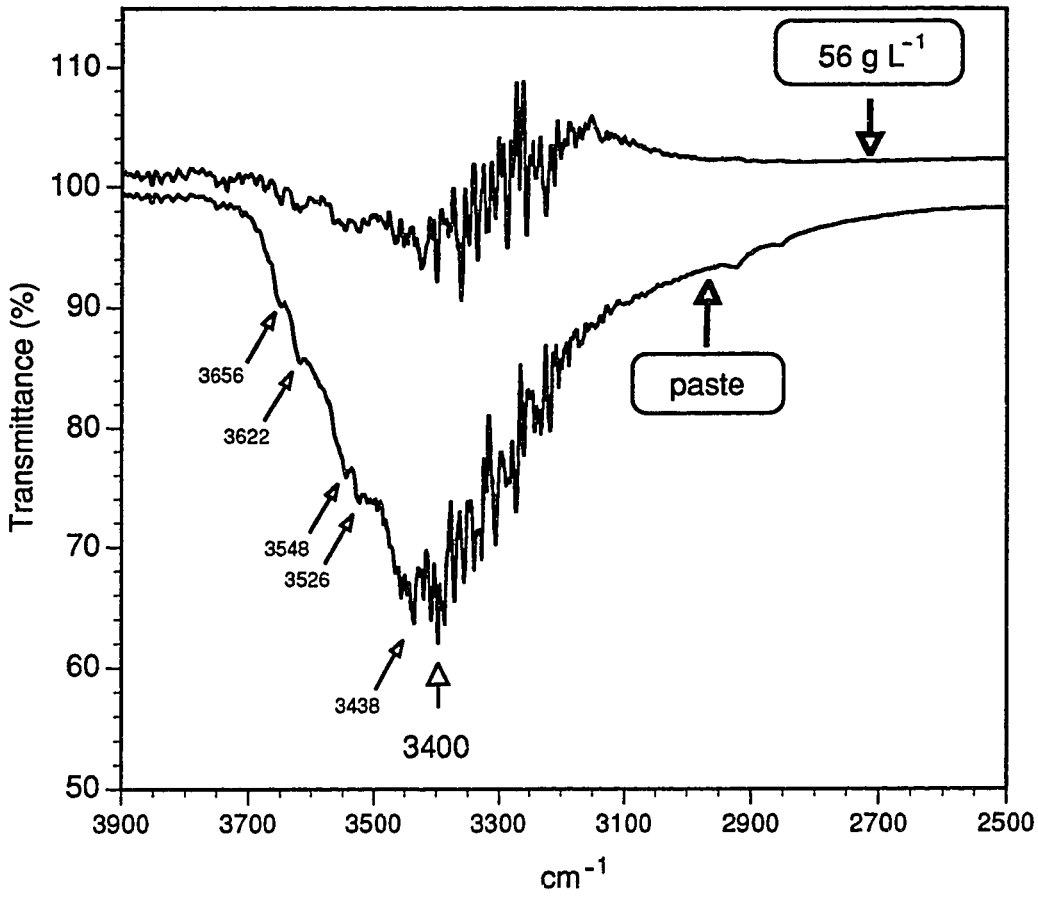

Figure 3.1 **The 3900 to 2500 cm^{-1} region of the HATR-FTIR spectra of a dialyzed alumina suspension (56 g L^{-1}) and alumina paste.**

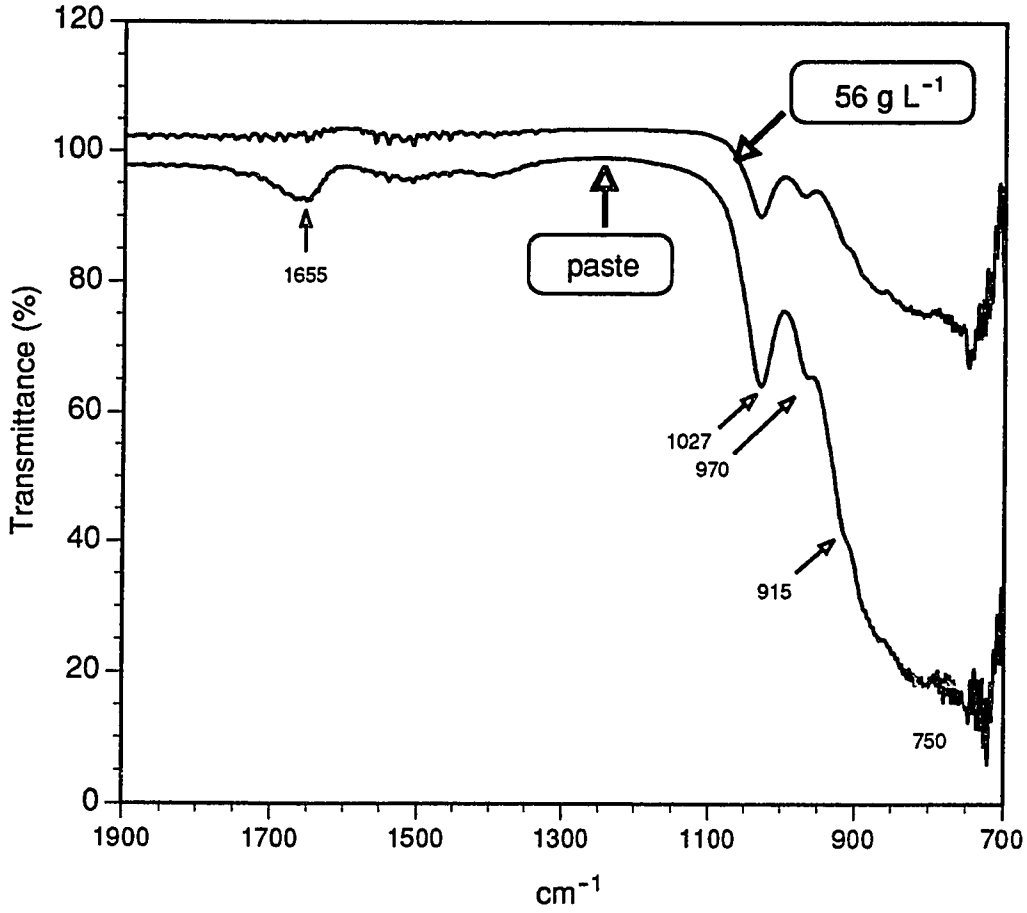

Figure 3.2 **The 1900 to 700 cm^{-1} region of the HATR-FTIR spectra of a dialyzed alumina suspension (56 g L^{-1}) and alumina paste.**

There are several absorption bands common to the spectra of the three aqueous alumina suspensions of varying concentration. Most notable is a broad band at 3400 cm^{-1} with several shoulders between 3656 cm^{-1} and 3438 cm^{-1}. The 3400 cm^{-1} band is located in the same region as the very broad and intense H_2O absorption band (0 % transmittance from 3390 to 3225 cm^{-1}) found in both the suspension and supernatant spectra between 3800 and 2650 cm^{-1} prior to spectral subtraction. As a result of the near complete IR absorption in this region, the subtraction process results in large residual noise, particularly on the low frequency side of the 3400 cm^{-1} band. This noise is reduced considerably by the signal-averaging of many scans (≥1000 scans) of both the suspension and supernatant prior to the subtraction process. However, some residual noise remains superimposed on the low frequency side of the 3400 cm^{-1} band, and thus this band is much more prominent in the spectrum of the suspension with the highest alumina particle concentration (the paste spectrum).

A smaller broad band at 1655 cm^{-1} is only visible in the paste spectrum and corresponds to the H-O-H bending region of surface-adsorbed H_2O (Ross, 1974). A sharp band located at 1027 cm^{-1} and several small shoulders on a broad absorbance centered at 750 cm^{-1} are also discernable. The bands between 1027 and 900 cm^{-1} correspond to the frequency range of Al-O-H bending modes (White, 1971). The 1027, 967, and 915 cm^{-1} bands are more easily seen in Fig. 3.4. The broad band at 3400 cm^{-1} is located in the OH stretching region of the IR spectrum,

and is attributable to surface OH groups and/or surface adsorbed H_2O on the alumina. All of the aforementioned bands are dependent on the particle concentration of alumina in the supernatant.

The effect of pH (pH 3 and 5) on the spectral bands of alumina suspensions of equal particle density (56 g L^{-1}) is shown in Figs. 3.3 and 3.4. As the pH of the suspension is decreased by additions of HCl, many of the bands seen in Figs. 3.1 and 3.2 (pH 6.5, no acid or base added) increase in intensity. No change in the location of bands with a decrease in pH was noted. The bands located at 3656, 3622, 3548, 3527, 3464, and 3438 cm^{-1} exhibit perhaps the most conspicuous pH dependence (Fig. 3.3). In the pH 3 spectrum, these bands no longer appear as shoulders on the broad band centered at 3400 cm^{-1}, but are now very sharp bands which partially obscure the 3400 cm^{-1} band. Since their intensity increases with an increase in H^+ activity in the suspension, this suggests that they may be due to the OH_2^+ surface group on the alumina surface, the prevalent surface functional group at low pH. To confirm the assignments of the low pH alumina bands, spectra were obtained of suspensions of equal pH (4.2) and varying particle concentration (11, 28, and 56 g L^{-1}). The spectra of the 28 g L^{-1} and the 56 g L^{-1} alumina suspensions at pH 4.2 appear in Figs. 3.5 and 3.6. All bands attributed to alumina in the suspension demonstrated the expected particle concentration dependence, with band intensities increasing with an increase in alumina particle density.

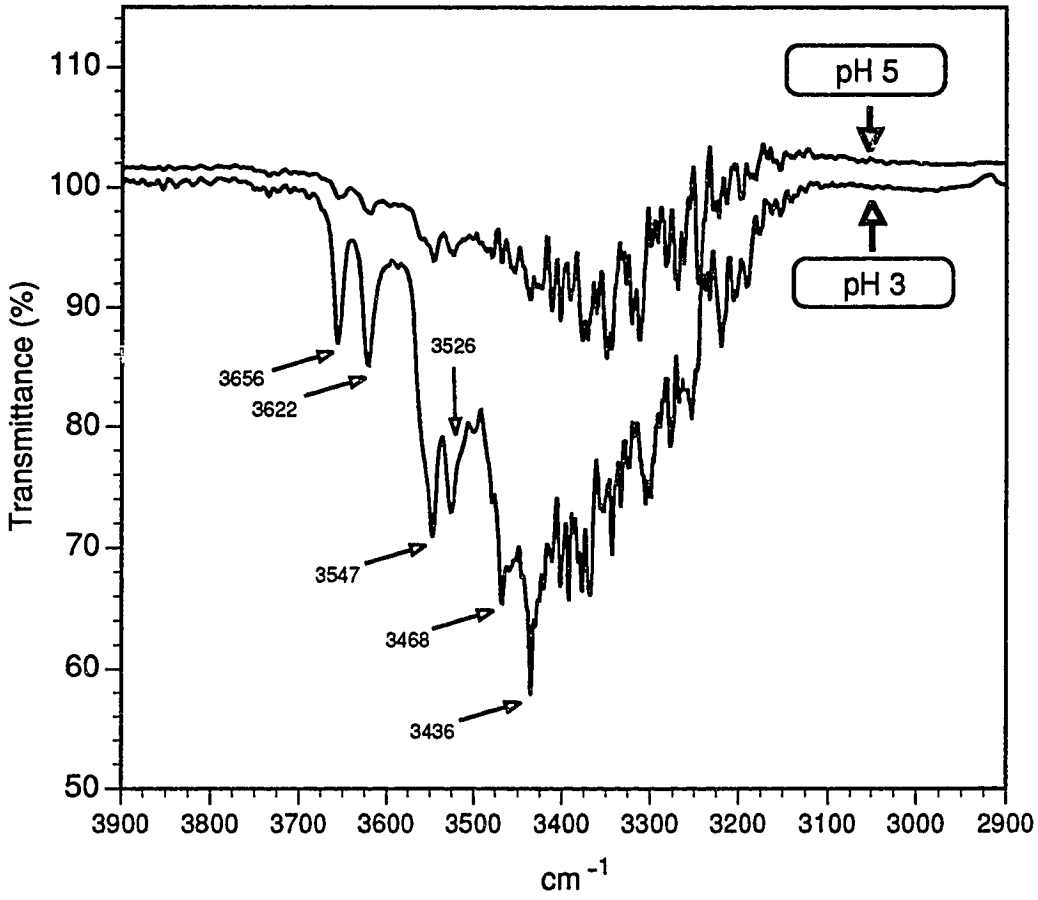

Figure 3.3 **The 3900 to 2900 cm^{-1} region of the HATR-FTIR spectra of alumina suspensions (56 g L^{-1}) at pH 3 and 5.**

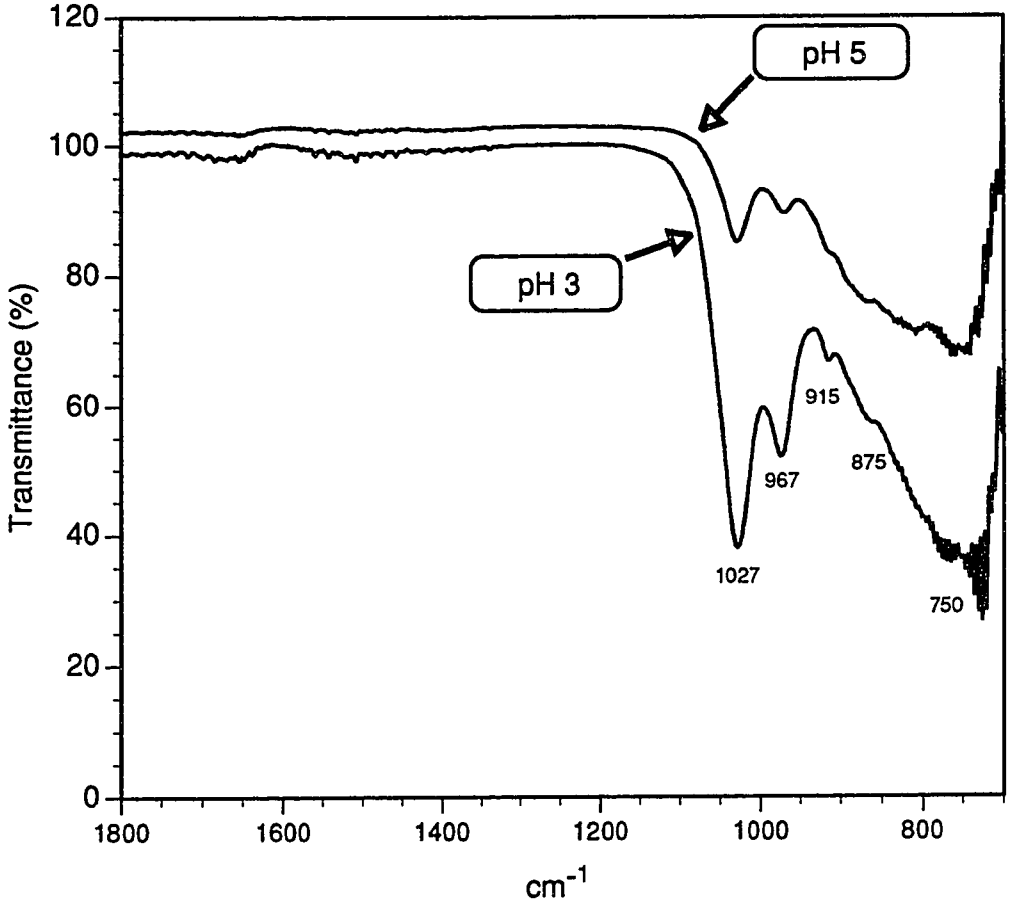

Figure 3.4 The 1800 to 750 cm^{-1} region of the HATR-FTIR spectra of alumina suspensions (56 g L^{-1}) at pH 3 and 5.

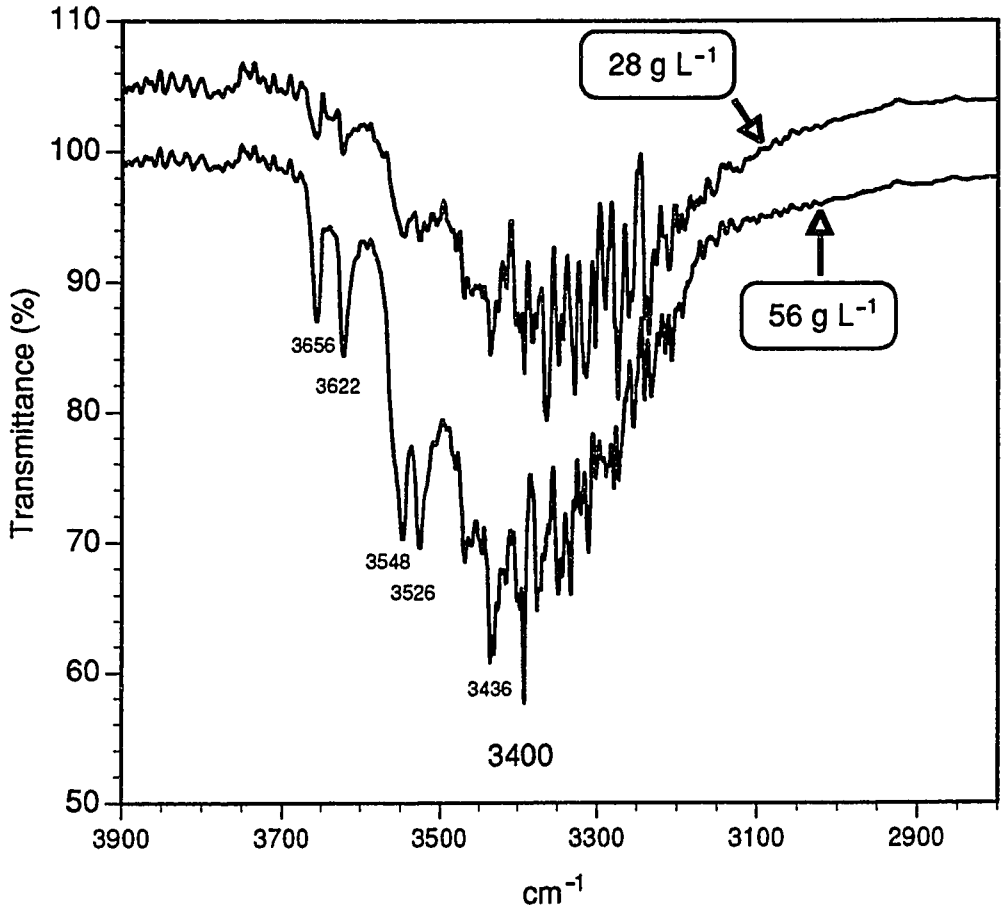

Figure 3.5 **The 3900 to 2800 cm^{-1} region of the HATR-FTIR spectra of alumina suspensions (28 g L^{-1} and 56 g L^{-1}) at pH 4.2.**

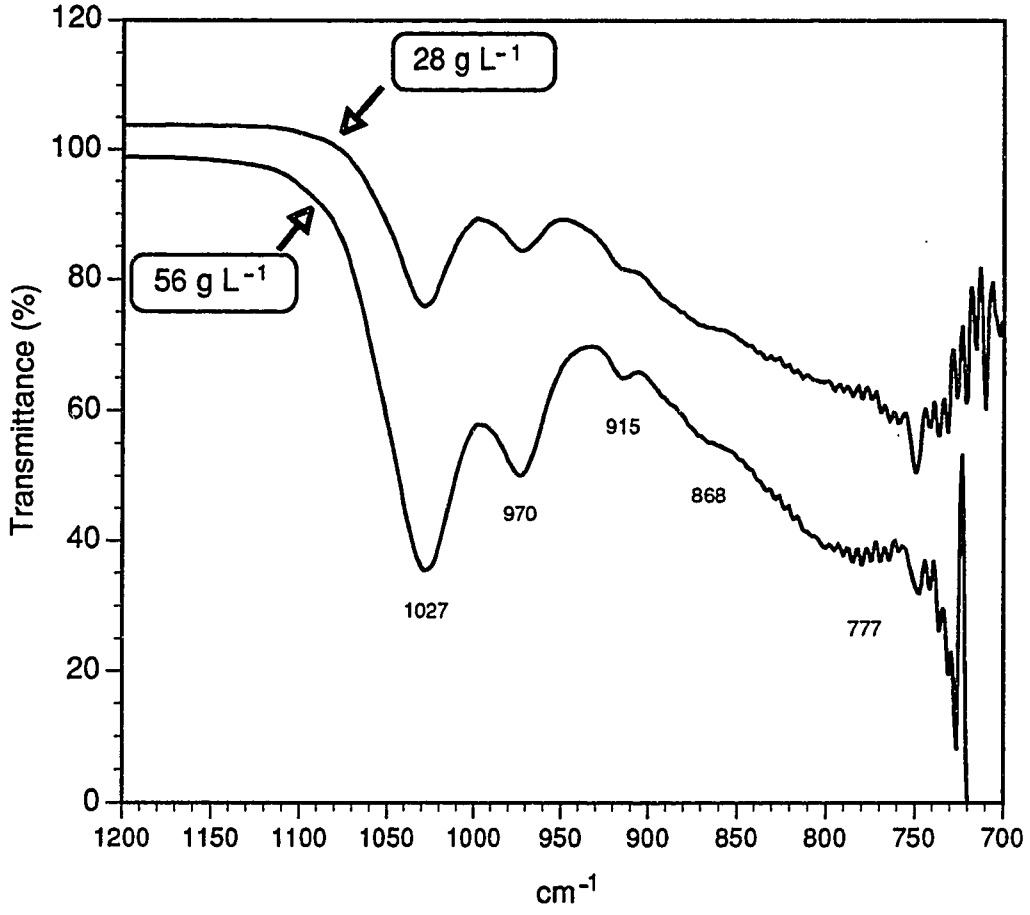

Figure 3.6 **The 1200 to 700 cm^{-1} region of the HATR-FTIR spectra of alumina suspensions (28 g L^{-1} and 56 g L^{-1}) at pH 4.2.**

The fact that all of the alumina bands, with the possible exception of the 3400 cm^{-1} band, are more intense in the low pH spectrum (including the 1027, and 967 cm^{-1} peaks) is anomalous, however. This would indicate that nearly all of the bands in the alumina spectrum are attributable to protonated surface functional groups since no other IR absorbing species would be expected to increase as a result of acid additions to the suspension. If these bands are attributable to OH_2^+ surface groups, they should be absent from the spectrum of alumina under very alkaline conditions (pH>>ZPC≈8). Furthermore, if these bands are due to proton bearing surface groups, they should relocate upon deuteration of the alumina suspension.

To test this hypothesis, spectra were obtained of an alumina suspension (56 g L^{-1}) adjusted to pH 11.5 (Figs. 3.7 and 3.8). At this pH, very few, if any, surface functional groups should be in the OH_2^+ form. All of the pH dependent bands of the alumina were more intense in the pH 11.5 spectrum than in the pH 6.5 spectrum (Figs. 3.1 and 3.2), indicating they do not pertain to OH_2^+ surface groups.

Treatment of the alumina with D_2O provides a means of distinguishing between surface OH and structural OH group bands in the oxide spectrum (Peri and Hannan, 1960). Spectra of alumina treated with and suspended in D_2O (a 55 g L^{-1} suspension and D_2O-alumina paste) are presented in Figs. 3.9 and 3.10. A new band centered near 2500 cm^{-1} is seen in the D_2O-alumina spectra and corresponds to the stretching vibration frequency of surface OD groups (Hair, 1967). Given the

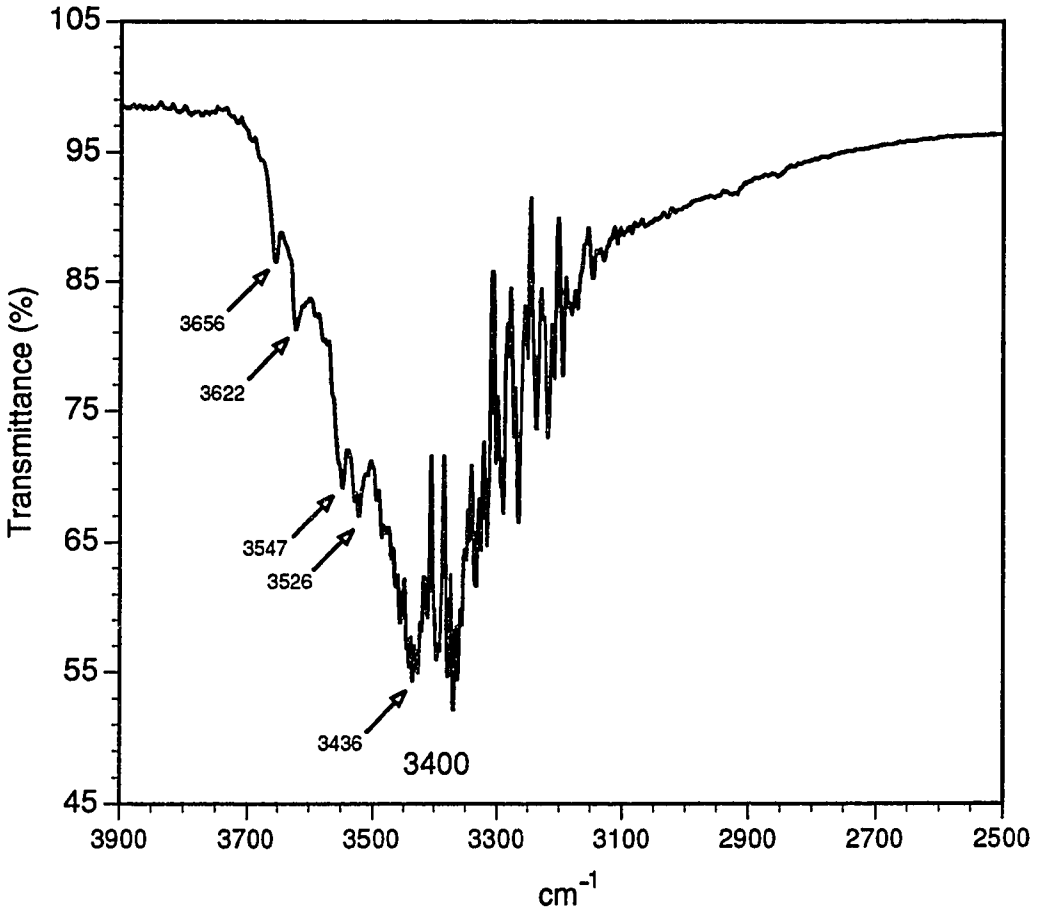

Figure 3.7 The 3900 to 2500 cm^{-1} region of the HATR-FTIR spectrum of an alumina suspension (56 g L^{-1}) at pH 11.5.

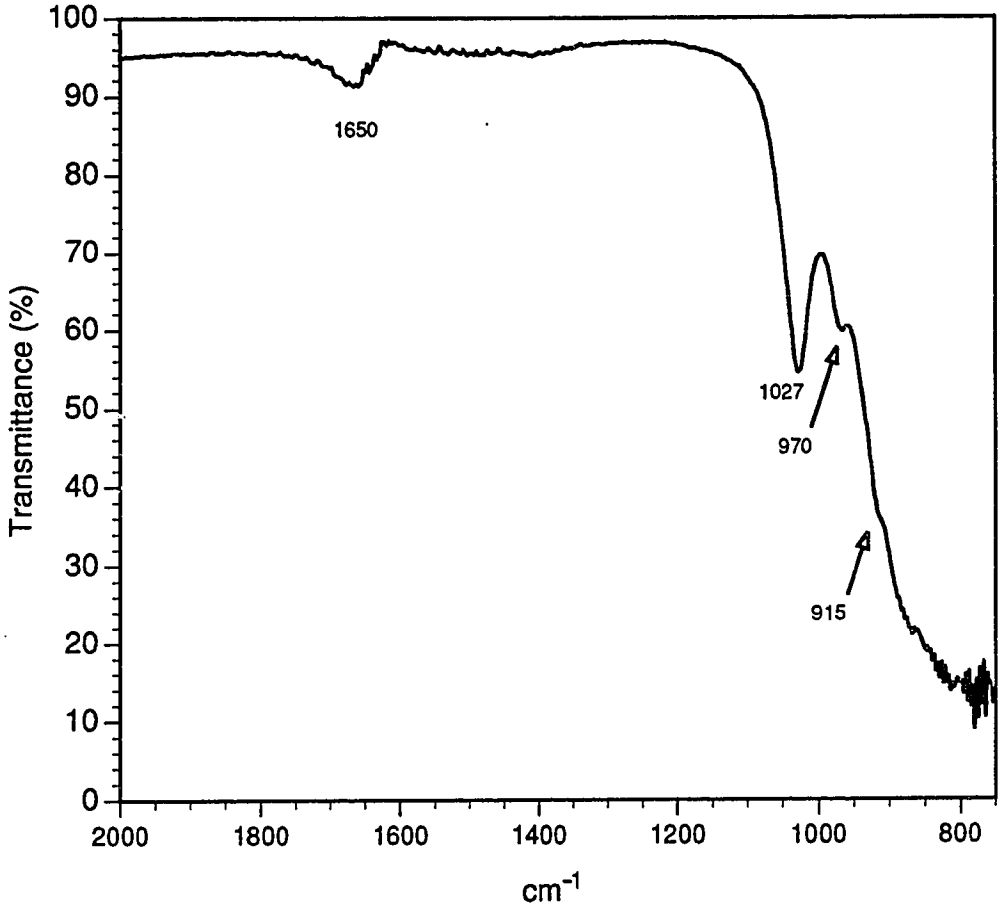

Figure 3.8 The 2000 to 750 cm^{-1} region of the HATR-FTIR spectrum of an alumina suspension (56 g L^{-1}) at pH 11.5.

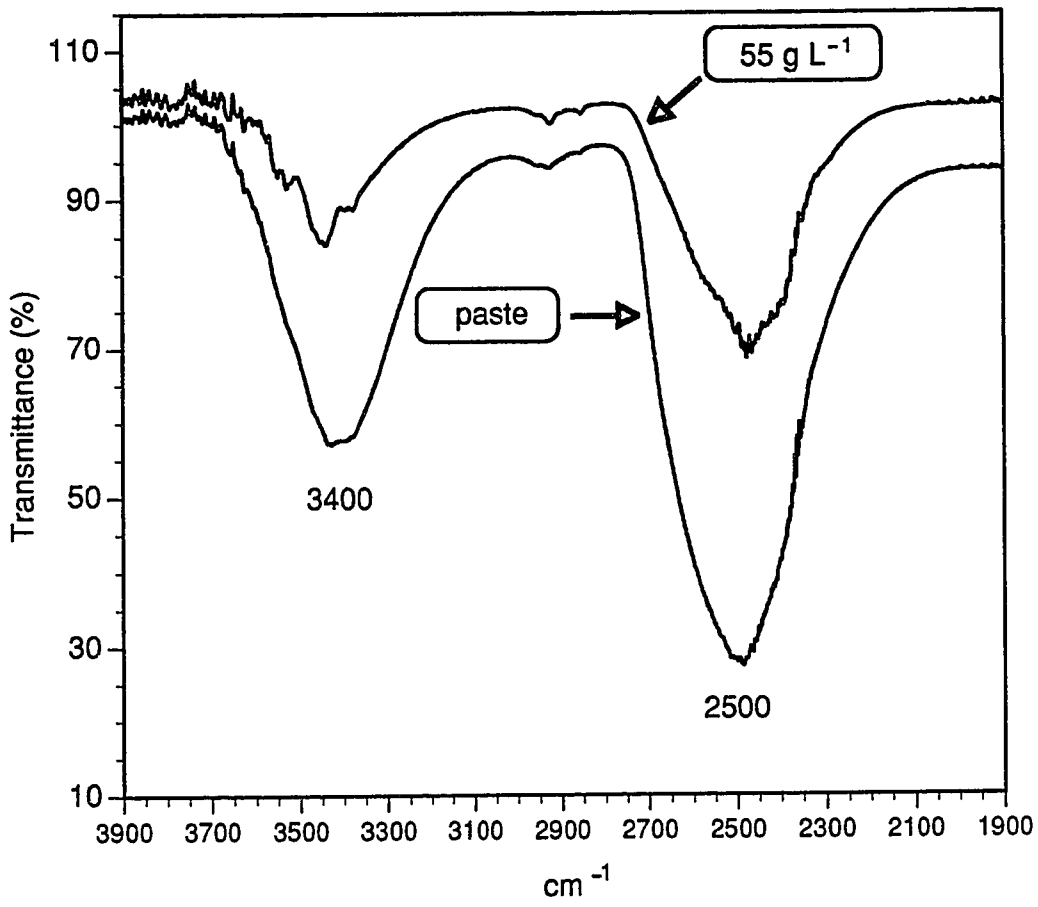

Figure 3.9 The 3900 to 1900 cm^{-1} region of the HATR-FTIR spectra of a deuterated alumina suspension (56 g L^{-1}) and a deuterated alumina paste.

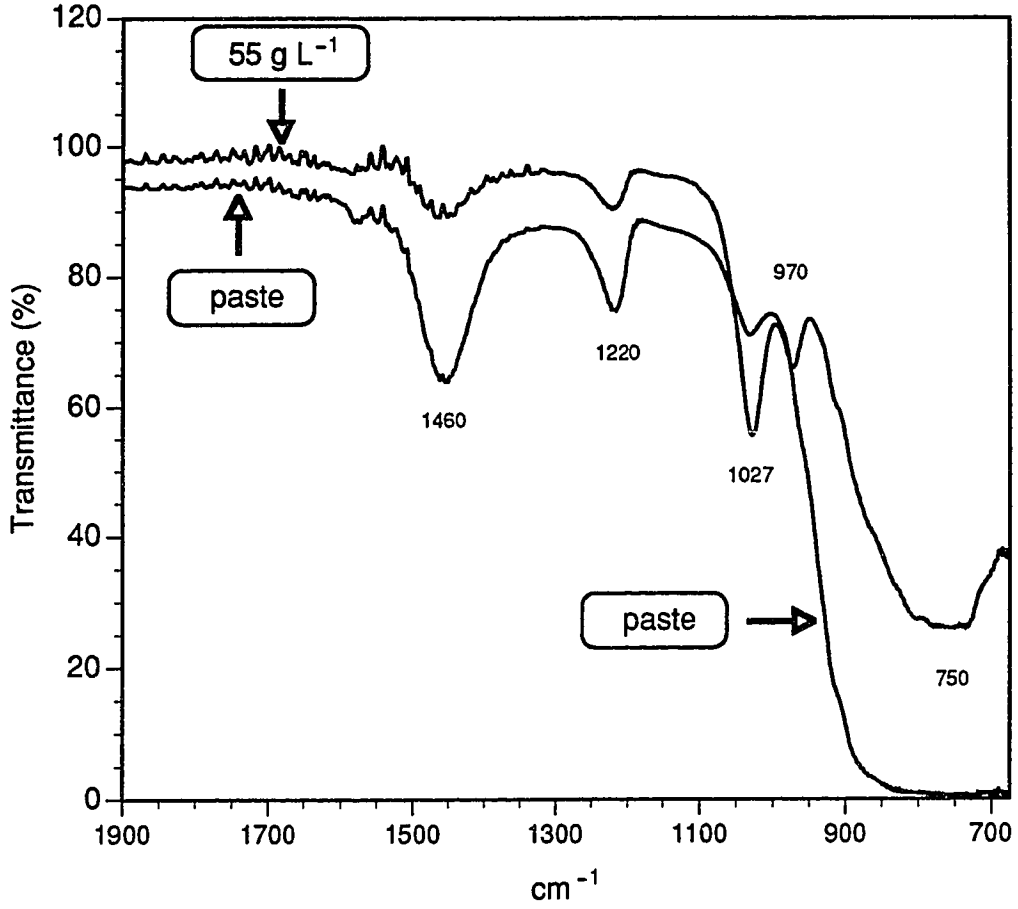

Figure 3.10 **The 1900 to 675 cm^{-1} region of the HATR-FTIR spectra of a deuterated alumina suspension (56 g L^{-1}) and a deuterated alumina paste.**

location of the 2500 cm^{-1} OD band and considering the atomic mass effects resulting from an exchange of D for H, the 3400 cm^{-1} band in the H_2O-alumina spectra (Figs. 3.1, 3.3, 3.5, and 3.7) must be due, at least in part, to a proton bearing surface group. However, rather than being replaced entirely by the 2500 cm^{-1} band, the 3400 cm^{-1} band remains in the D_2O-alumina spectrum. Persistence of the 3400 cm^{-1} band, in addition to the appearance of a new OD band at 2500 cm^{-1} following deuteration, was also found by White and coworkers in the spectrum of an aluminum hydroxide gel (White and Roth, 1986). The band at 3400 cm^{-1} in the D_2O-alumina spectrum may be due to adsorbed HDO and/or H_2O since the repeated washing with D_2O would only result in a dilution of the H_2O. Remaining traces of HDO and H_2O in the D_2O-alumina suspensions are thus expected following the D_2O wash. HDO absorbs in the 3400 cm^{-1} region of the IR spectrum, as well as near 1450 cm^{-1} (Falk and Ford, 1966). An absorption band at 1460 cm^{-1} appears prominently in the deuterated alumina spectra (Fig. 3.10). The new band found at 1220 cm^{-1} (Fig. 3.10) is due to adsorbed D_2O and replaces the 1650 cm^{-1} band due to adsorbed H_2O in the H_2O-alumina spectrum (Fig. 3.2). A comparison of the spectra of equivalent concentrations of alumina in H_2O and D_2O highlights the spectral changes resulting from the D_2O treatment (Figs. 3.1 and 3.9). In the spectrum of 55 g L^{-1} D_2O-alumina (Fig. 9), the bands between 3656 and 3438 cm^{-1} are still visible as shoulders on the 3400 cm^{-1} band. If these were due to surface hydroxyl groups they should be exchangeable with D in the supernatant

with a resultant change in band location. It appears, therefore, that these bands are due to structural OH in the bulk of the mineral which are not susceptible to D exchange.

The effect of D^+ activity in the suspension (pD) on the spectrum of D_2O-alumina is shown in Figs. 3.11 and 3.12. As in the H_2O-alumina spectra, the intensity of the bands at 3656, 3622, 3548, 3526, 3464, and 3438 cm^{-1}, as well the 1027, 970, and 915 cm^{-1} bands, are strongly dependent on acidity. These bands are much more intense at pD 2 (Figs. 3.11 and 3.12) than in the pD 6 spectrum (Figs. 3.9 and 3.10). Two additional bands are discernable at 3393 and 3375 cm^{-1} in the pD 2 spectrum without the interference of the H_2O subtraction noise (Fig. 3.11). The locations of the 3656 to 3438 cm^{-1} bands, as well as the 1027, 970, and 915 cm^{-1} bands, are not affected by a change from H_2O to D_2O in the supernatant. The bands appear sharper at low pD, however. This may result from a decrease in intensity of the broad band at 3400 cm^{-1}, further evidence that the H-bonded OH surface group, whose concentration decreases due to protonation and D exchange at low pD, contributes to the absorbance at 3400 cm^{-1}. The sharpness of the 3656 to 3375 cm^{-1} bands indicates an environment unaffected by the solvent. Hydrogen bonding between the solvent (D_2O and H_2O) and surface groups tends to broaden surface group bands (e.g., the 3400 cm^{-1} band). The absence of band broadening and exclusion from the solvent indicates these are structural OH group bands and not surface group bands.

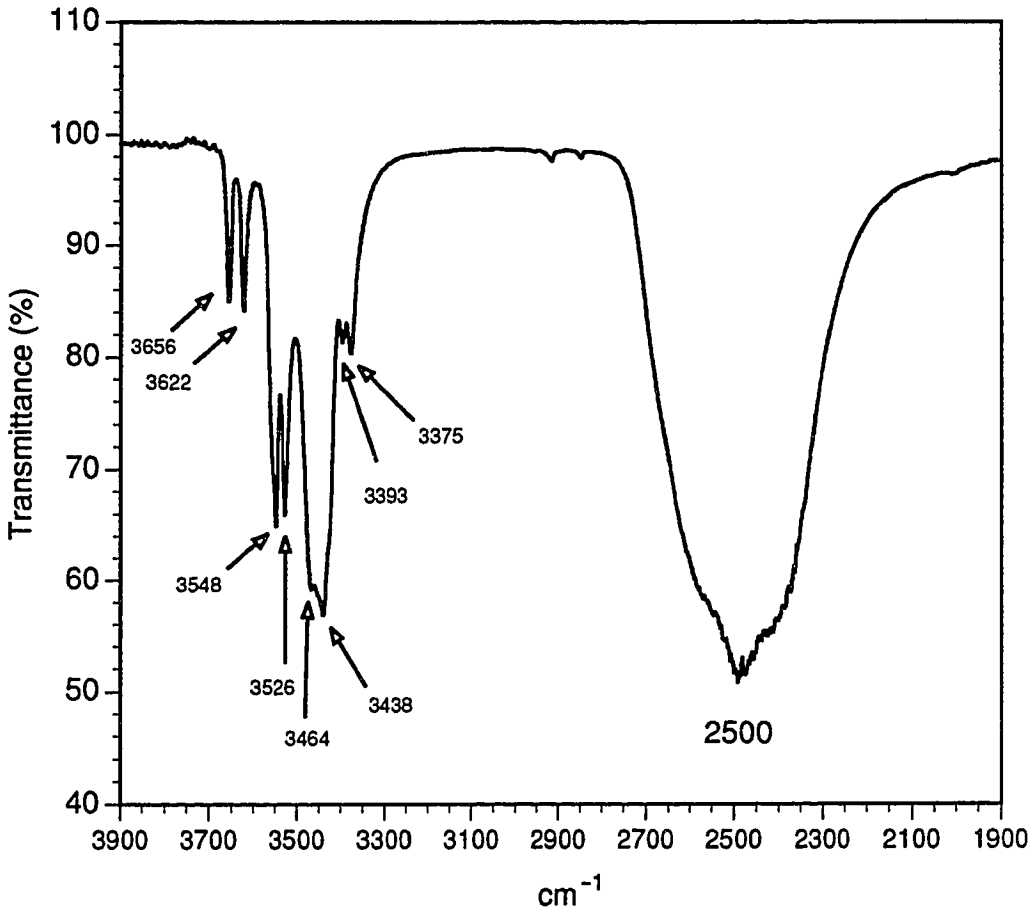

Figure 3.11 The 3900 to 1900 cm^{-1} region of the HATR-FTIR spectrum of a deuterated alumina suspension (55 g L^{-1}) adjusted to pD 2.

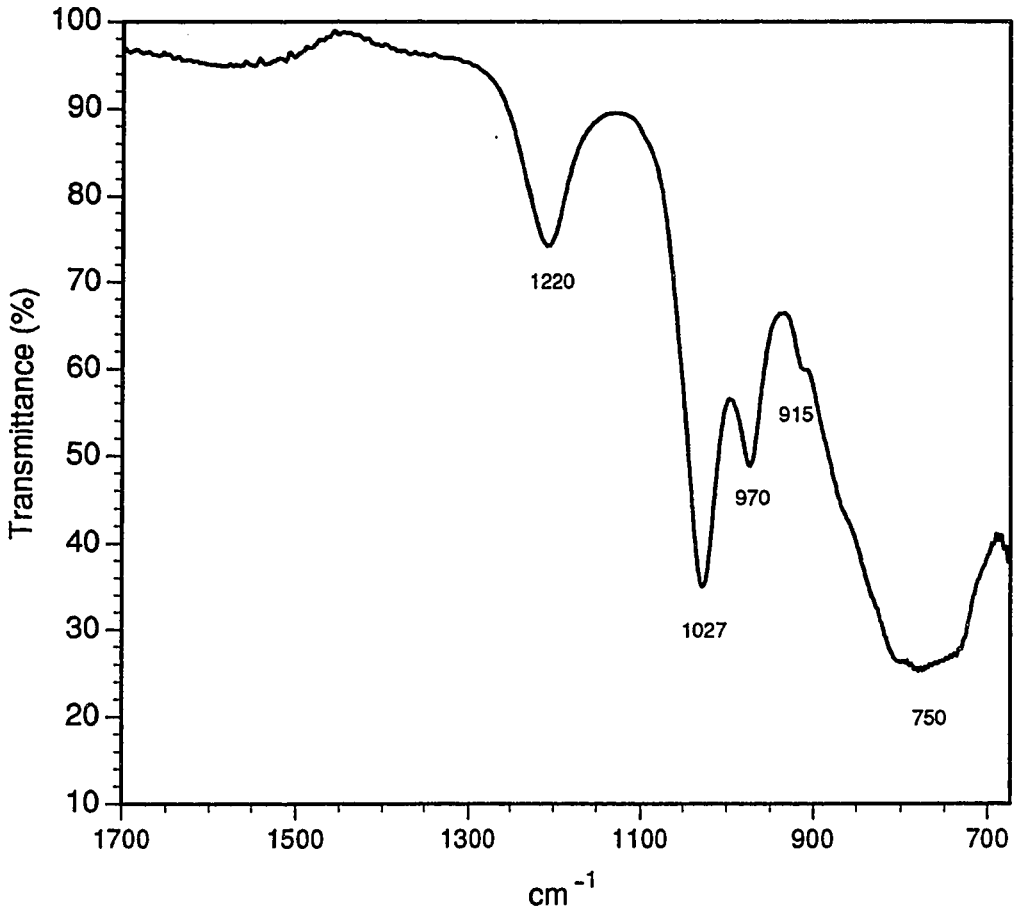

Figure 3.12 **The 1700 to 675 cm^{-1} region of the HATR-FTIR spectrum of a deuterated alumina suspension (55 g L^{-1}) adjusted to pD 2.**

The persistence of both the 3400 cm^{-1} band in the H_2O-alumina spectrum, and the 2500 cm^{-1} band in the D_2O-alumina spectrum, over a wide range of pH (pD) is difficult to explain if they are each attributed to only one form of the pH-dependent surface functional group. It would appear that these bands are actually overlapped surface OH (or OD) bands, OH_2^+ (or OD_2^+) surface group bands, and adsorbed solvent (H_2O, HDO and D_2O) bands. Band broadening as a result of hydrogen bonding precludes resolving the individual solvent and surface group bands. As pH or pD is decreased, the OH_2^+ and OD_2^+ groups, respectively, form at the expense of the neutral surface groups. Therefore, as the neutral surface group band intensity decreases, the protonated surface group band intensity increases. This results in very little net change in band intensity near 3400 cm^{-1} and 2500 cm^{-1} as pH or pD changes.

The unusual pH response of the aqueous alumina spectrum suggests an explanation other than an increase in concentration of the protonated surface site. It has been established that alumina dissolution occurs to a small extent in aqueous suspensions (Schulthess and Sparks, 1986) and that aqueous Al^{3+} hydrolyzes to form soluble polymeric aluminum species in solution. Precipitation of polymeric aluminum is favored near neutral pH. The undissolved alumina may act as a nucleation site facilitating the precipitation of aluminum polymers. This would result in a gibbsite-like layer coating the surface of the alumina. This layer may

redissolve at both low pH and high pH, affording the shallow-penetrating HATR-IR beam greater interaction with the bulk OH of the undissolved alumina.

To determine if a metastable Al-hydroxide coating on the alumina could explain the pH effects on the alumina spectrum, an Al-hydroxide gel suspension (41.4 g L^{-1}) was precipitated by neutralizing a 0.2 mol L^{-1} $Al(NO_3)_3$ solution with NaOH. The spectrum of the paste obtained by centrifuging this gel suspension appears in Figs. 3.13 and 3.14. No absorption bands found previously in the alumina spectra were visible in the spectrum of the precipitated Al-hydroxide. Two bands located at 1392 and 1352 cm^{-1} and a broad absorbance at 970 cm^{-1} are the most prominent features of the gel spectrum (Fig. 3.14). There also appears to be a broad band centered at 3520 cm^{-1} which is partially obscured by subtraction noise in the region of the strongest solvent absorption (Fig. 3.13).

Nail et al., (1976) prepared an Al-hydroxide gel by neutralizing (to pH 7.0) a $AlCl_3$ solution with NH_4OH. Infrared spectra of the Al-gel were obtained at several intervals throughout a 147 d aging period from air died films. The authors found that the resolution in the spectrum of the Al-gel increased over time indicating that the amorphous gel developed greater crystalline order as aging progressed. Increased crystallinity over time was confirmed by X-ray diffraction analysis. The spectrum of the freshly precipitated gel revealed only three diffuse bands, a very broad band between 3700 and 2900 cm^{-1} and two broadened bands of lesser intensity centered at 1640 cm^{-1} and 900 cm^{-1}. The authors assigned the

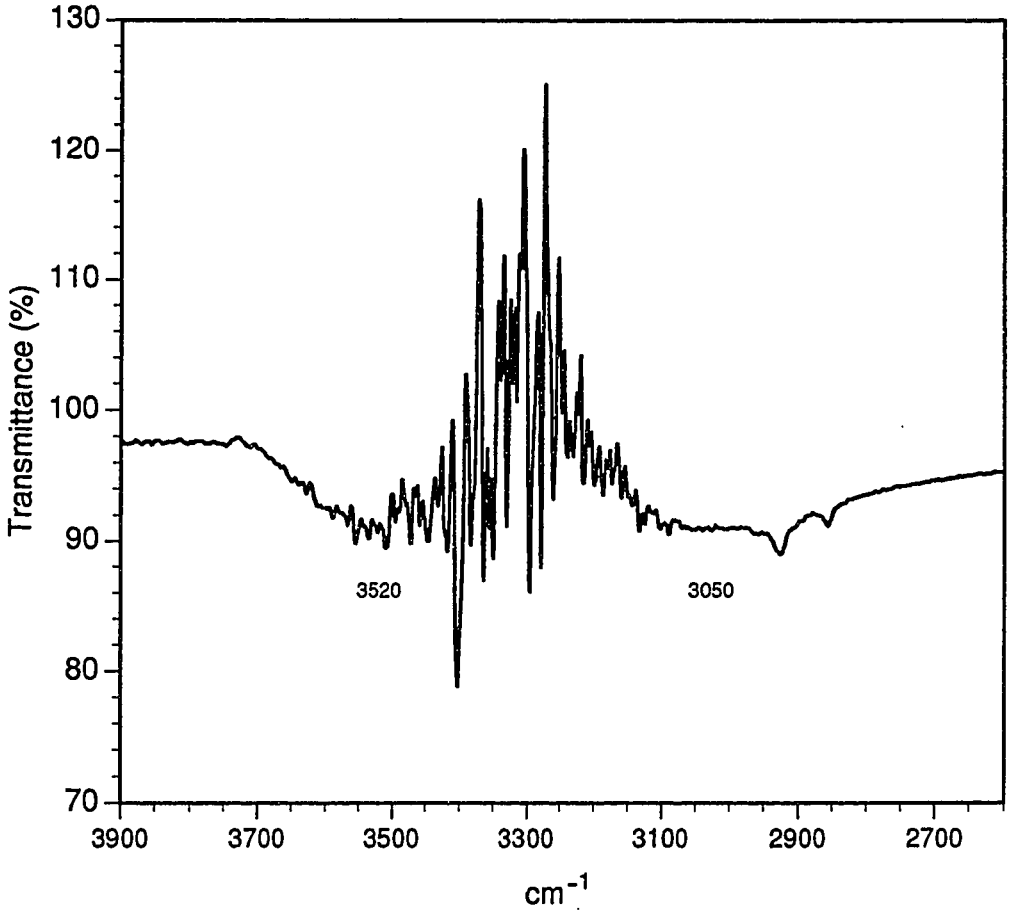

Figure 3.13 The 3900 to 2600 cm^{-1} region of the HATR-FTIR spectrum of a freshly precipitated $Al(OH)_3$ gel paste at pH 6.5.

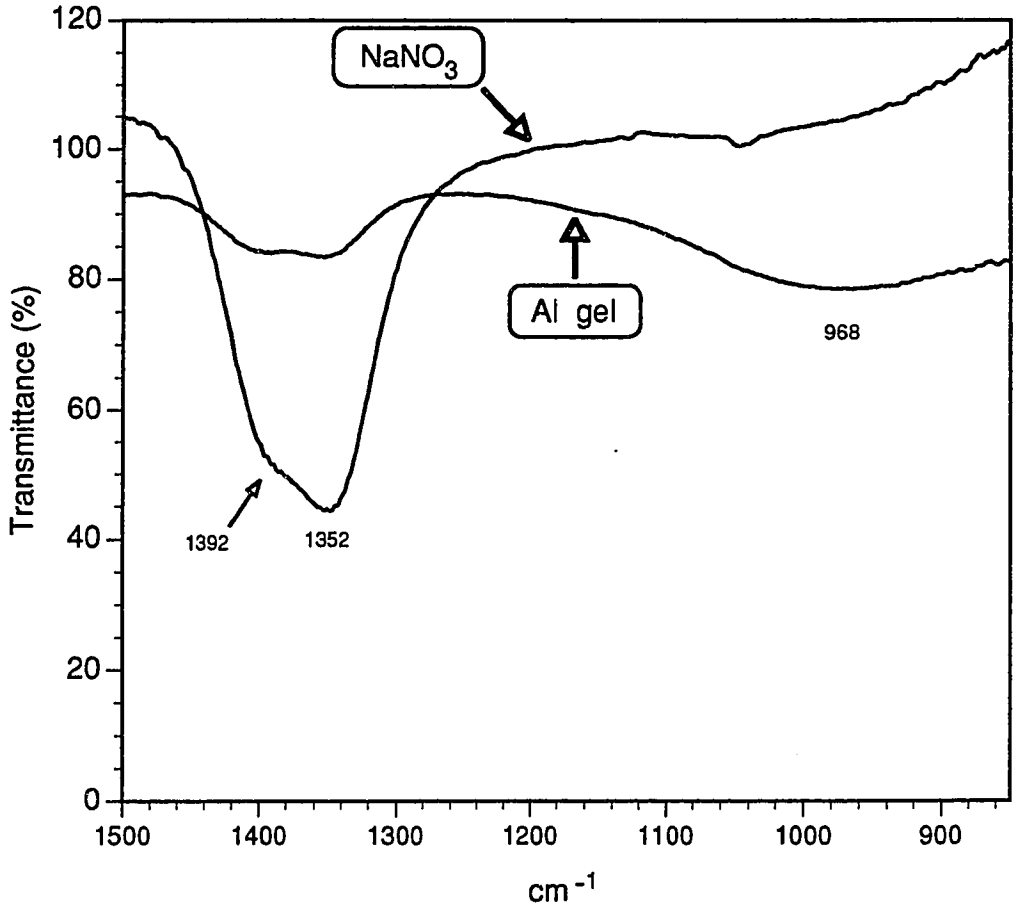

Figure 3.14 **The 1500 to 850 cm^{-1} region of the HATR-FTIR spectra of a freshly precipitated $Al(OH)_3$ gel paste at pH 6.5 and a 0.6 mol L^{-1} $NaNO_3$ solution.**

3700-2900 cm^{-1} band to stretching vibrations of OH groups of the gel structure. The 1640 cm^{-1} band was assigned to surface adsorbed H_2O, and the 900 cm^{-1} band to OH deformation vibrations. The broadness of the 3700-2900 cm^{-1} and 900 cm^{-1} bands was attributed to disorder in the structure resulting in a continuum of chemical environments for the OH groups. After 42 d, the gel spectra began to develop more numerous and well resolved bands, culminating in sharp bands superimposed on the 3700-2900 cm^{-1} band at 3612, 3520, and 3470 cm^{-1}, and a well resolved band at 1020 cm^{-1} with a less intense shoulder at 970 cm^{-1} after 124 d. Spectra were obtained of a 0.2 mol L^{-1} $Al(NO_3)_3$ solution (not shown), as well as a 0.6 mol L^{-1} $NaNO_3$ solution (Fig. 3.14). The 1392 and 1352 cm^{-1} bands were found in both the Al^{3+} and Na^+ solution spectra. The 1500 to 850 cm^{-1} region of the $NaNO_3$ spectrum is shown in Fig. 3.14. The 970 cm^{-1} band was found in the Al^{3+} solution and Al-gel spectra only. Serna et al. (1977) found absorption bands at 1395 and 1350 for NO_3^- bound by electrostatic attraction on an aluminum hydroxide gel. The bands in the Al-hydroxide gel spectrum can therefore be attributed almost entirely to the dissolved NO_3^- salts present.

In general, the Al-hydroxide gel spectra were relatively featureless compared to the alumina spectra of similar suspension density, particularly if the bands associated with the electrolyte in the gel suspension are ignored. Even in the case of the Al-hydroxide paste spectrum, the bands that were present were of relatively low intensity. This suggests that a thin amorphous hydroxide coating on

the alumina surface could reduce the intensity of alumina IR bands without characteristic bands of its own appearing in the spectrum of an aqueous alumina suspension of intermediate pH. This hypothesis is even more conceivable for HATR-FTIR spectra, where the spectral features of the surface of the colloid are accentuated relative to the bulk.

3.4.2 Aqueous and Adsorbed B Spectra

In order to establish the location of bands attributable to aqueous B species, spectra were obtained of $B(OH)_3$ dissolved in H_2O and in D_2O (0.35 mol L^{-1} B, pH/pD = 4.6) (Figs. 3.15 and 3.16). In each case, the spectrum of the pure solvent was subtracted from the solution spectrum. Bands attributable to dissolved B are located at 1405 and 1149 cm^{-1} in H_2O (Fig. 3.15), and 1392 and 892 cm^{-1} in D_2O (Fig. 3.16). Infrared bands near 1400 cm^{-1} have been assigned to the trigonal B-O asymmetric stretching (υ_3) vibration (Volkhin et al., 1983; Beyrouty et al., 1984), and near 1150 and 900 cm^{-1} to B-O-H and B-O-D bending vibrations, respectively. There is also a broad band at 3400 cm^{-1}, visible in both the H_2O and D_2O spectra, which may be due to H-bonded OH groups of aqueous B species in the H_2O solution or HDO in the D_2O solution. Spectra of 0.18 mol L^{-1} B solutions in H_2O and D_2O revealed that the intensity of these bands assigned to aqueous B are dependent on the concentration of dissolved B (not shown).

The 1600 to 750 cm^{-1} region of the spectrum of a 0.35 mol L^{-1} B solution at pH 10.6 is shown in Figure 3.17. The band at 1405 cm^{-1}, seen

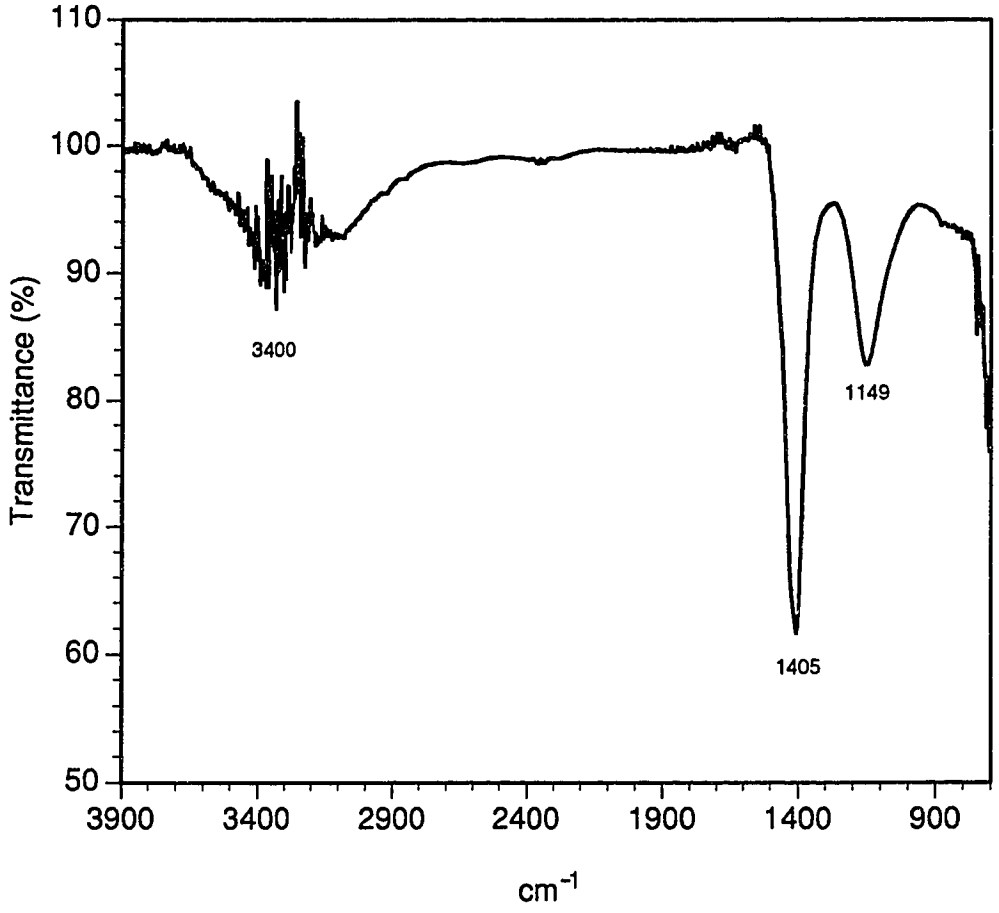

Figure 3.15 **The HATR-FTIR spectrum of a 0.35 mol L^{-1} B solution in H_2O (pH 4.6).**

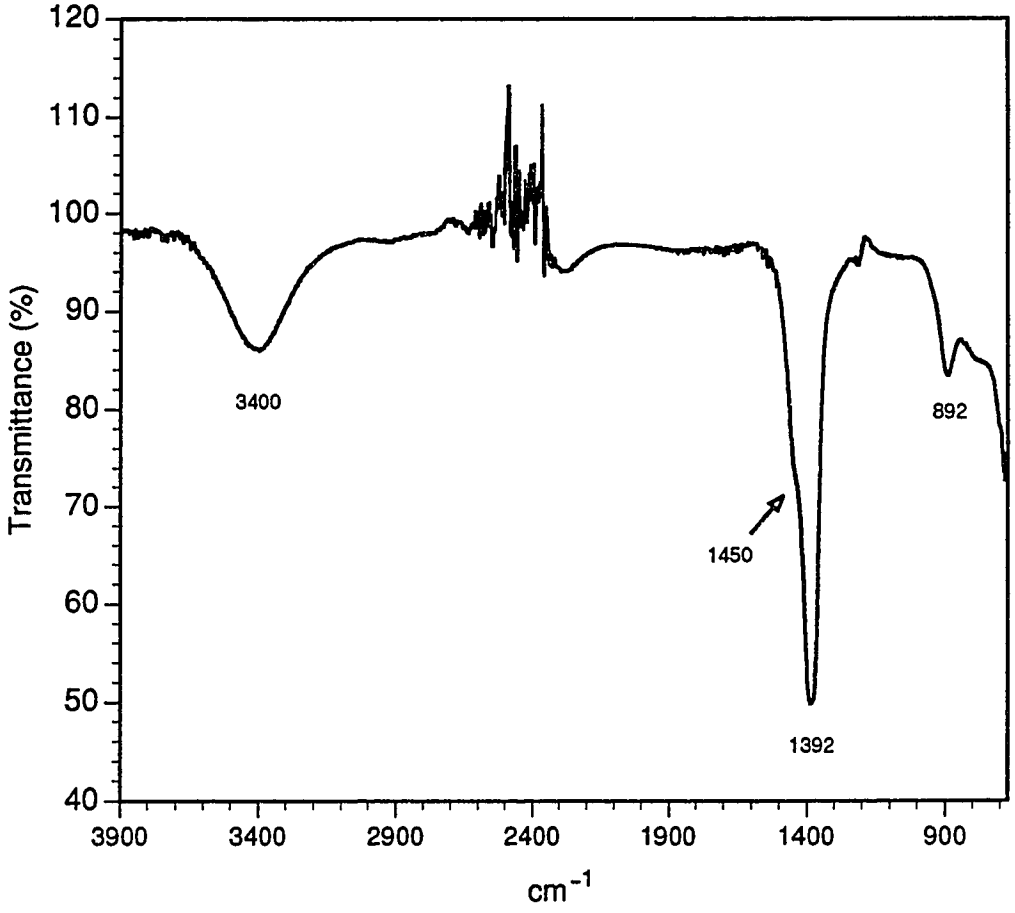

Figure 3.16 The HATR-FTIR spectrum of a 0.35 mol L^{-1} B solution in D_2O (pD 4.6).

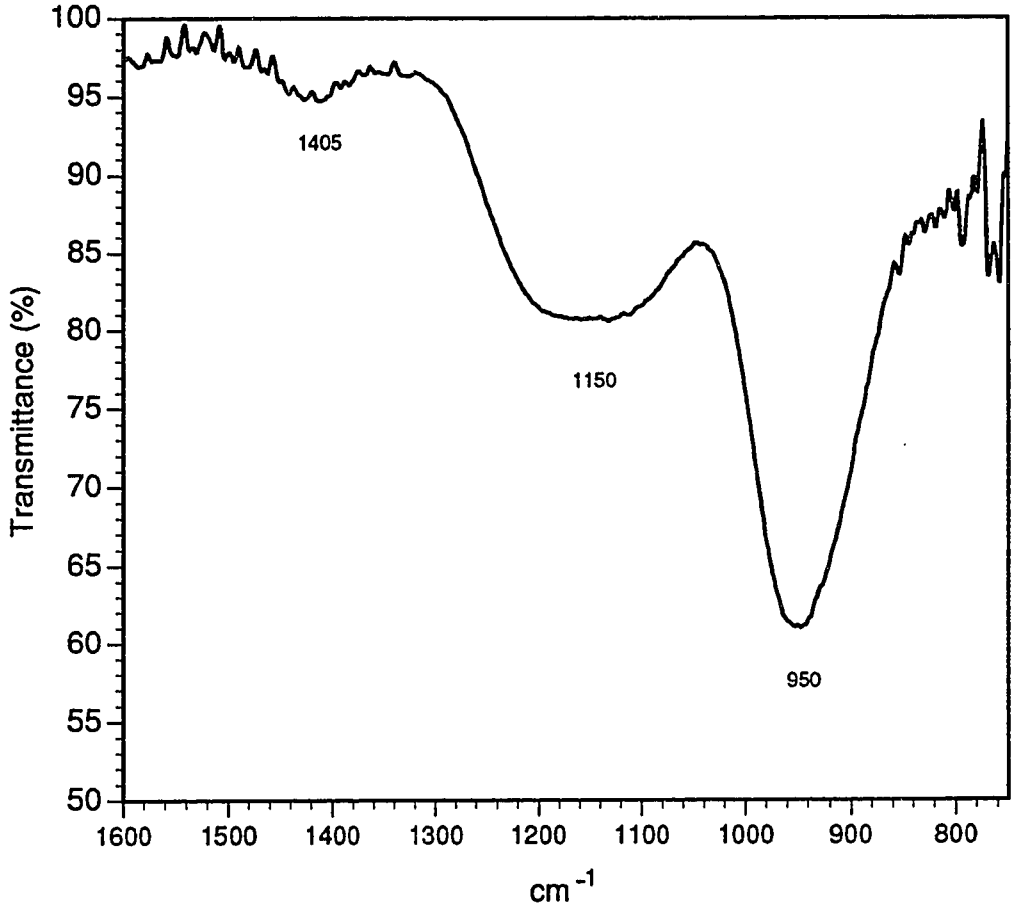

Figure 3.17 The HATR-FTIR spectrum of a 0.35 mol L^{-1} B solution in H_2O adjusted to pH 10.6.

previously at pH 4.6 (Fig. 3.15) is greatly diminished at high pH in favor of a new band at 950 cm^{-1}. Absorbance bands between 900 and 1000 cm^{-1} have been assigned to tetrahedral B-O υ_3 vibrations (Edwards et al., 1955; Ross, 1974). At pH 10.6, less than 4% of aqueous B remains as the trigonal BA monomer (Ingri et al., 1957). The balance exists as the tetrahedral BT monomer or aqueous polyborates of combined trigonal and tetrahedral coordination. The B-O-H bending vibration near 1150 cm^{-1} is only slightly dependent on B coordination and should not change significantly with a change from trigonal to tetrahedral coordination (Ross, 1974). It appears broader in the high-pH spectrum (Fig. 3.17), which indicates that it is due to a combination of both coordination states.

Two general approaches can be taken to study B adsorbed on alumina using IR spectroscopy, either noting changes in alumina surface group bands following B adsorption, and/or identifying new bands due to adsorbed B associated with the alumina surface. Of these two approaches, the former is the least feasible for aqueous alumina suspensions. In a suspension containing solvent, alumina and aqueous B, all largely comprised of OH groups, many different species will absorb IR radiation at approximately the same frequency as the alumina surface groups (~3400 cm^{-1}). Furthermore, band broadening effects of the solvent make this task even more unmanageable, and sorting the effects of the various contributors to absorbance at this frequency becomes extremely difficult. Spectra of alumina/B suspensions ranging from 0.02 to 0.18 mol L^{-1} total B produced insignificant

changes in absorbance intensity in the OH stretching region from spectra of alumina suspensions without adsorbed B (Fig. 3.18). Locating absorption bands attributable to adsorbed B in regions other than the OH stretching region then becomes the only practical means of determining the nature of the interaction between B and the alumina surface.

Evidence of adsorbed B can be seen in Figs. 3.18 and 3.19. A comparison of spectra obtained from pastes of alumina in H_2O with adsorbed B (Fig. 3.18) and without adsorbed B (Fig. 3.2) indicates the presence of two new bands at 1458 and 1301 cm^{-1} in the alumina with adsorbed B spectrum. These bands are not found in the spectrum of alumina in the absence of adsorbed B (Fig. 3.2). Studies of B adsorbed on $NiOH_2$ surfaces from $B(OH)_3$ solutions revealed a broad band centered near 1430 cm^{-1} which the authors assigned to the B-O υ_3 vibration of adsorbed B (Volkhin et al., 1983). Beyrouty and coworkers (1984) found bands at 1415 and 1300 cm^{-1} which they attributed to B adsorbed on gibbsite.

A comparison of the spectra of aqueous B (Figs. 3.15 and 3.17) and alumina with adsorbed B (Fig. 3.18) indicates that the bands at 1458 and 1301 cm^{-1} are unique to the adsorbed-B spectrum. The band at 1405 cm^{-1} in the aqueous-B spectra (Figs. 3.15 and 3.17) is absent in the adsorbed-B spectrum (Fig. 3.18). The aqueous-B band at 1405 cm^{-1} has been replaced by two new bands at 1458 and 1301 cm^{-1} in the adsorbed-B spectrum (Fig. 3.18). The 1149 cm^{-1} aqueous-B band

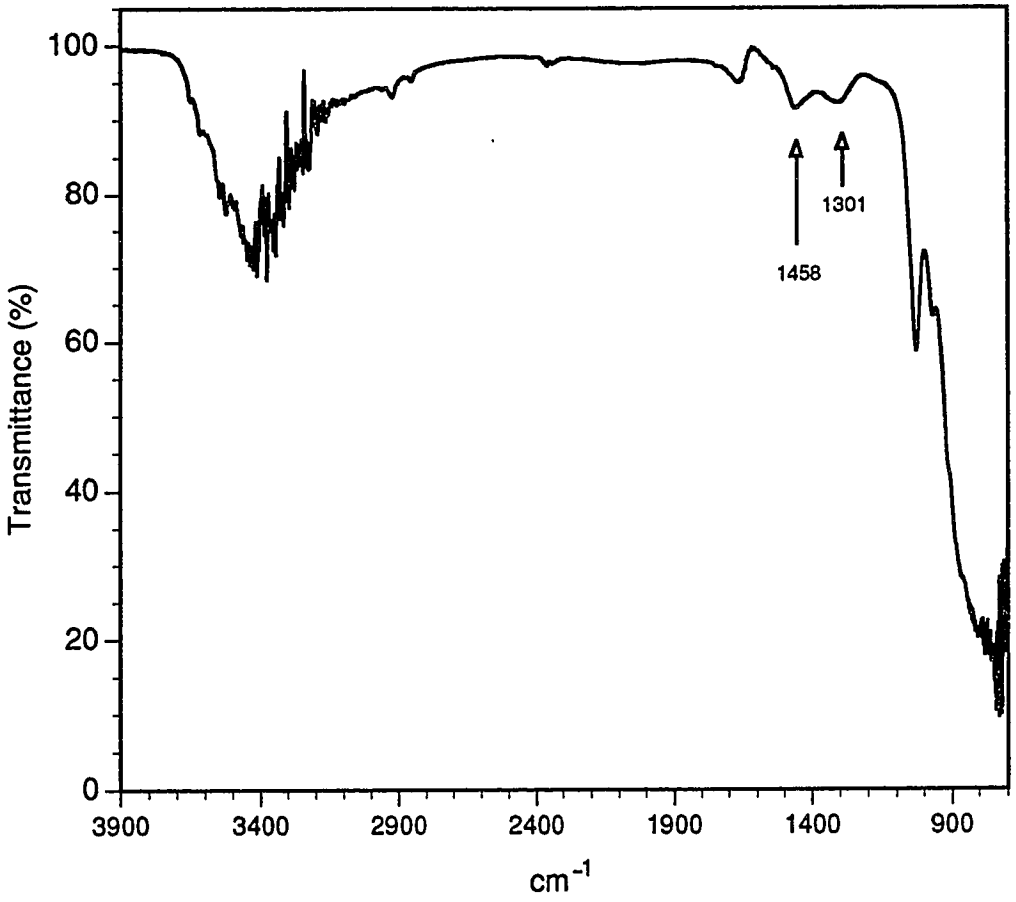

Figure 3.18 The HATR-FTIR spectrum of an alumina paste with adsorbed B. The paste was obtained from a 56 g L^{-1} alumina suspension with 0.18 mol total B L^{-1}.

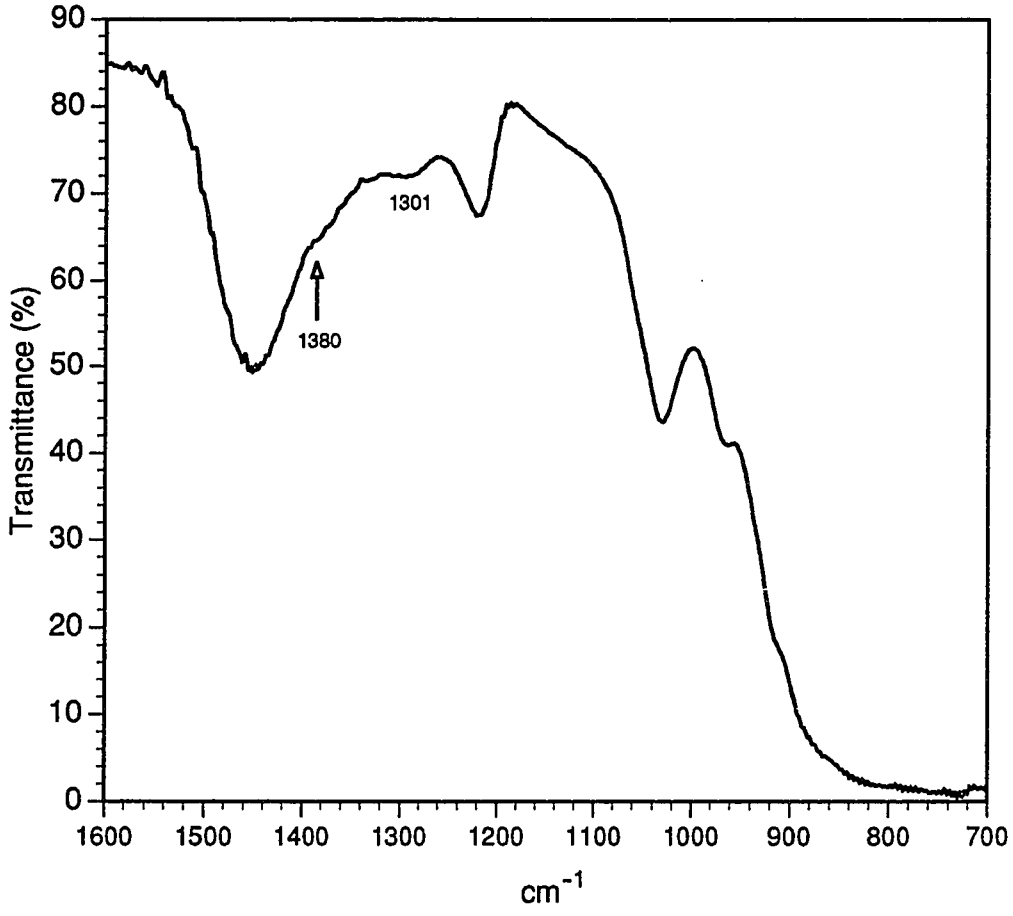

Figure 3.19 The HATR-FTIR spectrum of a deuterated alumina paste with adsorbed B. The paste was obtained from a 55 g L^{-1} alumina suspension with 0.18 mol L^{-1} total B in D_2O.

(Figs. 3.15 and 3.17) is also absent from the alumina with B spectrum. The relocation of aqueous B bands is consistent with the disruption of the trigonal symmetry and triple degeneracy of the hydroxyl groups of aqueous BA following coordination through one of its oxygens to surface Al^{3+} cations of alumina.

Splitting of aqueous oxy-anion bands as a result of adsorption was observed by Serna et al. (1977) in the IR spectra of NO_3^-, SO_4^{2-}, and CO_3^{2-} adsorbed to aluminum hydroxide gels from aqueous solutions. The degree of splitting is indicative of the type and strength of the bond formed with the surface. The magnitude of splitting upon electrostatic adsorption of NO_3^- was 45 cm^{-1} (1358 cm^{-1} aqueous, 1395 and 1350 cm^{-1} adsorbed) whereas the specifically adsorbed CO_3^{2-} exhibited a splitting of the υ_3 vibration of 65 cm^{-1} (1415 cm^{-1} aqueous, 1500 and 1435 cm^{-1} adsorbed). The degree of splitting of the 1405 cm^{-1} B-O υ_3 vibration (this study) following adsorption is 157 cm^{-1}, indicating a strong covalent bond is formed.

Due to the interference of the HDO band near 1450 cm^{-1}, the spectra of D_2O-alumina with adsorbed B are not conclusive regarding the assignments of the adsorbed-B bands. The band at 1301 cm^{-1} due to the B-O υ_3 vibration is again visible in the adsorbed B spectrum (Fig. 3.19). The 1301 cm^{-1} band is not present in the spectrum of BA dissolved in D_2O (Fig. 3.16) or in the alumina-D_2O paste in the absence of adsorbed B (Fig. 3.10). The intensity relationship of the 1450 and 1380 cm^{-1} bands is reversed in the adsorbed-B spectrum (Fig. 3.19) relative to the

spectrum of aqueous B (in D_2O) (Fig. 3.16), as the 1380 cm^{-1} band now appears as a shoulder on the more intense 1450 cm^{-1} HDO band. The 892 cm^{-1} band assigned to aqueous B-O-D bending modes is no longer visible in the paste spectrum (Fig. 3.19). This corresponds to the loss of the 1149 cm^{-1} aqueous B-O-H band in the H_2O system following adsorption (Fig. 3.18).

3.4.3 Summary of Infrared Results

The HATR-FTIR analyses of aqueous alumina suspensions indicate that the surface of alumina undergoes a transformation upon immersion in H_2O, producing a new aluminum hydroxide gel phase at its surface unlike the original structure of the synthesized alumina obtained in the dry state. This amorphous aluminum hydroxide gel coating on the alumina core is dissolved at relatively low and high pH, exposing the aqueous alumina surface.

The spectra of alumina with adsorbed B indicate that B forms a strong coordinate bond through surface oxygen atoms of the hydrous Al-oxide. This is indicated by significant splitting of IR bands found for aqueous B species following B adsorption.

The conclusions regarding the nature of the interaction of adsorbed B with the alumina surface are strengthened by the methodology chosen in this study. Because HATR-FTIR subtraction spectra yield absorption bands attributable to the solid and its aqueous interface (Tejedor-Tejedor and Anderson, 1985), the bands assigned to adsorbed B can be disassociated from the aqueous B species in the

suspensions. Since the spectral features of the bulk supernatant have been eliminated, the new bands found in the adsorbed B spectra could only arise from changes in the composition of the alumina or its aqueous interface.

Chapter 4

SUMMARY AND CONCLUSIONS

Boron adsorption and desorption reactions largely control the fate and availability of this essential plant nutrient in the root zone. In the dynamic environment of natural soils, the rates of these reactions govern the potential for deficient or excessive levels of B in the soil solution.

Pressure-jump chemical relaxation rate measurements obtained from alumina suspensions with adsorbed B indicate that the rates of B adsorption reactions on alumina surfaces are extremely rapid, occurring on millisecond time scales. The rates of B desorption are relatively slow; the adsorption rate is more than eight orders of magnitude greater than the desorption rate.

The correlation of pressure-jump reaction rate measurements to derived rate law expressions for B adsorption mechanisms indicates that the borate (BT) anion is adsorbed in a single-step ligand exchange reaction with neutral surface hydroxyl groups on alumina surfaces. As an indirect consequence of the kinetic confirmation of the BT reaction mechanism, specific adsorption of boric acid (BA) on neutral surface sites is also indicated. Water is the leaving ligand in both

reactions. Throughout the pH range of the pressure-jump study (pH 7.0 to 10.8), the amount of BT adsorbed is at least three times the amount of BA adsorbed.

Fourier transform infrared (FTIR) spectroscopic analyses of aqueous alumina suspensions, with and without adsorbed B, showed that the surface of the alumina may undergo a transformation upon immersion in H_2O, producing a new mineral phase at the surface unlike the original structure of the synthesized alumina obtained in the dry state. This new amorphous phase which coats the alumina core may not be identical in its chemical properties to the alumina core structure itself, particularly in adsorption reactions. In essence, aqueous alumina surfaces may only be exposed at relatively low and high pH, outside the normal pH range of natural waters. Moreover, the amorphous layer on the alumina in the intermediate pH range may become more ordered over time following immersion and dialysis, and thus its chemical reactivity will vary throughout this period. A standardized suspension aging period following dialysis would perhaps improve reproducibility in adsorption studies using this aluminum oxide.

In all probability, formation of a surface aluminum hydroxide gel surface layer is not an exclusive property of alumina. If other aluminum oxides undergo this same surface gel formation, this may indicate that these aluminum oxides have similar surface properties in aqueous suspensions near neutral pH (pH ~ 6 to 8), regardless of their structural dissimilarities in the dry state. Infrared studies of a variety of aluminum oxides in aqueous suspensions over a wide pH

range will reveal if this is in fact the case. These results suggest that colloid chemists may require more information regarding the similarities and differences of colloidal surfaces in the dry vs. wet state. Many characterization techniques used for colloidal substances require that samples be dry and it is assumed that wetting the colloid does not alter its composition or structure from the dry state. In light of the results of this study, that can no longer be considered a safe assumption.

The possibility that the alumina surface may have changed structurally throughout the pH range of the pressure-jump study (Chapter 2) is suggested by the IR results. The surface acidity "constants" of the oxide may also vary with the change in the surface structure, introducing a source of error in the determination of neutral surface site concentrations. Although, in the pH range of this study, the structure of the oxide surface may vary, it is nonetheless a hydrous oxide surface throughout. The surface functional groups of the suspended oxide would thus be similar compositionally, if not identical energetically. This may ultimately result in only small effects on the equilibrium and kinetics of B interactions with hydroxyl groups of the aluminum oxide, and the success of the pressure-jump analysis may be compromised only slightly. This is reflected in the slight disparity in the values of equilibrium constants obtained from kinetic and static analysis.

The FTIR spectra of alumina with adsorbed B indicate that B forms a strong coordinate bond through surface oxygen atoms of the hydrous aluminum oxide. In contrast to the modeling and analysis of pressure-jump relaxation data

obtained at high pH (pH > 7), the FTIR spectra indicate that most of the adsorbed B is three-coordinate rather than four-coordinate in the adsorbed state at low pH. Because the pressure-jump apparatus relies on conductivity detection, and only the BT adsorption reaction mechanism will result in a change in conductivity of the supernatant, the pressure-jump study was restricted to the range of pH > 7.0, where BT concentrations vary significantly. The FTIR analysis of adsorbed B was conducted at low pH (pH < 5), where B in solution is almost entirely in the trigonal BA form. Evidence of three-coordinate adsorbed B in the FTIR spectra is not unexpected under these experimental conditions. Because the FTIR spectra only reveal the coordination state of the adsorbed B after adsorption has taken place, it is not known if both BA and BT are reactants in the adsorption process at low pH.

The findings of the kinetic and spectroscopic analyses of B adsorption bear considerable significance to the management of B fertility in soils with sizable sesquioxide contents. Results of this study indicate that B in solution is extremely reactive with aluminum oxides having free surface hydroxyl groups. Boron is specifically adsorbed to aluminum oxide surfaces over a wide range of pH. As B enters the soil solution, either as a result of fertilizer applications or desorption from mineral surfaces, the likelihood of B fixation due to surface complex formation is very high in oxidic soils. In the case of desorbed B, readsorption may quickly occur before the plant can assimilate the released nutrient. Plant uptake of

B is believed to occur passively by diffusion and thus is a relatively slow process on the time scale of B adsorption reactions.

As B is removed from solution by plant uptake or leaching, it may take an extended period of time for B levels to regenerate in the soil solution by desorption. If the rate of plant uptake far exceeds the desorption rate, inadequate B levels in the soil solution will result.

If total B levels in a cultivated oxidic soil are high, a large percentage of total B may be in the fixed state. During periods of rapid plant uptake of B, such as would occur in cultivated soils during a growing season, the kinetics of B adsorption and desorption will favor a non-equilibrium state for adsorbed B. Following this condition, if extended periods of time transpire with no actively growing plant cover, (e.g., over winter) high soil solution B levels may gradually be restored by desorption, with the potential to induce plant injury in subsequent crops. Soils suspected of retaining large quantities of fixed B should be tested for excessive soil solution B levels following long periods of inactivity before planting crops which are particularly sensitive to elevated B levels.

In managing B soil fertility in the past, the processes by which B is fixed in soils have been surmised through indirect evidence. Most frequently, chemical adsorption of B on various inorganic soil constituents has been assumed to cause B fixation in soils. As a result of the reaction mechanisms identified through kinetic and FTIR analysis in this study, it has now been firmly established that B

undergoes ligand exchange reactions with aluminum oxides. In soils containing substantial quantities of aluminum oxides, this knowledge can be directly applied in predicting B fertility status. As is often the case, particularly in B-horizons of soils where these mineral weathering products have accumulated, these oxides occur as coatings on other minerals. This condition will cause the soil as a whole to behave chemically in similar fashion to the oxide, despite its relatively small contribution to total soil mass. Thus, soils which have extensive coatings of oxides will have a great capacity to fix B through chemical adsorption to their surfaces.

The oxide chosen for this study is not a common soil oxide. Alumina was selected as the adsorbent for this study because it has been used widely for adsorption studies by other researchers and thus would facilitate comparison of the findings to those of other studies. Several infrared spectroscopic studies of dry alumina have also been conducted. In order to know with more certainty how the rates of B adsorption and desorption reactions on alumina compare with naturally occurring soil oxides, such as gibbsite ($Al(OH)_3$ and boehmite (AlOOH), similar kinetic measurements should be obtained for B adsorption and desorption using these oxides.

REFERENCES

Adriano, D. C., A. L Page, A. A. Elseewi, A. C. Chang, and I. Straughn. 1980. Utilization and disposal of fly ash and other coal residues in terrestrial ecosystems: a review. J. Environ. Qual. 9:333-344.

Aharoni, C., and D. L. Sparks. 1991. Kinetics of soil chemical reactions—A theoretical treatment. *In* Rates of soil chemical processes. D. L. Sparks and D. L. Suarez (eds.) Soil Sci. Soc. Am., Inc., Madison WI.

Anderson, D. G., J. K. Duffer, J. M. Julian, R. W. Scott, T. M. Sutliff, M. J. Vaickus, and J. T. Vandeberg. 1980. An infrared spectroscopy atlas for the coatings industry. Federation of Societies for Coatings Technology, Philadelphia, PA.

Anderson, J. L., E. M. Eyring, and M. P. Whittaker. 1964. Temperature jump rate studies of polyborate formation in aqueous boric acid. J. Phys. Chem. 68:1128-1132.

Ashida, M., M. Sasaki, H. Kan, T. Yasunaga, K. Hachiya, and T. Inoue. 1978. Kinetics of proton adsorption-desorption at TiO_2-H_2O interface by means of pressure-jump technique. J. Colloid Interface Sci. 99:183-186.

Astumian, R. D., M Sasaki, T. Yasunaga, and Z. A. Schelly. 1981. Proton adsorption-desorption kinetics on iron oxides in aqueous suspensions, using the pressure-jump method. J. Phys. Chem. 85:3832-3835.

Balz, R., U. Brandle, E. Kammerer, D. Kohnlein, O. Lutz, A. Nolle, R. Schafitel, and E. Veil. 1986. ^{11}B and ^{10}B NMR investigations in aqueous solutions. Z. Naturforsch. 41:737-742.

Bassett, R. L. 1980. A critical evaluation of the thermodynamic data for boron ions, ion pairs, complexes, and polyanions in aqueous solution at 298.15 K and 1 bar. Geochim. Cosmochim. Acta. 44:1151-1160.

Bernasconi, C. F. 1976. Relaxation kinetics. Academic Press, New York, NY.

Beyrouty, C. A., G. E. Van Scoyoc, and J. R. Feldkamp. 1984. Evidence supporting specific adsorption of boron on synthetic aluminum hydroxides. Soil Sci. Soc. Am. J. 48:284-287.

Biggar, J. W., and M. Fireman. 1960. Boron adsorption and release by soils. Soil Sci. Soc. Am. Proc. 24:115-120.

Bingham, F. T. and A. L. Page. 1971. Specific character of boron adsorption by an amorphous soil. Soil Sci. Soc. Am. Proc. 35:892-893.

Bingham, F. T., A. L. Page, N. T. Coleman, and K. Flach. 1971. Boron adsorption characteristics of selected amorphous soils from Mexico and Hawaii. Soil Sci. Soc. Am. Proc. 35:546-550.

Bloesch, P. M., L. C. Bell, and J. D. Hughes. 1987. Adsorption and desorption of boron by goethite. Aust. J. Soil Res. 25:377-3990.

Boeseken, J. 1949. The use of boric acid for the determination of the configuration of carbohydrates. Adv. Carbohydrate Chem. 4:189-210.

Bowden, J. W., S. Nagarajah, S. Barrow, A. M. Posner, and J. P. Quirk. 1980. Describing the adsorption of phosphate, citrate and selenite on a variable-charge mineral surface. Aust. J. Soil Res. 18:49-60.

Bowden, J. W., A. M. Posner, and J. P. Quirk. 1977. Ionic adsorption on variable charge mineral surfaces. Theoretical-charge development and titration curves. Aust. J. Soil Res. 15:121-136.

Boyd, G. E., A. W. Adamson, and L. S. Meyers, Jr. 1947. The exchange adsorption of ions from aqueous solutions by organic zeolites. II. Kinetics. J. Am. Chem. Soc. 69:2836-2848.

Chang, A. C., L. J. Lund, A. L. Page, and J. E. Warneke. 1977. Physical properties of fly ash-amended soils. J. Environ Qual. 6:267-270.

Cook, R. L., and C. E. Millar. 1939. Some soil factors affecting boron availability. Soil Sci. Soc. Am. Proc. 4:297-301.

Couch, E. L., and R. E. Grimm. 1968. Boron fixation by illites. Clays Clay Miner. 16:249-256.

Davis, J. A., and L. O. Leckie. 1980. Surface ionization and complexation at the oxide/water interface. III. Adsorption of anions. J. Colloid Interface Sci. 74:32-43.

Edwards, J. O., and V. Ross. 1960. Structural principles of the hydrated polyborates. J. Inorg. Nucl. Chem. 15:329-337.

Edwards, J. O., G. C. Morrison, V. F. Ross, and J. W. Schultz. 1955. The structure of the aqueous borate ion. J. Amer. Chem. Soc. 77:266-268.

Eigen, M., and L. DeMaeyer. 1963. Relaxation methods. *In* A. Weissberger (ed.) Techniques in organic chemistry. Vol. VIII. Part 2. 2nd ed. Wiley Interscience, New York, NY.

Eisenberg, D., and D. Crothers. 1979. Physical chemistry with applications to the life sciences. Benjamin/Cummings Publ. Co., Inc., Menlo Park, CA.

Elrashidi, M. A., and G. A. O'Connor. 1982. Boron sorption and desorption in soils. Soil Sci. Soc. Am. J. 46:27-31.

Epperlein, B. W., O. Lutz, and A. Schwenk. 1975. Fourier transform NMR studies on boron-10 and boron-11 in aqueous solutions. Z. Naturforsch. 30:955-958.

Evans, C. M. 1983. The kinetics and mechanisms of boron adsorption and desorption in Mid-Atlantic Coastal Plain soils. Masters thesis. Univ. of Delaware, Newark, DE.

Evans, L. J. 1988. Boron retention in Ontario soils. Final report of OMAF Project 778. Department of Land Resource Science, University of Guelph, Guelph, Ontario.

Falk, M., and T. A. Ford. 1966. Infrared spectrum and structure of liquid water. Can. J. Chem. 44:1699-1707.

Farmer, V. C. 1974. Vibrational spectroscopy in mineral chemistry. *In* V. C. Farmer (ed.) The infrared spectra of minerals. Mineralogical Society, London, England.

Fleming, G. A. 1980. Essential micronutrients: Boron and molybdenum. *In* B. E. Davies (ed.) Applied soil trace elements. John Wiley and Sons. New York, N. Y.

Fleet, M. E. L. 1965. Preliminary investigations into the sorption of boron by clay minerals. Clay Minerals. 6:3-16.

Goldberg, S., and H. S. Forster. 1991. Boron sorption on calcareous soils and reference calcites. Soil Sci. 152:304-310.

Goldberg, S., and R. A. Glaubig. 1985. Boron adsorption on aluminum and iron oxide minerals. Soil Sci. Soc. Am. J. 49:1374-1379.

Goldberg, S., and R. A. Glaubig. 1986a. Boron adsorption on California soils. Soil Sci. Soc. Am. J. 50:1173-1176.

Goldberg, S., and R. A. Glaubig. 1986b. Boron adsorption and silicon release by the clay minerals kaolinite, montmorillonite, and illite. Soil Sci. Soc. Am. J. 50:1442-1448.

Goldberg, S., and R. A. Glaubig. 1988. Boron and silicon adsorption on an aluminum oxide. Soil Sci. Soc. Am. J. 52:87-91.

Goldberg, S., and G. Sposito. 1984. A chemical model of phosphate adsorption by soils: I. Reference oxide minerals. Soil Sci. Soc. Am. J. 48:772-778.

Greulach, V. A. 1973. Plant function and structure. MacMillan Publ. Co., NY.

Gruenewald, B., and W. Knoche. 1979. Recent developments and applications of pressure jump methods. *In* W. J. Gettins and E. Wyn-Jones (eds.) Techniques and applications of fast reactions in solution. Reidel Publ. Co., Dordrecht, The Netherlands.

Griffin, R. A., and R. G. Burau. 1974. Kinetic and equilibrium studies of boron desorption from soil. Soil Sci. Soc. Am. Proc. 38:892-897.

Gupta, U. C. 1979. Boron nutrition of crops. Adv. Agron. 31:273-307.

Gupta, U. C., Y. A. Jame, C. A. Campbell, A. J. Leyshon, and W. Nicholaichuk. 1985. Boron toxicity and deficiency: a review. Can J. Soil Sci. 65:381-409.

Hachiya, K., M. Ashida, M. Sasaki, H. Kan, T. Inoue, and T. Yasunaga. 1979. Study of the kinetics of adsorption-desorption of Pb^{+2} on a γ-Al_2O_3 surface by means of relaxation techniques. J. Phys. Chem. 83:1866-1871.

Hachiya, K., M. Ashida, M. Sasaki, M. Karasuda, and T. Yasunaga. 1980. Study of the adsorption-desorption of IO_3^- on a TiO_2 surface by means of relaxation techniques. J. Phys. Chem. 84:2292-2296.

Hachiya, K, M. Sasaki, T. Ikeda, N. Mikami, and T. Yasunaga. 1984. Static and kinetic studies of the adsorption-desorption of metal ions on a γ-Al_2O_3 surface. Kinetic study by means of pressure-jump technique. J. Phys. Chem. 88:27-31.

Hadas, A., and J. Hagin. 1972. Boron adsorption by soils as influenced by potassium. Soil Sci. 113:189-193.

Hair, M. L. 1967. Infrared spectroscopy in surface chemistry. Marcel Dekker, Inc., New York, NY.

Harder, H. 1961. Einbau von Bor im detritisch Tonminerale. Geochim. Cosmochim. Acta. 21: 284-294.

Harrick, N. J, and N. H. Riederman. 1965. Infrared spectra of powders by means of internal reflection spectrometry. Spectrochim. Acta 21:2135-2139.

Hatcher, J. T., and C. A. Bower. 1958. Equilibria and dynamics of boron adsorption by soils. Soil Sci. 85:319-328.

Hatcher, J. T., C. A. Bower, and M. Clark. 1967. Adsorption of boron by soils as influenced by hydroxy aluminum and surface area. Soil Sci. 104:422-426.

Hayes, K. F., J. O. Leckie. 1986. Mechanism of lead ion adsorption at the goethite-water interface. *In* J. A. Davis and K. F. Hayes (eds.) Geochemical processes at mineral surfaces. ACS SYM. 323. Am. Chem. Soc., Washington, DC.

Hayes, K. F., and J. O. Leckie. 1987. Modeling ionic strength effects on cation adsorption at hydrous oxide/solution interfaces. J. Colloid Interface Sci. 115:564-572.

Hayes, K. F., G. Redden, W. Ela, and J. O. Leckie. 1991. Surface complexation models: an evaluation of model parameter estimation using FITEQL and oxide mineral titration data. J. Colloid Interface Sci. 142:448-469.

Heilman, M. D., D. L. Carter, and C. L. Gonzalez. 1965. The ethylene glycol monoethyl ether (EGME) technique for determining soil-surface area. Soil Sci. 100:409-413.

Heller, G. 1986. A survey of structural types of borates and polyborates. Top. Curr. Chem. 131:39-98.

Hiemstra. T., W. H. Van Riemsdijk, and G. H. Bolt. 1989. Multisite proton adsorption modeling at the solid/solution interface of (Hydr)oxides: A new approach. J. Colloid Interface Sci. 133:91-104.

Hingston, F. J. 1964. Reactions between boron and clays. Aust. J. Soil Res. 2:83-95.

Hingston, F. J. 1981. A review of anion adsorption. *In* M. A. Anderson and A. J. Rubin (ed.) Adsorption of inorganics at solid-liquid interfaces. Ann Arbor Science Publ., Inc., Ann Arbor, MI.

Hingston, F. J., A. M. Posner, and J. P. Quirk. 1972. Anion adsorption by goethite and gibbsite: I. The role of the proton in determining adsorption envelopes. J. Soil Sci. 23:177-192.

Hoffmann, H., J. Stuehr, and E. Yeager. 1964. Studies of relaxation effects in electrolytic solutions with the pressure-jump method. *In* B. E. Conway and R. G. Barradus (eds.) Chemical physics of ionic solutions. J. Wiley and Sons, Inc., NY.

Ikeda, T., M. Sasaki, R. D. Astumian, and T. Yasunaga. 1981. Kinetics of the hydrolysis of zeolite 4A surface by the pressure-jump relaxation method. Bul. Chem. Soc. Jpn. 54:1885-1886.

Ikeda, T., M. Sasaki, K. Hachiya, R. D. Astumian, T. Yasunaga, and Z. A. Schelly. 1982a. Adsorption-desorption kinetics of acetic acid on silica-alumina particles in aqueous suspensions, using the pressure-jump relaxation method. J. Phys. Chem. 86:3861-3866.

Ikeda, T., M. Sasaki, and T. Yasunaga. 1982b. Kinetics of the hydrolysis of hydroxyl groups on zeolite surfaces using the pressure-jump relaxation method. J. Phys. Chem. 86:1678-1680.

Ikeda, T., M. Sasaki, and T. Yasunaga. 1983. Kinetic studies of ion exchange of alkylammonium ion for sodium ion in aqueous suspensions of zeolite 4A using the pressure-jump method. J. Phys. Chem. 87:745-749.

Ikeda, T., and T. Yasunaga. 1984. Kinetic studies of ion exchange of the ammonium ion for H^+ in zeolite H-ZSM-5 by the chemical relaxation method. J. Colloid Interface Sci. 99:165-166.

Ingri, N. 1962. Equilibrium studies of polyanions: VIII. On the first equilibrium steps in the hydrolysis of boric acid, a comparison between equilibria in 0.1 M and 3.0 M $NaClO_4$. Acta Chem. Scanda. 16:439-448.

Ingri, N., G. Lagerstrom, M. Frydman, and L. G. Sillen. 1957. Equilibrium studies of polyanions: II. Polyborates in $NaClO_4$ medium. Acta Chem. Scand. 11:1034-1058.

Janda, R., and G. Heller. 1979. ^{11}B-NMR spectroscopic studies on aqueous polyborate solutions. Z. Naturforsch. 34:1078-1083.

Jones, H. E., and G. D. Scarseth. 1944. The calcium-boron balance in plants as related to boron needs. Soil Sci. 57:15-24.

Keren, R., and F. T. Bingham. 1985. Boron in water, soils, and plants. *In* B. A. Stewart (ed.) Advances in Soil Science. Vol. 1. Springer-Verlag New York Inc., New York, NY.

Keren, R., and R. G. Gast. 1981. Effects of wetting and drying, and of exchangeable cations, on boron adsorption and release by montmorillonite. Soil Sci. Soc. Am. J. 45:478-482.

Keren, R., R. G. Gast, and B. Bar-Yosef. 1981. pH-dependent boron adsorption by Na-montmorillonite. Soil Sci. Soc. Am. J. 45:45-48.

Keren, R., and U. Mezumen. 1981. Boron adsorption by clay minerals using a phenomenological equation. Clays Clay Miner. 29:198-204.

Keren R., and H. Talpaz. 1984. Boron adsorption by montmorillonite as affected by particle size. Soil Sci. Soc. Am. J. 48:555-559.

Kiselev, A. V., and V. I. Lygin. 1975. Infrared spectra of surface compounds. John Wiley and Sons, New York, NY.

Klein, C., and C. S. Hurlbut, Jr. 1985. Manual of mineralogy. 20th ed. John Wiley and Sons. New York, NY.

Knoche, W. 1974. Pressure-jump methods. *In* G. G. Hammes (ed.) Investigations of rates and mechanisms of reactions. Part 2. 3rd ed. John Wiley, New York.

Knoche, W., and H. Strehlow. 1979. Data capture and processing in chemical relaxation measurements. *In* W. J. Gettins and E. Wyn-Jones (ed.) Techniques and applications of fast reactions in solution. D. Reidel Publ. Co., Dordrecht, Holland.

Knoche, W., and G. Wiese. 1974. An improved apparatus for pressure-jump relaxation measurements. Chem. Instrum. 5:91-98.

Krizan, M., and H. Strehlow. 1973-1974. On the evaluation of chemical relaxation measurements with sampling technique and on-line processing. Chem. Instr. 5:99-108.

Lee, S., and S. Aranoff. 1967. Boron in plants; a biochemical role. Science. 158:798-799.

Maeda, M., T. Hirao, M. Kotaka, and H. Kakihana. 1979. Raman spectra of polyborate ions in aqueous solution. J. Inorg. Nucl. Chem. 41:1217-1220.

Makkee, M., A. P. G. Kieboom, and H. van Bekkum. 1985. Studies on borate esters: III. Borate esters of D-mannitol, D-glucitol, D-fructose, and D-glucose in water. Recl. Trav. Chim. Pays-Bas. 104:230-235.

Mattigod, S. V., J. A. Frampton, and C. H. Lim. 1985. Effect of ion-pair formation on boron adsorption by kaolinite. Clays Clay Miner. 33:433-437.

Maya, L. 1976. Identification of polyborate and flouroborate ions in solution by Raman spectroscopy. Inorg. Chem. 15:2179-2184.

McPhail, M., A. L. Page, and F. T. Bingham. 1972. Adsorption interactions of monosilicic and boric acid on hydrous oxides of iron and aluminum. Soil Sci. Soc. Am. J. 36:510-514.

Mesmer, R. E., C. F. Baes, Jr., and F. H. Sweeton. 1972. Acidity measurements at elevated temperatures. VI. Boric acid equilibria. Inorg. Chem. 11:537-543.

Mezumen, U., and R. Keren. 1981. Boron adsorption by soils using a phenomenological adsorption equation. Soil Sci. Soc. Am. J. 45:722-726.

Midgley, A. R., and D. E. Dunklee. 1939. The effect of lime on the fixation of borates in soils. Soil Sci. Soc. Am. Proc. 4:302-307.

Mikami, N., M. Sasaki, K. Hachiya, R. D. Astumian, T. Ikeda, and T. Yasunaga. 1983a. Kinetics of the adsorption-desorption of phosphate on the γ-Al_2O_3 surface using the pressure-jump technique. 87:1454-1458.

Mikami, N., M. Sasaki, K. Hachiya, and T. Yasunaga. 1983b. Kinetic study of the adsorption-desorption of the uranyl ion on a γ-Al_2O_3 surface using the pressure-jump technique. J. Phys. Chem. 87:5478-5481.

Mikami, N., M. Sasaki, T. Kikuchi, and T. Yasunaga. 1983c. Kinetics of the adsorption-desorption of chromate on γ-Al_2O_3 surfaces using the pressure-jump technique. 87:5245-5248.

Momii, R. K., and N. H. Nachtrieb. 1967. Nuclear magnetic resonance study of borate-polyborate equilibria in aqueous solution. Inorg. Chem. 6:1189-1192.

Naftel, J. A. 1937. Soil liming investigations: V. The relation of boron deficiency to over-liming injury. J. Am. Soc. Agron. 29:761-771.

Nail, S. L., J. L. White, and S. L. Hem. 1975. Comparison of IR spectroscopic analysis and X-ray diffraction of aluminum hydroxide gel. J. Pharm. Sci. 64:1166-1169.

Oertli, J. J., and E. Grgurevic. 1975. Effect of pH on the absorption of boron by excised barley roots. Agron. J. 67:278-280.

Oertel, R. P. 1972. Raman study of aqueous monoborate-polyol complexes. Equilibria in the monoborate-1,2-ethanediol system. Inorg. Chem. 11:544-549.

Ogwada, R. A., and D. L. Sparks. 1986. Kinetics of ion exchange on clay minerals and soil: I. Evaluation of methods. Soil Sci. Soc. Am. J. 50:1158-1162.

Okazaki, E., and T. T. Chao. 1968. Boron adsorption and desorption by some Hawaiian soils. Soil Sci. 105:255-259.

Osugi, J., M. Sato, and T. Fujii. 1968. Pressure-jump technique applied in study of solutions. Nippon Kagaku Zasshi 89:562-565.

Pagenkopf, G. K., and J. M. Connolly. 1982. Retention of boron by coal ash. Environ. Sci. Technol. 16:609-616.

Parker, D. R., and E. H. Gardner. 1981. The determination of hot-water-soluble boron in some acid Oregon soils using a modified azomethine-H procedure. Commun. in Soil Sci. Plant Anal. 12:1311-1322.

Parks, R. Q., and B. T. Shaw. 1941. Possible mechanisms of boron fixation in soil: I. Chemical. Soil Sci. Soc. Am. Proc. 6:219-223.

Parks, W. L., and J. L. White. 1952. Boron retention by clay and humus systems saturated with various cations. Soil Sci. Soc. Am. Proc. 16:298-300.

Pasdeloup, M., and C. Brisson. 1981. NMR study of the complexation of boric acid with catechol (1,2-dihydroxybenzene). Org. Magn. Reson. 16:164-167.

Peri, J. B. 1965. Infrared and gravimetric study of the surface hydration of γ-alumina. J. Phys. Chem. 69:211-219.

Peri, J. B., and R. B. Hannan. 1960. Surface hydroxyl groups on γ-alumina. J. Phys. Chem. 64:1526-1530.

Peryea, F. J., F. T. Bingham, and J. D. Rhoades. 1985a. Kinetics of post-reclamation boron dissolution. Soil Sci. Soc. Am. J. 49:836-839.

Peryea, F. J., F. T. Bingham, and J. D. Rhoades. 1985b. Mechanisms for boron regeneration. Soil Sci. Soc. Am J. 49:840-843.

Pizer, R., and L. Babcock. 1977. Mechanism of the complexation of boron acids with catechol and substituted catechols. Inorg. Chem. 16:1677-1681.

Rajartnam, J. A., J. B. Lowry, P. N. Avadhani, and R. H. V. Corley. 1971. Boron: Possible role in plant metabolism. Science. 172:1142-1143.

Reisenauer, H. M., L. M. Walsh, and R. G. Hoeft. 1973. Testing soils for sulfur, boron, molybdenum, and chlorine. *In* L. M. Walsh and J. D. Beaton (ed.) Soil Testing and Plant Analysis. Soil Sci. Soc. Am., Madison WI.

Rhoades, J. D., R. D. Ingvalson, and J. T. Hatcher. 1970. Adsorption of boron by ferromagnesian minerals and magnesium hydroxide. Soil Sci. Soc. Am. Proc. 34:938-941.

Ross, S. D. 1974. Borates. *In* V. C. Farmer (ed.) The infrared spectra of minerals. Mineralogical Society, London, England.

Russell, J. D. 1974. Instrumentation and techniques. *In* V. C. Farmer (ed.) The infrared spectra of minerals. Mineralogical Society, London, England.

Salentine, C. G. 1983. High field ^{11}B NMR of alkali borates. Aqueous polyborate equilibria. Inorg. Chem. 22:3920-3924.

Schindler, P. W., and H. Gamsjäger. 1972. Acid-base reactions of TiO_2 suspensions. Kolloid Z. Z. Polym. 250:759-763.

Schulthess, C. P., and D. L. Sparks. 1986. Backtitration technique for proton isotherm modeling of oxide surfaces. Soil Sci. Soc. Am. J. 50:1406-1411.

Serna, C. J., J. L. White, and S. L. Hem. 1977. Anion-aluminum hydroxide gel interactions. Soil Sci. Soc. Am. J. 41:1009-1013.

Sharma, H. C., N. S. Pasricha, and M. S. Bajwa. 1989. Comparison of mathematical models to describe boron desorption from salt-affected soils. Soil Sci. 147:79-84.

Sims, J. R., and F. T. Bingham. 1967. Retention of boron by layer silicates, sesquioxides, and soil materials: I. Layer silicates. Soil Sci. Soc. Am. Proc. 31:728-732.

Sims, J. R., and F. T. Bingham. 1968a. Retention of boron by layer silicates, sesquioxides, and soil materials: II. Sesquioxides. Soil Sci. Soc. Am. Proc. 32:364-369.

Sims, J. R., and F. T. Bingham. 1968b. Retention of boron by layer silicates, sesquioxides, and soil materials: III. Iron-and aluminum-coated layer silicates and soil materials. Soil Sci. Soc. Am. Proc. 32:369-373.

Singh, S. P. N., and S. V. Mattigod. 1992. Modeling boron adsorption on kaolinite. Clays Clay Miner. 40:192-205.

Singh, S. S. 1964. Boron adsorption equilibria in soils. Soil Sci. 98:383-387.

Skoog, D. A. 1985. Principles of instrumental analysis. 3rd ed. Saunders College Publ., Philadelphia, PA.

Smith, H. D., and R. J. Wiersema. 1972. Boron-11 nuclear magnetic resonance study of polyborate ions in solution. Inorg. Chem. 11:1152-1154.

Smith, R. A. 1985. Boric oxide, boric acid, and borates. *In* W. Gerhartz (ed.) Ullmann's encyclopedia of industrial chemistry. Vol. A4. 5th ed. VCH Publishers, Deerfield Beach, FL.

Sparks, D. L. 1986. Kinetics of reactions in pure and mixed systems. *In* D. L. Sparks (ed.) Soil physical chemistry. CRC Press, Boca Raton, FL.

Sparks, D. L. 1989. Kinetics of soil chemical processes. Academic Press, Inc., San Diego, CA.

Sparks D. L., and P. C. Zhang. 1991. Relaxation methods for studying kinetics of soil chemical phenomena. *In* Rates of soil chemical processes. D. L. Sparks and D. L. Suarez (eds.) Soil Sci. Soc. Am., Inc, Madison WI.

Spectra-Tech Contact Sampler™ User's Manual, Spectra-Tech Inc., Stamford, CT.

Spessard, J. E. 1970. Investigations of borate equilibria in neutral salt solutions. J. Inorg. Nucl Chem. 32:2607-2613.

Stevenson, F. J. 1982. Humus chemistry: genesis, composition, reactions. Wiley, NY.

Stubican, V. and R. Roy. 1962. Boron substitution in synthetic micas and clays. Am. Minerologist. 45:1166-1173.

Stumm, W., C. P Huang, and S. R. Jenkins. 1970. Specific chemical interaction affecting the stability of dispersed systems. Croat. Chem. Acta 42:223-245.

Stumm, W., H. Hohl, and F. Dalang. 1976. Interaction of metal ions with hydrous oxide surfaces. Croat. Chem. Acta 48:491-504.

Stumm, W., R. Kummert, and L. Sigg. 1980. A ligand exchange model for the adsorption of inorganic and organic ligands at hydrous oxide interfaces. Croat. Chem. Acta 53:291-312.

Takahashi, M. T., and R. A. Alberty. 1969. The pressure-jump methods. *In* K. Kustin (ed.) Methods in Enzymology. Volume 16. Reidel Publ., Dordrecht, The Netherlands.

Tejedor-Tejedor, M. I., and M. A. Anderson. 1986. "In situ" attenuated total reflection Fourier transform infrared studies of the goethite (α-FeOOH)-aqueous solution interface. Langmuir. 2:203-210.

Tisdale, S. L., W. L. Nelson, and J. D. Beaton. 1985. Soil fertility and fertilizers. 4th ed. Macmillan Publ. Co., New York, NY.

Van Duin, M., J. A. Peters, A. P. G. Kieboom, and H. van Bekkum. 1985. Studies on borate esters: II. Structure and stability of borate esters of polyhydroxycarboxylates and related polyols in aqueous alkaline media as studied by ^{11}B NMR. Tetrahedron. 41:3411-3421.

Volkhin, V. V., T. K. Tomchuk, and G. V. Leonteva. 1983. Sorption of boron from solution by hydroxides of divalent metals. J. Applied Chem. USSR. 56:729-734.

Westall, J., and H. Hohl. 1980. A comparison of electrostatic models for the oxide/solution interface. Adv. Coll. Interface Sci. 12:265-294.

Westall, J. C. 1982. FITEQL. A program for the determination of chemical equilibrium constants from experimental data (Version 2.0). Dept. of Chemistry. Oregon State Univ., Corvallis, OR.

White, J. L. 1971. Interpretation of infrared spectra of soil minerals. Soil Sci. 112:22-31.

White, J. L., and C. B. Roth. 1986. Infrared spectroscopy. *In* A. Klute (ed.) Methods of soil analysis. Part 1. Physical and mineralogical methods. 2nd ed. Agronomy 9:291-330.

White, G. N., and L. W. Zelazny. 1986. Charge properties of soil colloids. *In* D. L. Sparks (ed.) Soil Physical Chemistry. CRC Press, Boca Raton, FL.

Yates, D. E., S. Levine, and T. E. Healy. 1974. Site-binding model of the electric double layer at the oxide/water interface. Chem. Soc. Faraday Trans., I, 70:1807-1818.

Yermiyaho, U. R., R. Keren, and Y. Chen. 1988. Boron sorption on composted organic matter. Soil Sci. Soc. Am. J. 52:1309-1313.

Yoshino, K., M. Kotaka, M. Okamoto, and H. Kakihana. 1979. ^{11}B-NMR study of the complex formation of borate with catechol and L-dopa. Bull. Chem. Soc. Japan. 52:3005-3009.

Yost, E. C., M. I. Tejedor-Tejedor, and M. A. Anderson. 1990. In situ CIR-FTIR characterization of salicylate complexes at the goethite/aqueous solution interface. Environ. Sci. Technol. 24:822-828.

Zeltner, W. A., E. C. Yost, M. L. Machesky, M. I. Tejedor-Tejedor, and M. A. Anderson. 1986. Characterization of anion binding on goethite using titration calorimetry and cylindrical internal reflection-Fourier transform infrared spectroscopy. *In* J.A. Davis and K. F. Hayes (eds.) Geochemical processes at mineral surfaces. American Chemical Society. Washington, DC.

Zhang, P. C., and D. L. Sparks. 1989. Kinetics and mechanisms of molybdate adsorption/desorption at the goethite/water interface using pressure-jump relaxation. Soil Sci. Soc. Am. J. 53:1028-1034.

Zhang, P. C., and D. L. Sparks. 1990a. Kinetics and mechanisms of sulfate adsorption/desorption on goethite using pressure-jump relaxation. Soil Sci. Soc. Am. J. 54:1266-1273.

Zhang, P. C., and D. L. Sparks. 1990b. Kinetics of selenate and selenite adsorption/desorption at the goethite/water interface. Environ. Sci. Technol. 24:1848-1856.